UNIVERSITY OF CALIFORNIA
SANTA CRUZ

INDIVIDUALS TO CLADES: AN EXAMINATION OF INTRASPECIFIC AND INTERSPECIFIC VARIATION IN SEA OTTERS AND OTHER CHARISMATIC MUSTELOIDS

A dissertation submitted in partial satisfaction
of the requirements for the degree of

DOCTOR OF PHILOSOPHY

in

Ecology and Evolutionary Biology

by

Chris J. Law

June 2019

The Dissertation of Chris J. Law is approved:

_____
Professor Rita Mehta, chair

_____
Professor Terrie Williams

_____
Professor Kathleen Kay

_____
Tim Tinker, Ph.D.

_____
Professor Graham Slater

_____
Lori Kletzer
Vice Provost and Dean of Graduate Studies

Table of Contents

List of Figures and Tables

while the black arrow shows the critical value required to reject the null constant rates model derived from parametric bootstrapping.

Figure 1.4. Lineage diversification rates through time. (a) Phylorate plot of lineage diversification based on the "pruned-before" MCC phylogeny. Colors at each point in time along the branches of the phylorate plot denote instantaneous rate of diversification. Warmer colors (red) indicate faster rates and cooler colors (blue) indicate slower rates. Below the phylorate plot is the global deep-sea oxygen isotope records (modified from (Zachos et al. 2008)). These records indicate a rapid decrease in global temperatures following the Eocene-Oligocene Transition and the Mid-Miocene Climate Transition (Zachos et al. 2008), giving rise to more open vegetation habitats such as grasslands and woodlands (Singh 1988; Prothero and Berggren 2014; Leopold et al. 2014). However, the lack of rate shifts suggests that there are no significant increases in diversification rates after these climate events. (b–d). Diversification-through-time plots depicting family-specific net diversification trajectories computed from the joint posterior density of macroevolutionary rate parameters in BAMM. The black lines denote the background diversification rate (the rate of all musteloids minus the rate of each respective family). Shading intensity of the colored lines indicate the 5% through 95% Bayesian credible regions on the distribution of rates at any point in time for Mustelidae (b), Procyonidae (c), and Mephitidae (d). The black lines denote the mean background diversification rate-through-time (the rate of all musteloids minus the rate of each respective family), and

the grayscale shading illustrates the 95% credible interval of the distribution of background rates through time.

Figure 1.5. Rate-through-time plot in extant musteloids using BAMM (a) and in fossil musteloids using PyRate (b). Net diversification rates are shown in black, speciation rates in blue, and extinction rates in red. The grayscale shading illustrates the 95% credible interval for net diversification. EOCT, Eocene-Oligocene Climate Transition; MMCT, Mid-Miocene Climate Transition.

Figure 1.6. Rate-through-time plot in fossil mephitids (a), ailurids (b), procyonids (c), and mustelids (d) from PyRate. Net diversification rates are shown in black, speciation rates in blue, and extinction rates in red. The grayscale shading illustrates the 95% credible interval for net diversification.

Figure 1.7. Species richness of Mustelidae (a), Procyonidae (b), Ailuridae (c), and Mephitidae (d) across the past 37 Ma. The black curve in each of plot denotes total musteloid richness. The grey bar indicates the Mid-Miocene Climate Transition. Colored curves denote species richness of each respective clade: green squares = neomustelids; pink circles = paleomustelids; blue triangles = procyonids; red stars = ailurids; orange diamonds = mephitids.

Figure 1.8. Rate-through-time plots depicting net body length evolutionary rate in Mustelidae (a), Procyonidae (b), and Mephitidae (c). Shading intensity of the colored lines indicates the 5% through 95% Bayesian credible regions on the distribution of rates at any point in time for Mustelidae (a), Procyonidae (b), and Mephitidae (c). The black curve in each plot denotes the mean background diversification rate-through-time (the rate of all musteloids minus the rate of each respective family), and the grayscale shading illustrates the 95% credible interval of the distribution of background rates through time. Mustelids (mean rate, 0.0023; 95% HPD, 0.0016–0.0033) exhibit greater body length evolutionary rates than procyonids (mean rate, 0.0011; 95% HPD, 0.0004–0.0023) and mephitids (mean rate, 0.0011; 95% HPD, 0.0004–0.0023).

Figure 1.9. Phylorate plot of phenotypic (body length) evolution rates through time. (a) Phylorate plot of the mean phenotypic evolutionary rate of body length across all shift configurations based the MCC phylogeny. (b–d) Phylorate plots of 4 distinct shift configurations with the highest posterior probability. Rate shifts, shown as red circles with sizes proportional to the marginal probability of the shift, demonstrate significant increase in evolutionary rate. 3 distinct shift configurations account for the majority of the posterior probability of the data but result in conflicting rate configurations. The most frequent shift configuration (*f = 0.35*) signifies no rate shift (b) whereas the second most frequent shift configuration (*f = 0.33*) indicates an increase in evolutionary rate at the node leading to the divergence of Ictonychinae,

Mustelinae, and Lutrinae (c). Conversely, the third most frequent shift configuration (*f = 0.16*) reveals a rate shift at the root of Mustelidae (d).

Table 1.1. Parameter estimates (speciation rate λ, extinction rate μ, and clade carrying capacity K) and model support for constant rate (CR) and diversity-dependent models with shifts in clade-wide (SR) or clade-specific Key Innovation related (KI) carry capacities. See text for model names.

Figure 2.1. Time calibrated phylogeny of Musteloidea. Shaded blue box indicates the mustelid subclade (Helictidinae, Guloninae, Ictonychinae, Mustelinae, and Lutrinae) that exhibits decoupled diversification dynamics, specifically higher species carrying capacity relative to the rest of Musteloidea. Shaded green box indicates the mustelid subclade (Ictonychinae, Mustelinae, and Lutrinae) that exhibits an increase in the evolutionary rate of body length without an increase in the evolutionary rate of body mass.

Figure 2.2. Measurements of body regions used to calculate VSI. L_X = lengths and H_X = heights.

Figure 2.3. Box and whisker plots of VSI (A), underlying morphological components (B–G), body size (H), forelimb length (I), and hindlimb length (J). Designation of the three 2-peak models are depicted on the pruned phylogeny. The first model (OUM_A) tested for a transition in VSI between a designated clade consisting of the

branches leading to the most recent common ancestors of Helictidinae, Guloninae, Ictonychinae, Mustelinae and Lutrinae and the remaining musteloids {Law:2018ft}. The second model (OUM_B) tested for a transition in VSI between a designated clade consisting of the branches leading to the most recent common ancestors of Ictonychinae, Mustelinae and Lutrinae and the remaining musteloids {Law:2018ft}. The third model (OUM_C) tested for a transition in VSI between a designated clade consisting of just musteline weasels and polecats and the remaining musteloids.

Figure 2.4. PGLS regressions of (A) ln geometric mean (body size) versus ln VSI (body shape), (B) VSI residuals versus forelimb length residuals, and (C) VSI residuals versus hindlimb length residuals. VSI and limb length residuals were extracted from the residuals of each trait against the geometric mean. Shaded polygons indicate the 95% confidence intervals. diamonds, Mephitidae; upside down triangle, Ailuridae; squares, Procyonidae; black circles, miscellaneous Mustelidae; pentagon, Guloninae; stars, Ictonychinae; triangles, Lutrinae; green circles, Mustelinae.

Table 2.1. Parameter estimates and model fits of (A) VSI, (B) body size, (C) forelimb length residuals, and (D) hindlimb length residuals. Optima have been converted back to raw values from ln transformed values.

Figure 3.1. Landmarks (large black circles) and semi-landmarks (small white circles) used for geometric morphometric analysis of skull shape and size.

Figure 3.2. PGLS regressions between A) the degree of cranial size dimorphism and cranial shape dimorphism, B) the degree of cranial size dimorphism and bite force dimorphism, and C) the degree of cranial shape dimorphism and bite force dimorphism with 95% confidence intervals (shaded polygons).

Figure 3.3. Ancestral state reconstruction of A) social systems and B) dietary regimes mapped onto a pruned time-calibrated phylogeny of 63 musteloid species. Pie charts on each node show the relative Bayesian posterior probability of each character state across 1000 simulations.

Figure 3.4. Density plots of the estimated optima from the best-fitting generalized Ornstein–Uhlenbeck (OU) model of A) cranial size dimorphism, B) cranial shape dimorphism, and C) bite force dimorphism. Multi-peak OU models with separate optima under dietary regimes (herbivory, green; aquatic carnivory, blue; omnivory, orange; and terrestrial carnivory, red) were the best-fitting models for cranial size dimorphism and bite force dimorphism. A single peak OU model was the best-fitting model for cranial shape dimorphism.

Table 3.1. Comparisons of evolutionary model fits for cranial size, cranial shape, and bite force. Mean Akaike information criterion (AICc) is the averaged AICc over 1000 replications and ΔAICc is the model's mean AICc minus the minimum AICc between

models. Bolded rows represent the best-fit model as indicated by Akaike weights (w_A). * indicate models that were unable to converge. OUMA and OUMVA models did not converge for all sexual dimorphism metrics.

Figure 4.1. Photographs of male sea otter skulls illustrating changes in size and shape throughout development at 1 month (pup), 7 months (immature), 2.5 years (subadult), 4.5 years (adult), and 10 years (aged adult). Scale bar represents 2 cm.

Figure 4.2. Ontogenetic changes of the ventral cranium. Vectors on landmarks and semilandmarks show the direction and magnitude of change from the mean pup shape to the mean aged adult shape of females (**A**) and males (**B**) after centroid size is scaled to the same size for each specimen. Vectors were magnified by a factor of 3 to display shape changes. P_D = Procrustes distance between youngest individual and oldest individual in each sex.

Figure 4.3. Ontogenetic changes of the lateral cranium. Vectors on landmarks and semilandmarks show the direction and magnitude of change from the mean pup shape to the mean aged adult shape of females (**A**) and males (**B**) after centroid size is scaled to the same size for each specimen. Vectors were magnified by a factor of 3 to display shape changes. P_D = Procrustes distance between youngest individual and oldest individual in each sex.

Figure 4.4. Ontogenetic changes of the mandible. Vectors on landmarks and semilandmarks show the direction and magnitude of change from the mean pup shape to the mean aged adult shape of females (**A**) and males (**B**) after centroid size is scaled to the same size for each specimen. Vectors were magnified by a factor of 3 to display shape changes. P_D = Procrustes distance between youngest individual and oldest individual in each sex.

Figure 4.5. Ontogenetic shape changes of the ventral cranium (**A–E**), lateral cranium (**F–J**), and mandible (**K–O**) within each age class. Vectors on the landmarks and semilandmarks of each skull view show the direction and magnitude of change from the mean youngest shape to the mean oldest shape within each given age class. Skull views that exhibit significant shape changes through ontogeny are highlighted in yellow. *SD* indicates significant effect of sex on shape changes. Vectors were magnified by a factor of 3 to display shape changes. P_D = Procrustes distance between youngest individual and oldest individual within each age class. Asterisks "*" indicate significant P_D based on permutation tests.

Figure 4.6. Ventral cranial (**A–B**), lateral cranial (**C–D**), and mandibular (**E–F**) shape differences between female and male southern sea otters in the adult and aged adult age classes. Red landmarks/semilandmarks indicate female shape and blue landmarks/semilandmarks indicate male shape. Lines linking female and male

landmarks/semilandmarks indicate the relative direction and magnitude of change. Lines were magnified by a factor of 3 to display shape differences between the sexes.

Figure 4.7. Growth curves for skull shape (ventral cranium (**A**), lateral cranium (**B**), and mandible (**C**)) and skull size (ventral cranium (**D**), lateral cranium (**E**), and mandible (**F**)). Circles represent female skulls, triangles represent male skulls, and colors represent the 5 age classes. The red (darker) curves are the female growth curves, and the blue (lighter) curves are the male growth curves. Only the lateral cranium and mandible exhibited significantly intersexual differences in asymptotic values, and only the cranium exhibited significantly intersexual differences in growth rates (See Table 4.3). Red (darker) and blue (lighter) dashed lines indicate the times at which cranium shapes reach 95% of their asymptotic values for females and males, respectively, whereas the black dashed line indicate the ages at which mandibular shape reaches the minimum for the 95% confidence range for the asymptotic values for females and males combined. On the x-axis, *W* indicates age of weaning, *D* indicates age of complete gain of permanent dentition, and SM♀ and SM♂ indicate earliest age of sexual maturity for female and male southern sea otters, respectively.

Figure 4.8. Growth curves for temporalis mechanical advantage to the canine (**A**) and premolar (**B**) and for masseter mechanical advantage to the canine (**C**) and the premolar (**D**). Circles represent female skulls, triangles represent male skulls, and colors represent the 5 age classes. The red (darker) curves are the female growth

curves, and the blue (lighter) curves are the male growth curves. There was no significant difference in mechanical advantage between the sexes rates (See Table 3). Black dashed lines indicate the ages at which mechanical advantage reach 95% of their asymptotic values for both females and males combined. On the x-axis, *W* indicates age of weaning, *D* indicates age of complete gain of permanent dentition, and SM♀ and SM♂ indicate earliest age of sexual maturity for female and male southern sea otters, respectively.

Figure 4.9. Growth curves for body mass (A) and body length (B). The red curves are the female growth curves, and the blue curves are the male growth curves. Shaded red and blue represent 95% interval confidence range of the female and male growth curves, respectively.

Figure 4.10. Timeline illustrating the maturation ages of southern sea otter skull morphology and mechanical advantage in relation to major life history events. Maturation age was defined as the age at which skull shape/size/mechanical advantage and body size reached 95% of their asymptotic values.

Table 4.1. Results from Procrustes ANOVAs for ontogenetic changes and sex differences in cranial and mandibular shape across the entire lifespan.

Figure 5.1. A) Photograph of the two major jaw adductor muscles of an adult male

sea adult. B) Forces of the temporalis and masseter muscles ($\mathbf{F_T}$ and $\mathbf{F_M}$) are applied at given distances (MAT and MAM) from the fulcrum (triangle), creating rotation of the lower jaw. Bite forces, at given distances (O_C and O_M), balance these muscle forces. Using the model $BF_X = 2\left[\frac{(\mathbf{F_T}*MAT+\mathbf{F_M}*MAM)}{\boldsymbol{O_X}}\right]$, theoretical bite forces are calculated at the canine (BF_C) and the molar (BF_M). C) and D) Cranial dimensions used in this study. CBL, condylobasal length; ZB, zygomatic breadth; and CH, cranial height.

Figure 5.2. Scaling of A) condylobasal length on body mass for female and male southern sea otters, B) bite force at the molar on condylobasal length, and C) bite force at the molar on body mass. Red circles indicate female otters and blue triangles indicate male otters. Red and blue solid lines represent SMA regressions for female and male, respectively. Dotted lines indicate line of isometry. Asterisk indicates slope is significantly different from isometry. See Table 5.1 and Table 5.2 for more details.

Figure 5.3. Scaling of temporalis and masseter muscle masses on condylobasal length. Red circles indicate female otters and blue triangles indicate male otters. Red and blue solid lines represent SMA regressions for female and male, respectively. Dotted lines indicate line of isometry. Asterisk indicates slope is significantly different from isometry. See Table 5.4 for more details.

Figure 5.4. Scaling of out-levers and in-levers on condylobasal length. Red circles

INDIVIDUALS TO CLADES: AN EXAMINATION OF INTRASPECIFIC AND INTERSPECIFIC VARIATION IN SEA OTTERS AND OTHER CHARISMATIC MUSTELOIDS

Chris J. Law

Abstract

The remarkable phenotypic diversity between and within species represents one of the most salient patterns across the Tree of Life. Why some clades exhibit low species diversity and morphological stasis for much of their evolutionary history whereas others have diversified into numerous species and morphological forms? And similarly, why do some populations exhibit greater intraspecific variation compared to other populations? In this dissertation, I used the carnivoran clade Musteloidea (badgers, minks, otters, raccoons, red panda, skunks, weasels) to examine how phenotypic variation between and within musteloid species contribute to their overall biological diversity. In my first two chapters (Chapters 1 and 2), I used a variety of phylogenetic comparative methods and osteological specimens to reveal that musteloids exhibited increased species richness due to evolutionary shifts to more elongate bodies. This morphological innovation potentially allowed these elongate musteloids to exploit novel habitats and prey associated with the climatic changes of the Mid-Miocone Climate Transition. In Chapter 3, I used 3D geometric morphometrics of musteloid crania and found that dietary divergence rather than sexual selection was a greater factor in maintaining cranial sexual dimorphism in musteloids. These results provide evidence that sexual selection is not always the

primary force that maintains sexual dimorphism and demonstrate the importance of diet in reducing intraspecific competition for resources as an important mechanism that maintains the evolution of sexual dimorphism in extant musteloids. In my last two chapters (Chapters 4 and 5), I used 2D geometric morphometric and gross dissection approaches to quantify the size and shape of southern sea otter skulls and estimated their bite force. I found significant sexual dimorphism in adult sea otter skulls and bite force that arose through differences in developmental and growth rates and duration of the craniomandibular morphology. I postulate that males are selected to attain mature crania faster to presumably reach adult biting ability sooner, gaining a competitive advantage in obtaining food and in male–male agonistic interactions. Overall, my dissertation demonstrates how phenotypic variation can lead to increased diversification within certain clades as well as increases in potential competitive advantages within a single population.

Acknowledgements

I would like to thank my advisor, Rita Mehta, for her continual support and enthusiasm throughout my time at Santa Cruz. Who would have thought I ended up in Rita's lab as a graduate student considering she ignored all three of my emails to her when I was applying for graduate schools. I guess she didn't like polychaete worms…But I finally met Rita back in the 2013 SICB annual meeting and I guess I impressed her with "want[ing] to build a phylogenetic tree and map things on it." So, thank you Rita for bringing me into your lab to build a tree and map things on it as well as your mentorship, teaching, and guidance. I have learned a great deal about research and mentorship over the past 6 years and look forward to working on more cool projects in the future as well as beating you in volleyball again.

I also thank members of my PhD committee, Dr. Kathleen Kay, Dr. Graham Slater, Dr. Tim Tinker, and Dr. Terrie Williams. Kathleen provided great phylogenetic comparative methods advice during my committee meeting as well as during our occasional joint comparative methods lab meetings between the Kay and Mehta labs. Always fun to talk comparative methods with a bunch of people. Graham provided much needed help with the phylogenetic comparative methods when I first started out. Graham's expertise made Chapters 1 and 2 possible and gave me a much much greater appreciation for the fossil record. Tim is brilliant. I would learn something new about sea otters and/or modelling every time I met with him. Tim has a way of explaining these complex models in a way that makes complete sense until the moment I go back into my office and wished I had transcribed the entire

conversation. So, thank you Tim for teaching me about modeling and of course giving me the opportunity to work with super adorable sea otters. Lastly, thank you Terrie for your support, enthusiasm, and insight with musteloids. It has been fun talking with someone who has personally raised fun minks for research. I will be picking Terrie's brain about that once I start my giant ant farm weasel body elongation project.

I am grateful to all the funding I have received for my research: National Science Foundation (NSF) Graduate Research Fellowship, a NSF Doctoral Dissertation Improvement Grant, a Collection Study Grant through the American Museum of Natural History, a Visiting Scholarship through the Field Museum, a James L. Patton Award through the American Society of Mammalogists, a Rosemary Grant Student Research Award through the Society for the Study of Evolution, a Fellowship of Graduate Student Travel through the Society of Integrative and Comparative Biology, a Packard Foundation Grant, the Rebecca and Steve Sooy Fellowship, the Friends of the Long Marine Lab, the Lerner Gray Fund, Sigma Xi Grant-in-aid-of-Research, the Myers Trust Grant, and an American Cetacean Society grant. I also thank the following natural history museums and their collection managers and curators for allowing me to visit and/or loan specimens: the American Museum of Natural History, Academy of Natural Sciences of Drexel University, Burke Museum, California Academy of Sciences, Cornell University Museum of Vertebrates, Denver Museum of Nature & Science, Field Museum, Florida Museum of Natural History, KU Natural History Museum, Natural History Museum of Los

Angeles County, Louisiana Museum of Natural History, Museum of Comparative Zoology, Moore Laboratory of Zoology, Museum of Southwestern Biology, Museum of Vertebrate Zoology, National Museum of Natural History, Texas Cooperative Wildlife Collection, University of Arkansas Collections Facility, and University of Michigan Museum of Zoology. Museums are essential for research. I also thank members of UC Santa Cruz, U.S. Geological Survey, Monterey Bay Aquarium, and the California Department of Fish and Wildlife for the sea otter work. I especially thank Tim Tinker, Joe Tomoleoni, Colleen Young, Francesca Batac, Erin Dodd, Jessica Fujii, Dr. Jim Estes, Michelle Staedler, and Dr. Mike Murray. None of this work would have been possible with these people and organizations.

I thank past and present members of the Mehta lab including Vikram Baliga, Ben Higgins, Sarah Kienle, Jacob Harrison, Kat Dale, Kelley Voss, Sam Gartner, and Noe Castaneda. Everyone has contributed to making the Mehta lab a fun place to work in. Thank you Vikram for your guidance in everything stats. And thank you Kat for letting me tag along on your Catalina and Baja trips so I could beat you in board games. I hope the lab continues the tradition of “meeting basic requirements.” I am also grateful for all the students I had the opportunity to mentor including Ana Moreland, Carly Sanchez, Parker Kaye, Jennilyn Stenske, Ekai Richards, Sam Sambado, Kaz Jones, Meghan Yap-Chiongco, Shohei Burns, Emma Duran, Isaac Sanchez, Vikram Venkatram, Anna Wadhwa, and Nancy Hung. It was definitely fun watching their careers grow.

Thank you to all the people I have met at Santa Cruz. You have definitely made living in Santa Cruz and doing a PhD an awesome experience. Thank you to the volleyball crew outdoor times. The #moreballslesstalk era with team #BearClaw and team #Dragon was truly a Golden Age of volleyball. Thank you Jen (aka Chocolate Bear), Rosa (aka Dragon1) Dmitriy (aka Dragon2), and Tash. The second Golden Age of volleyball expanded to be a larger group of people including Megan, Tina, Joe, Bea, Tony, Sam^2, Sammy-J, Jae, Sid, and Ravi. With that came the Taco Thursdays, karaoke, and of course the Bar-Boardwalk games. I also thank the basketball crew because basketball is first love. Thank you Remy, Joel, Zach, Gary, Jacob, Mike, Vikram, and other members of my IM and Parks n' Rec teams. I also thank members of my cohort: Carla, Chris K., Pauline, Sarah, Tash, Sarah McKay, Kate, and honorary cohort members Dmitriy, Sean, and Jen. All of our cohort dinners and board games have been a blast. Lastly, I thank our ~~pub~~ pop bio group, Jason, Luis, Theresa, and Logan, for our weekly discussion about science.

Lastly, I thank my family for their support that got me to where I am today. I am grateful to my grandmother and uncle for raising me as a kid and teaching me the importance of school. I also thank my mom, dad, and sisters for their excitement about studying animals. I'm pretty they think I'm swimming with sea otters all day. And finally, I thank Rosa Chung Law for her continual support and love. I'm excited to continue our adventures and travels across the world, starting with the Concrete Jungles of New York.

Statement of Contribution

The text of this dissertation includes reprints of the following previously published material:

Chapter 1. Law CJ, Slater G, & Mehta RS. 2018. Lineage diversity and size disparity in Musteloidea: testing patterns of adaptive radiation using molecular and fossil-based methods. *Systematic Biology*. 67:127–144.

I designed the study, collected the sequence, body size, and fossil data, performed the majority of data analyses, and drafted the manuscript. Graham Slater helped compile fossil data to date the phylogeny and performed the DDD analyses. Rita Mehta and Graham Slater helped develop the approach, provided crucial insights, and revised the manuscript. All authors read and approved the final manuscript.

Chapter 2. Law CJ, Slater G, & Mehta RS. In revision. Shared extremes by ectotherms and endotherms: body elongation in mustelids is associated with small size and reduced limbs. *Evolution*.

Graham Slater, Rita Mehta, and I conceived the study. I collected the VSI data, performed the macroevolutionary analyses, and drafted the manuscript. Rita Mehta helped collect VSI data. Graham Slater provided crucial insights on macroevolutionary methods. Rita Mehta and Graham Slater helped develop the

approach and revised the manuscript. All authors read and approved the final manuscript.

Chapter 3. Law CJ & Mehta RS. 2018. Degree of carnivory drives the evolution of sexual dimorphism in crania size and bite force in Musteloidea. *Evolution*. 72:1950–1961.

I designed the study, collected geometric morphometric data, carried out data analysis, and drafted the manuscript; Rita Mehta helped develop the approach, provided crucial insight, and revised the manuscript. Both authors read and approved the final manuscript.

Chapter 4. Law CJ, Baliga VB, Tinker MT, & Mehta RS. 2017. Asynchrony in craniomandibular development and growth in *Enhydra lutris nereis* (Carnivora: Mustelidae): Are southern sea otters born to bite? *Biological Journal of Linnean Society*. 121:420-438.

I designed the study, collected geometric morphometric data, carried out data analyses, and drafted the manuscript; Vikram Baliga helped perform data analyses; Tim Tinker collected body size data and helped perform data analyses; and Rita Mehta and Vikram Baliga helped develop the approach, provided crucial insight, and revised the manuscript. All authors read and approved the final manuscript.

Chapter 5. Law CJ, Young C, and Mehta RS. 2016. Ontogenetic scaling of theoretical bite forces in southern sea otters (*Enhydra lutris nereis*). *Physiological and Biochemical Zoology* 89:347-363.

I designed the study, performed dissections, collected data, carried out data analyses, and drafted the manuscript; Colleen Young obtained specimens and helped with dissections; Rita Mehta helped develop the approach, provided crucial insight, and revised the manuscript. All authors read and approved the final manuscript.

Introduction

Overview

The remarkable disparity in both species richness and phenotypic diversity among clades represents one of the most salient patterns across the Tree of Life. Why some clades exhibit low species diversity and morphological stasis for much of their evolutionary history whereas others have diversified into numerous species and morphological forms continues to remain a central question in evolutionary biology. While disparity may be more obvious at the macroevolutionary level, microevolution often drives these broad scale patterns. Species' genetic and phenotypic diversity varies among geographically and/or temporally isolated populations (Futuyma 1997; Thompson 2005) as well as within a single population (Bolnick et al. 2003; 2011). Although researchers have long documented that sexual dimorphism (Darwin 1871) and ontogeny (Polis 1984) contribute to phenotypic and ecological variation within a population, a growing number of researchers have recognized that even individuals within a single sex and age class exhibit intraspecific phenotypic variation that can alter ecological dynamics within a single community (Bolnick et al. 2003; 2011).

As a comparative biologist, I am interested in understanding how phenotypic variation both between and within species contributes to overall biological diversity. To examine these evolutionary processes, I take an integrative approach to examine how morphological variation affects various aspects of animal biology (Arnold 1983; Wainwright 1991; Koehl 1996). These include performance, the ability of an organism to perform ecological tasks; behavior, which determines whether an

organism chooses to use its abilities; and ecology, the interaction of an organism with its environment. Placed under a phylogenetic context, this whole organism approach helps us understand how ecomorphological mechanisms contribute to the success and survival of species across evolutionary time as well as between individuals within single populations.

I used the carnivoran superfamily Musteloidea (e.g. badgers, martens, minks, otters, raccoons, red panda, weasels, etc.) as my model clade to examine phenotypic diversity between and within species. Musteloids are species rich with 85 putative species in 33 genera. Equally impressive is their morphological and ecological diversity. Habitats occupied by members of Musteloidea include arctic tundra, tropical and temperate forests, grasslands, deserts, and aquatic habitats such as inland waterways and coastal intertidal zones (Wilson et al. 2009). Musteloids also exhibit a range of locomotor lifestyles (e.g. arboreal, cursorial, fossorial, aquatic) and diverse dietary ecologies ranging from the generalist diets of raccoons, skunks, and badgers to the specialized diets of the herbivorous red panda, hypercarnivorous weasels, and piscivorous otters (Wilson et al. 2009). In addition to great interspecific variation, musteloids also exhibit great intraspecific variation. It is well documented that different populations of a single musteloid species exhibit geographic variation in phenotypic and ecological traits (Ralls et al. 1985; Erlinge 1987; Dayan and Simberloff 1994; Suzuki et al. 2013). Various factors including climate, prey resources, and habitat use are hypothesized to contribute to these geographic variations in body size, craniodental traits, sexual dimorphism, and diet (Ralls et al.

1985; Erlinge 1987; Dayan and Simberloff 1994; Suzuki et al. 2013). In addition, single musteloid populations also exhibit variation, albeit these studies are much fewer. The greatest example is the population of southern sea otters in the Monterey Bay, which exhibit intraspecific specialization in diets as well as in tool-use behavior (Tinker et al. 2008; 2012; Fujii et al. 2015).

Dissertation Outline

In Chapters 1 and 2, I examined the influence of body shape on increased species diversification within Musteloidea. In **Chapter 1**, I tested the hypothesis that patterns of lineage diversification and phenotypic evolution in Musteloidea are consistent with adaptive radiation theory. That is, I predicted that musteloids exhibited rapidly increasing rates of diversification and phenotypic evolution at the onset of ecological opportunity. To accomplish my goals, I constructed a novel time-calibrated phylogeny of 75 musteloid species (88%) that encompasses all 33 genera by compiling a 46 mitochondrial and nuclear gene dataset and then estimating divergence times using the fossilized birth–death (FBD) model with 74 musteloid fossils. I then assessed patterns of lineage diversification using molecular- (i.e. DDD and BAMM) and fossil-based (i.e. PyRate) methods and assessed evolutionary rates of body mass and body length to determine if ecological opportunity led to early bursts in rates of phenotypic evolution. In **Chapter 2**, I tested hypotheses that some mustelid clades (i.e. weasels, polecats, martens, otters) exhibited evolutionary shifts towards more elongate body shapes, which may have served as a morphological

innovation leading to their increased species richness. To accomplish my goals, I quantified musteloid body shapes using the vertebrate shape index (VSI) (Collar et al. 2013) with osteological specimens. I then used a generalized evolutionary modeling approach (Hansen 1997; Butler and King 2004; Beaulieu et al. 2012) to explicitly test hypotheses that clades within Mustelidae exhibited evolutionary transitions towards more elongate bodies.

In **Chapter 3**, I examined how sexual selection and niche divergence influenced the evolution of sexual dimorphism in the crania of musteloids. Sexual selection is often hypothesized to have driven the evolution of sexual dimorphism (Moors 1980). Researchers, however, have also found interspecific differences in the feeding apparatus (Wiig 1986; Thom et al. 2004) and diet (Moors 1980; Birks and Dunstone 1985; Zalewski 2007; Elliott Smith et al. 2015), providing evidence that niche divergence may also be an important selective force in the evolution of sexual dimorphism in musteloids. To test these hypotheses, I used 3D geometric morphometric and generalized evolutionary modeling approaches (Hansen 1997; Butler and King 2004; Beaulieu et al. 2012) to examine how social systems (a proxy for sexual selection) and diet (a proxy for natural selection via niche divergence) correspond with the evolution of sexual dimorphism in cranial shape, cranial size, and bite force across Musteloidea.

In Chapters 4 and 5, I examined the effects of ontogeny and sexual dimorphism within a single musteloid population, the southern sea otter (*Enhydra lutris nereis*). In **Chapter 4**, I investigated the growth and development of the

southern sea otter (*Enhydra lutris nereis*) skull to examine when juveniles have reached sufficient maturity to transition to a durophagous diet and if these ontogenetic patterns differ between the sexes. To accomplish my goals, I used 2D geometric morphometrics and nonlinear modeling to quantify ontogenetic changes in skull shape and size as well as measured the rate and duration of development and growth. In **Chapter 5**, I tested the hypothesis that the scaling patterns of bite force in southern sea otters and the underlying anatomical components differ between the sexes. To test my hypothesis, I first investigated the anatomical traits that contribute to bite force generation. I then simultaneously determined the scaling patterns of theoretical bite forces and skull components across ontogeny and assessed whether these scaling patterns differed between the sexes. Last, I elucidated which of these factors are responsible for the strong allometric patterns of bite force production.

References

Arnold S.J. 1983. Morphology, performance and fitness. Amer. Zool. 23:347–361.

Beaulieu J.M., Jhwueng D.-C., Boettiger C., O'Meara B.C. 2012. Modeling stabilizing selection: Expanding the Ornstein-Uhlenbeck model of adaptive evolution. Evolution. 66:2369–2383.

Birks J.D.S., Dunstone N. 1985. Sex-related differences in the diet of the mink *Mustela vison*. Holarctic Ecology. 8:245–252.

Bolnick D.I., Amarasekare P., Araújo M.S., Bürger R., Levine J.M., Novak M., Rudolf V.H.W., Schreiber S.J., Urban M.C., Vasseur D.A. 2011. Why intraspecific trait variation matters in community ecology. 26:183–192.

Bolnick D.I., Svanbäck R., Fordyce J.A., Yang L.H. 2003. The ecology of individuals: incidence and implications of individual specialization. Am Nat. 161:1–28.

Butler M.A., King A.A. 2004. Phylogenetic comparative analysis: a modeling approach for adaptive evolution. Am Nat. 164:683–695.

Collar D.C., Reynaga C.M., Ward A.B., Mehta R.S. 2013. A revised metric for quantifying body shape in vertebrates. Zool. 116:246–257.

Darwin C. 1871. The Descent of Man and Selection in Relation to Sex. London: John Murray.

Dayan T., Simberloff D. 1994. Character displacement, sexual dimorphism, and morphological variation among British and Irish mustelids. Ecology. 75:1063–1073.

Elliott Smith E.A., Newsome S.D., Estes J.A., Tinker M.T. 2015. The cost of reproduction: differential resource specialization in female and male California sea otters. Oecologia. 178:17–29.

Erlinge S. 1987. Why do European stoats Mustela erminea not follow Bergmann's rule? Holarctic Ecology. 10:33–39.

Fujii J.A., Ralls K., Tinker M.T., Tinker M.T. 2015. Ecological drivers of variation in tool-use frequency across sea otter populations. Behav Ecol. 26:519–526.

Futuyma D.J. 1997. Evolutionary Biology. Sunderland, Massachusetts: Sinauer Associates, Inc.

Hansen T.F. 1997. Stabilizing selection and the comparative analysis of adaptation. Evolution. 51:1341–1351.

Koehl M. 1996. When does morphology matter? Annu. Rev. Ecol. Syst. 27:501–542.

Moors P.J. 1980. Sexual dimorphism in the body size of mustelids (Carnivora): the roles of food habits and breeding systems. Oikos. 34:147–158.

Polis G.A. 1984. Age Structure Component of Niche Width and Intraspecific Resource Partitioning - Can Age-Groups Function as Ecological Species. Am Nat. 123:541–564.

Ralls K., Harvey P.H., Harvey P.H. 1985. Geographic variation in size and sexual dimorphism of North American weasels. Biol J Linn Soc. 25:119–167.

Suzuki S., Peng J.-J., Chang S.-W., Chen Y.-J., Wu Y., Lin L.-K., Kimura J. 2013. Insular Variation of the Craniodental Morphology in the Siberian Weasel Mustela sibirica. J. Vet. Med. Sci. 75:575–581.

Thom M.D., Harrington L.A., Macdonald D.W. 2004. Why are American mink sexually dimorphic? A role for niche separation. Oikos. 105:525–535.

Thompson J.N. 2005. The Geographic Mosaic of Coevolution. University of Chicago Press.

Tinker M.T., Bentall G., Estes J.A. 2008. Food limitation leads to behavioral diversification and dietary specialization in sea otters. Proc Natl Acad Sci USA. 105:560–565.

Tinker M.T., Guimarães P.R. Jr, Novak M., Marquitti F.M.D., Bodkin J.L., Staedler M., Bentall G., Estes J.A. 2012. Structure and mechanism of diet specialisation: testing models of individual variation in resource use with sea otters. Ecology Letters. 15:475–483.

Wainwright P.C. 1991. Ecomorphology: experimental functional anatomy for ecological problems. Amer. Zool. 31:680–693.

Wiig Ø. 1986. Sexual dimorphism in the skull of minks *Mustela vison*, badgers *Meles meles* and otters *Lutra lutra*. Zool J Linn Soc. 87:163–179.

Wilson D.E., Mittermeier R.A., Mittermeier R.A. 2009. Handbook of the Mammals of the World. Lynx Edicions.

Zalewski A. 2007. Does size dimorphism reduce competition between sexes? The diet of male and female pine martens at local and wider geographical scales. Acta Theriol. 52:237–250.

Syst. Biol. 67(1):127–144, 2018
DOI:10.1093/sysbio/syx047

Lineage Diversity and Size Disparity in Musteloidea: Testing Patterns of Adaptive Radiation Using Molecular and Fossil-Based Methods

CHRIS J. LAW [1], GRAHAM J. SLATER [2], AND RITA S. MEHTA [1]

[1]Department of Ecology and Evolutionary Biology, Long Marine Lab, University of California, Santa Cruz, 115 McAllister Way, Santa Cruz, CA 95060, USA; and [2]Department of the Geophysical Sciences, University of Chicago, 5734 S. Ellis Avenue, Chicago, IL 60637 USA
Correspondence to be sent to: Department of Ecology and Evolutionary Biology, Long Marine Lab, University of California, Santa Cruz, 115 McAllister Way, Santa Cruz, CA 95060, USA;
E-mail: cjlaw@ucsc.edu.

Received 4 June 2015; reviews returned 18 April 2017; accepted 28 April 2017
Associate Editor: Tanja Stadler

Abstract.—Adaptive radiation is hypothesized to be a primary mechanism that drives the remarkable species diversity and morphological disparity across the Tree of Life. Tests for adaptive radiation in extant taxa are traditionally estimated from calibrated molecular phylogenies with little input from extinct taxa. With 85 putative species in 33 genera and over 400 described extinct species, the carnivoran superfamily Musteloidea is a prime candidate to investigate patterns of adaptive radiation using both extant- and fossil-based macroevolutionary methods. The species diversity and equally impressive ecological and phenotypic diversity found across Musteloidea is often attributed to two adaptive radiations coinciding with two major climate events, the Eocene–Oligocene transition and the Mid-Miocene Climate Transition. Here, we compiled a novel time-scaled phylogeny for 88% of extant musteloids and used it as a framework for testing the predictions of adaptive radiation hypotheses with respect to rates oflineage diversification and phenotypic evolution. Contrary to expectations, we found no evidence for rapid bursts oflineage diversification at the origin of Musteloidea, and further analyses of lineage diversification rates using molecular and fossil-based methods did not find associations between rates oflineage diversification and the Eocene–Oligocene transition or Mid-Miocene Climate Transition as previously hypothesized. Rather, we found support for decoupled diversification dynamics driven by increased clade carrying capacity in the branches leading to a subclade of elongate mustelids. Supporting decoupled diversification dynamics between the subclade of elongate mustelids and the ancestral musteloid regime is our finding ofincreased rates of body length evolution, but not body mass evolution, within the decoupled mustelid subclade. The lack of correspondence in rates of body mass and length evolution suggest that phenotypic evolutionary rates under a single morphological metric, even one as influential as mass, may not capture the evolution of diversity in clades that exhibit elongate body shapes. The discordance in evolutionary rates between body length and body mass along with evidence of decoupled diversification dynamics suggests that body elongation might be an innovation for the exploitation of novel Mid-Miocene resources, resulting in the radiation of some musteloids. [adaptive radiation; body size evolution; Carnivora; evolutionary rates; key innovation; lineage diversification; phylogeny.]

The remarkable disparity in both species richness and morphological diversity among clades represents one of the most salient macroevolutionary patterns across the Tree of Life. Since Darwin, many have asked why some clades exhibit low species diversity and morphological stasis for much of their evolutionary history whereas other clades diversified into numerous species and morphological forms. One mechanism theorized to drive species diversity and morphological disparity is adaptive radiation (Simpson 1955; Schluter 2000). In adaptive radiation theory, the occurrence of ecological opportunity and/or evolution of novel morphological innovation(s) create new adaptive zones. In turn, these new niches promote rapid increases in lineage diversification that coincides with increases in phenotypic disparity as colonizing lineages rapidly evolve adaptive traits that are highly correlated to their new resources (Schluter 2000). A key prediction of adaptive radiation theory is, therefore, that rapidly increasing rates of diversification and phenotypic evolution should be highest when ecology opportunity is greatest, typically early in the clade's evolutionary history (Harmon et al. 2003; Rabosky and Lovette 2008a, 2008b; Gavrilets and Losos 2009; but see Mahler et al. 2013; Hopkins and Smith 2015; Slater 2015). These rates are subsequently expected to slow down as niche space fills to capacity (Harmon et al. 2003; Rabosky and Lovette 2008b).

Rates of diversification and phenotypic evolution through time can be estimated from calibrated molecular phylogenies of extant taxa (e.g., Harmon et al. 2003; Adams et al. 2009; Tran 2014; Colombo et al. 2015). A variety of methods have been developed to quantify the processes that have shaped the evolutionary history of a clade, assess rate variation among lineages, and, more recently, investigate rate variation through time (Rabosky 2006; Rabosky and Lovette 2008b; Alfaro et al. 2009; Stadler 2011; Etienne and Haegeman 2012; Rabosky et al. 2014). Interestingly, investigation of diversification and phenotypic evolutionary rates in some vertebrate clades hypothesized to have undergone adaptive radiations—for example, cetaceans (Slater et al. 2010), ovenbirds and woodcreepers (Derryberry et al. 2011), and New World monkeys (Aristide et al. 2015)—have revealed a lack of congruence between lineage diversification and phenotypic disparity: whereas rates of phenotypic evolution show evidence for declining rates through time, lineage diversification often does not exhibit an expected early burst (Slater et al. 2010; Derryberry et al. 2011; Aristide et al. 2015). A possible

explanation for the lack of signal for an early burst of diversification is the absence offossil data in these macroevolutionary analyses. Previous studies have shown that fossil data are important in understanding macroevolutionary processes (Quental and Marshall 2010; Liow et al. 2010); however, the majority of current macroevolutionary methods rely solely on time-calibrated phylogenies of extant taxa and do not account for extinct taxa in estimations of evolutionary rates. As a result, some researchers postulate the absence of extinct taxa in these analyses may have erased signatures of early rapid diversification that remain in patterns morphological disparity (Slater et al. 2010 ; Derryberry et al. 2011; Aristide et al. 2015). Although fossil-based methods for inferring diversification dynamics exist and have recently become more prominent in the evolutionary biology community (e.g., Alroy 2014 ; Silvestro et al. 2014a), many groups of organisms lack the adequate fossil record needed to assess diversification rates through time.

With approximately 85 putative extant species in 33 genera and over 400 described extinct species, the carnivoran superfamily Musteloidea is a prime candidate clade in which to investigate patterns of adaptive radiation using both extant- and fossil-based macroevolutionary methods. Musteloid habitats encompass several biomes including the arctic tundra, tropical and temperate forests, grasslands, deserts, and aquatic habitats such as inland waterways and coastal intertidal zones (Wilson and Mittermeier 2009). Equally impressive is the great ecomorphological diversity found across Musteloidea (Fabre et al. 2013 , 2015; Dumont et al. 2015). Within each environment, musteloids exhibit diverse lifestyles, with taxa that are arboreal, fossorial, or aquatic as well as a variety of diets ranging from the generalist diets of raccoons, skunks, and badgers to the specialized diets of the herbivorous red panda, hypercarnivorous weasels, and piscivorous otters (Wilson and Mittermeier 2009). The incredible ecological and phenotypic diversity in Musteloidea is often attributed to adaptive radiation (Koepfli et al. 2008; Sato et al. 2009, 2012). Previous studies have postulated associations between the advent of ecological opportunity and rapid bursts of diversification during two distinct time periods in musteloid evolutionary history (Koepfli et al. 2008 ; Sato et al. 2009, 2012). The first putative burst of rapid diversification occurred 28–33 million years ago (Ma) right after the Eocene–Oligocene transition (33.5 Ma) and gave rise to Mephitidae (skunks and stink badgers), Ailuridae, (red panda), Procyonidae (raccoons and allies), and Mustelidae (badgers, martens, minks, otters, and weasels) (Sato et al. 2009, 2012). The second burst occurred near the root of extant Mustelidae (9.5–14 Ma), right after the Mid-Miocene Climate Transition, and gave rise to six of the eight extant subfamilies within Mustelidae (Koepfli et al. 2008). In both instances, rapid diversification closely followed major climatic events characterized by a sudden decrease in global temperatures (Zachos et al. 2008). These periods of abrupt cooling and drying resulted in a dramatic expansion of more open vegetation habitats such as grasslands and woodlands (Singh 1988; Estep et al. 2014 ; Leopold et al. 2014 ; Prothero and Berggren 2014), and, in turn, led to the diversification of rodent species (Finarelli and Badgley 2010 ; Calede et al. 2011 ; Fabre et al. 2012), which are the predominate prey of many mustelids (Wilson and Mittermeier 2009). The occurrence of ecological opportunity and rapid diversification at the roots of Musteloidea and Mustelidae led researchers to hypothesize that adaptive radiation may be the underlying process that promoted the ecological—and therefore phenotypic diversity—we observe within subsequent clades.

Although Musteloidea has qualitatively been described to exhibit two bursts of adaptive radiation (Koepfli et al. 2008 ; Sato et al. 2009, 2012), the quantitative evidence for the adaptive radiation hypotheses has yet to be investigated. Most importantly, incorporation of fossil data into current diversification analyses may help to link species with phenotypic diversification. The fossil record indicates that extinct musteloids were species-rich, and many of these groups are also hypothesized to have originated near major climate transitions; paleomustelids arose just after the Eocene–Oligocene transition (Baskin 1998 ; Finarelli 2008) and leptarctines originated near the Mid-Miocene Climate Transition (Bever and Zakrzewski 2009). Thus, how paleomustelids, leptarctinae, and other extinct musteloids may have contributed to patterns oflineage diversification remains unknown. In this study, we tested the hypothesis that patterns oflineage diversification and phenotypic evolution in Musteloidea are consistent with adaptive radiation theory. To accomplish our goals, we first constructed a novel time-calibrated phylogeny of 75 musteloid species (88%) that encompasses all 33 genera by compiling a 46 mitochondrial and nuclear gene dataset and then estimating divergence times using the fossilized birth–death (FBD) model with 74 musteloid fossils. We then tested for quantitative signatures of adaptive radiation within Musteloidea. We first examined decoupled diversification dynamics within Musteloidea using the program DDD. We then assessed patterns oflineage diversification using both molecular-based methods with extant taxa in the program BAMM as well as fossil-based methods with 453 extinct and extant musteloids (total of 2168 specimens) in the program PyRate. Lastly, to determine if ecological opportunity led to early bursts in rates of phenotypic evolution, we assessed evolutionary rates of body mass and body length in BAMM. We examined body size because it scales with many traits associated with the ecomorphology of species.

Materials and Methods

Taxon Sampling

Previous musteloid phylogenetic studies primarily focused within individual families and genera,

particularly within Mustelidae (e.g., Koepfli and Wayne 1998; Koepfli et al. 2007 ; Fulton and Strobeck 2007 ; Koepfli et al. 2008 ; Harding and Smith 2009 ; Sato et al. 2009). Investigation of the phylogenetics of Musteloidea has focused on resolving relationships among the four families, and the largest musteloid phylogeny to date contains approximately 52% of extant musteloid species (Sato et al. 2012). To reconstruct a more comprehensive phylogeny, we downloaded GenBank sequence data from these previous studies, the majority of which came from Koepfli et al. (2008), Yu et al. (2011), and Sato et al. (2012) (see Supplementary Table S1 available at Dryad at http://dx.doi.org/10.5061/dryad.nj1bp for complete reference list). We obtained 46 genes (4 mitochondrial and 42 nuclear genes) from 75 of the 85 putative musteloid species (88.2% of musteloid species), representing all 33 musteloid genera (Wilson and Mittermeier 2009). Our dataset accounts for 8 of the 12 mephitids, 13 of the 14 procyonids, 53 of the 58 mustelids, and the single ailurid species (Supplementary Table S1 available on Dryad; see Supplementary Table S2 available on Dryad for missing species). The ursid Ursus arctos and phocid Phoca vitulina were chosen as outgroups based on previous studies indicating that Ursidae and Pinnipedia are the closest extant clades to Musteloidea (Flynn et al. 2005 ; Eizirik et al. 2010). The final 46-gene dataset consists of 34,857 base pairs (bps) with an average of 767 bps per gene (range 194–1419), and each gene was represented by an average of 40 species (range 15–76) (Supplementary Table S3 available on Dryad). Total percentage of missing genes was 48.7% (1680 of 3450).

Phylogenetic Analyses

We reconstructed the musteloid phylogeny using a supermatrix approach. Prior to phylogenetic analyses, the individual 46 gene datasets (Supplementary Table S3 available on Dryad) were aligned with MUSCLE 3.8 (Edgar 2004) under default settings and edited manually where needed using Mesquite (Maddison and Maddison 2011). Alignments were also trimmed to start and end with the first and third codon positions, and protein translations of protein coding sequences were checked for stop codons and frameshift mutations as well as the presence of nuclear mitochondrial DNA (numts) in the mitochondrial dataset. To ensure no mislabeled sequences, we constructed individual gene trees using MrBayes v. 3.2.2 (Ronquist et al. 2012) on the CIPRES (Cyberinfrastructure for Phylogenetic Research at the UC San Diego Supercomputer Center) Portal (Miller et al. 2010) using four runs of one chain, 10 million Markov Chain Monte Carlo (MCMC) generations sampled every 1000 generations, and the first 25% of samples discarded as burnin. We found no mislabeled sequences. We selected a 14 partition scheme using PartitionFinder (Lanfear et al. 2012) under the default settings with Bayesian information criterion scores and a greedy search and allowed each partition to have its own independent substitution model (Supplementary Table S4 available on Dryad).

The 46 individual gene datasets were concatenated and analyzed using maximum likelihood (ML) and Bayesian inference (BI) methods. ML analyses were performed in RAxML 8.0.9 (Stamatakis 2014) as a 14 partitioned dataset under the General Time Reversible + Gamma (GTR + G) model. Nonparametric bootstrap values were estimated using 1000 pseudo replicates under the same model conditions. BI analyses were conducted using MrBayes 3.2.2 (Ronquist et al. 2012) on the CIPRES Portal (Miller et al. 2010). Appropriate evolutionary models were applied to each respective partition (Supplementary Table S4 available on Dryad). The data partitions were unlinked for parameter estimations and ran on 4 parallel MCMC chains (one cold, three heated) for 2 independent sets at 10 million generations per set, sampling trees every 1000 generations. Convergence of these values and effective sample sizes was assessed in the program Tracer, 1.6 (Rambaut et al. 2014). Approximately 25% of sampled trees were discarded as burn-in, and the remaining trees were used to construct a majority rule consensus tree.

We also estimated species trees using supertree and multispecies coalescent methods. For the supertree analysis, a matrix representation with parsimony (MRP) matrix (Ragan 1992) was then compiled from the 46 Bayesian gene trees (from above) in the program Clann 3.2.3 (Creevey and McInerney 2005). With the MRP matrix, reconstruction of the supertree phylogeny was performed in PAUP* 4.0b10 (Swofford 2003) using a parsimony-based heuristic search with tree bisection and reconnection. For the coalescent analysis, we used ASTRAL-II v4.7.8 with 100 replicates of multilocus bootstrapping (Mirarab et al. 2014).

Estimation of Divergence Times

We estimated musteloid divergence times using the FBD tree process prior (Heath et al. 2014), extended to allow for sampled ancestors (Gavryushkina et al. 2014) as implemented in BEAST v2.3.2 (Bouckaert et al. 2014). The use of this model circumvents the need to define arbitrary age priors on nodes while maximizing the amount offossil data that can be used. We compiled age ranges of 74 fossil musteloids from the literature (Appendix 1). Only fossil taxa that have been subject to formal phylogenetic analysis and could be robustly placed within a musteloid clade were included in our dataset. Our final dataset consisted of 4 stem arctoids, 4 stem musteloids, 9 stem mephitids, 8 ailurids, 16 procyonids, 7 oligobunines, 11 leptarctines, and 13 neomustelids. For each fossil, we also surveyed the literature to identify its stratigraphic range. Fossil ages were assigned a uniform distribution for their stratigraphic range, spanning age uncertainty in the case of taxa known from a single fossil or from first and last appearance dates in the case of taxa known from multiple localities.

We used an uncorrelated lognormal relaxed molecular clock model with exponential prior distributions on the mean and standard deviation of the clock rate. The same 14 partition scheme (Supplementary Table S4 available on Dryad) was used for the molecular data, and we allowed each partition to have its own independent substitution model. Three parameters are used in the MCMC optimization under the FBD model: net diversification rate, turnover rate, and fossil sampling rate. Preliminary diversification rate analyses suggested musteloids exhibit low-diversification rates; thus we used an exponential prior distribution with a mean of 1 for the net diversification rate parameter and uniform prior distributions on the range [0,1] for turnover rate and fossil sampling proportion. Lastly, we accounted for incomplete taxon sampling by setting the parameter ρ (Rho) to 0.88 for the 88% of extant species sampled.

Four separate MCMC analyses with 150 million generations sampled every 15,000 generations were run to provide independent posterior probability distribution estimations of model parameters and node ages, and a random starting tree was used for each analysis. Convergence of parameters and effective sample sizes were assessed in the program Tracer, 1.6 (Rambaut et al. 2014); all effective samples sizes were >200 after discarding the first 35% of the combined samples as burn-in. Sampled trees from the four analyses were combined using LogCombiner v2.2.1 (http://beast.bio.ed.ac.uk/LogCombiner), pruned to remove all fossil taxa, and summarized as a maximum clade credibility (MCC) tree using TreeAnnotator v2.2.1 (http://beast.bio.ed.ac.uk/TreeAnnotator). The resulting posterior probabilities and corresponding 95% credible intervals for the mean divergence time estimates were visualized using the program FigTree v1.40 (http://beast.bio.ed.ac.uk/FigTree).

Estimation of Species Diversification

To test for temporally distinct adaptive radiations within Musteloidea, we employed the likelihood-based approach developed by (Etienne et al. 2012 ; Etienne and Haegeman 2012), implemented in the R library DDD v 3.2. We compared the fit of a suite of decoupled diversity dependent models against null models assuming either a time-homogenous constant rates birth–death process (CR0) or a diversity dependent process in which a single carrying capacity operated over musteloid history with diversity dependent speciation and constant extinction (CR1). The first set of alternative models assumes a shift in carrying capacity and/or rates operating across musteloid phylogeny at some time t in the past. We fit four variants of this process in which (i) only carrying capacities varied before and after t (SR1), (ii) carrying capacities and speciation rates varied before and after time t (SR2), (iii) carrying capacities and extinction rates varied before and after time t (SR3), and (iv) all parameters varied before and after time t (SR4). The shift point t was itselfinferred from the data in all cases. The second set of alternative models that we considered tested for shifts in diversification parameters associated with clade-specific key innovations (KI models). Based on analyses of body length evolutionary rates (see below), we identified two putative branches within which key innovations may have evolved; the base of Mustelidae (KI_M) and in the branch leading to the most recent common ancestor of Ictonychinae, Mustelinae and Lutrinae (KI_IML). We further tested for decoupled dynamics in the branch leading to the most recent common ancestor of this clade plus Helictinae plus Martinae (KI_M2), as this is the most inclusive clade exhibiting dramatic body elongation. Missing species were assigned as appropriate to the clade to which they belong for all analyses and model fitting was conditioned on nonextinction of the phylogeny (Supplementary Table S2 available on Dryad). We fit the same four variants of the KI models as for the SR models and assessed relative model support using Akaike weights (w_A).

Etienne et al. (2016) showed that the use of Akaike weights for model choice may be inappropriate when comparing the fit of diversity dependent and constant rates model as the likelihood ratio (LR) statistic is often not chi-square distributed. They suggested instead to use a parametric bootstrap procedure to determine the appropriate value for accepting or rejecting diversity dependence at a specified level of significance. Although such a procedure is not appropriate for decoupled models as they are not nested within either a constant rates or single diversity dependent process (R. Etienne pers. comm), we can still use the parametric bootstrap procedure to more generally evaluate the reliability of model selection when comparing constant rates and diversity dependent models. Following Etienne et al. (2016), we used 1000 parametric bootstrap replicates to assess type I error, the appropriate critical value of the LR statistic at $\alpha = 0.05$, and power of the test for diversity dependence.

We also estimated the rates of diversification across the musteloid phylogeny using BAMM v2.5.0 (Rabosky et al. 2013; Rabosky 2014). BAMM uses a reversible jump Markov Chain Monte Carlo (RJMCMC) to explore candidate models oflineage diversification and trait evolution as well as quantify heterogeneity in evolutionary rates (Rabosky 2014). We performed 4 independent BAMM runs of 10 million generations on our MCC musteloid phylogeny from BEAST, sampling every 1000 generations and with priors chosen using the function setBAMMpriors (Rabosky et al. 2014). We assessed the convergence of the BAMM run using the R (R Core Team 2015) package BAMMtools v2.0 (Rabosky et al. 2014) and used the CODA library to check the effective sample sizes oflog-likelihoods and the number of shift events present in each sample; all parameters had effective sample sizes >1000. We accounted for incomplete taxon sampling using the analytical correction implemented in BAMM (Supplementary Table S2 available on Dryad). We note that some aspects of BAMM have recently been criticized (Moore et al. 2016 , but see Rabosky et al. 2017);

nevertheless, we cautiously retain our analyses here for comparative purposes, noting that they are one of several diversification rate analyses employed.

To incorporate fossil data in our analyses, we estimated lineage diversification rates from the fossil record using a birth–death MCMC (BDMCMC) analysis implemented in the program PyRate v. 0.604 (Silvestro et al. 2014a , 2014b). PyRate simultaneously estimates the speciation and extinction rates for each species using a birth-death process. The birth-death process uses each species' temporal distribution in the fossil record to model the diversification dynamics by exploring alternative diversification models with different number of rate shifts that may underlie changes in diversity (Silvestro et al. 2014a, 2014b). We obtained musteloid fossil data from the Paleobiology Database, Fossilworks, and NOW Database (accessed 9/02/15) and included only fossils that were identified to the species level. Our complete fossil dataset comprised of 453 species (total of 2168 specimens), of which 404 are extinct (Supplementary Table S5 available on Dryad). We then used the R function extract.ages from the PyRate package to randomly resample the age offossil occurrences 10 times. We assumed independent preservation rates for each epoch. Each replicate was analyzed independently for 15 million generations with the number of extant species set to 85 using Python 2.7.6 (python.org). Convergence of the BDMCMC sample and effective sample sizes was assessed in the program Tracer, 1.6 (Rambaut et al. 2014), and mean diversification rates through time were estimated after discarding the first 25% of the logged rate estimates as burn-in and combining the remaining samples across all 10 replicates. We also performed separate PyRate analyses for each of the major families: Mephitidae, Ailuridae, Procyonidae, and Neomustelidae. We did not include paleomustelids as the phylogenetic placement of the majority of these taxa is unknown. We used the same procedure as above.

We also plotted species richness of all putative extinct and extant musteloids using the same fossil dataset obtained from the Paleobiology Database, Fossilworks, and NOW Database as well as extant musteloids not represented in the fossil record. The combined database was pruned to exclude taxa that could not be placed within the taxonomic groups Mephitidae, Ailuridae, Procyonidae, Paleomustelidae, and Neomustelidae. Our complete dataset comprised of 447 putative musteloids (40 mephitids, 21 ailurids, 46 procyonids, 46 paleomustelids, and 294 neomustelids). We used the R package Paleotree (Bapst 2012) to calculate species richness within each taxonomic group over the past 36 Ma in 1 Ma intervals.

Lastly, we used PyRateContinuous to examine whether evolutionary (speciation and extinction) rates correlate with changes in clade diversity, suggesting diversity dependence, or with changes in global temperature. PyRateContinuous uses a birth–death model to quantify correlation parameters between time-varying evolutionary rates with a time continuous variable such as the clade's own diversity or temperature (Silvestro et al. 2015). For each birth–death model—the diversity-dependent and temperature-dependent models—we discarded the first 25% of the logged rate estimates as burn-in combined the remaining samples across the 10 replicates, and ran each analysis independently for 1.25 million MCMC iterations with sampling frequency of 1000. For the temperature-dependent model, we used global temperature data derived from stable isotope proxies (Zachos et al. 2008) and rescaled for analyses in PyRate (Silvestro et al. 2015). We used Tracer, 1.6 (Rambaut et al. 2014) to examine the mean values and 95% HPD (highest posterior density) intervals of the posterior samples of the parameters. Following Silvestro et al. (2015), we considered the correlation to be statistically significant if 0 was not within the 95% HPD of the correlation parameter. We also used PyRateContinuous to examine if there was a shift in correlation parameters before and after the Mid-Miocene Climate Transition.

Estimation of Phenotypic Evolutionary Rates

It is a basic biological phenomenon that several ecological, physiological, and morphological traits scale with size (Schmidt-Nielsen 1984 ; LaBarbera 1989). Previous investigations of rates of phenotypic evolution in mammals have therefore used either body length or body mass as proxies for organismal size (Slater et al. 2010; Wilson et al. 2012 ; Aristide et al. 2015). Since both characters were readily attainable in the literature, we used BAMM to test for variation in rates of phenotypic evolution with both body size metrics as proxies for musteloid ecomorphology. We compiled the mean adult body length—excluding the tail length—and mean adult body mass for each species in our phylogeny and log-transformed the measurements prior to analysis (Supplementary Table S6 available on Dryad). Mean body sizes rather than maximum sizes were used to limit the effects of outliers and/or misreported measurements. Although most species of musteloids exhibit sexual dimorphism, we did not test body size rates between males and females because body size measurements based on sex are scarce in the literature. We performed 4 independent BAMM runs on our MCC musteloid phylogeny, with 10 million generations sampling every 1000 generations, and assessed convergence of the BAMM run as described above. Again, we accounted for incomplete taxon sampling using the analytical correction implemented in BAMM.

Results

Phylogenetic Analyses and Estimation of Divergence Times

Supermatrix-based phylogenetic analyses with ML and BI methods resulted in identical topologies. We recovered a successive sister group relationship of Mephitidae (Node 1) and Ailuridae (Node 9), to a clade (Node 10) consisting of Procyonidae and Mustelidae

(Fig. 1; Supplementary Text and Supplementary Table S7 available on Dryad). Species tree estimations using MRP and coalescent-based methods revealed similar topologies as the supermatrix approaches with the exception of the topological placement of some mustelid subfamilies (Appendix 2; Supplementary Fig. S1 available on Dryad).

Our time-tree estimated using the FBD tree prior with 74 fossil taxa infers that the initial radiation of extant musteloid families (the basal-most nodes of the extant sample) occurred during a ~3 million year time interval (from 31.21 to 28.09 Ma) beginning in the Early Oligocene and continuing into the Late Oligocene (Fig. 2; Supplementary Fig. S2 and Supplementary Table S7 available on Dryad). When attempting to summarize our results as a MCC tree, we found that pruning all fossil taxa prior to identifying the MCC tree resulted in unconventional but weakly supported (posterior probability = 0.69) higher level branching pattern, where Mephitidae and Ailuridae form a sister group, with Mephitidae diverging from Ailuridae around 28.09 Ma (node 9; 95% HPD, 24.30–32.15 Ma). Pruning fossils after finding the MCC tree resulted in the traditional higher level relationships of (Mephitidae, (Ailuridae, (Procyonidae, Mustelidae))); however, the placement offossil taxa in our posterior sample of trees is somewhat arbitrary as we did not include morphological data in our analyses. We therefore focus our discussion on the results generated using the MCC tree recovered after pruning fossils from input trees, despite its unconventional higher level branching order. Reassuringly, diversification analyses using both time trees displayed identical results, suggesting that this minor topological distinction does not greatly impact macroevolutionary inferences. Regardless of the position of Ailuridae, we infer that Procyonidae and Mustelidae diverged from each other around 28.75 Ma (node 10; 95% HPD, 25.71–32.12 Ma) during the Late Oligocene.

Diversification Rates Through Time

Comparison of constant rates and simple diversity dependent diversification models to those allowing for decoupled diversification dynamics yielded strong support (~85% of w_A) for a decoupling of the diversification process along the branch leading to Helictidinae, Guloninae, Ictonychinae, Mustelinae and Lutrinae (KI_M2 models; Table 1). The best-fitting models, receiving ~27 and ~31 % of weight, respectively, suggest a slightly larger carrying capacity for the decoupled sub-clade than for the main clade (56 vs. 32 species) with no change in intrinsic speciation or extinction rates, or else a much larger carrying capacity (~70 species) for the sub-clade coupled with a shift in extinction rates from 0.15 to 0.01. Key innovation models associated with crown Mustelidae (KI_M) or Ictonychinae, Mustelinae and Lutrinae (KI_IML) received negligible support (<5% w_A), as did simple homogeneous or clade-wide shift models. Diversity dependence with a single K is not significantly preferred over a constant rates process using a classical LR test based on the chi-square distribution with one degree offreedom (LR statistic = 0.088, P = 0.77) or AIC (Akaike information criterion) (w_A [constant rates]) = 0.72). Parametric bootstrapping yields a critical value for significance at α = 0.05 level of 5.47, some 1.4 times larger than the critical value of 3.84 implied by a χ^2 test (Fig. 3a). This increases the explanatory power of the constant rates process (P = 0.96) and suggests that model selection based on AIC may be inappropriate (type I error rate using classical (likelihood ratio test likelihood r = 0.11). However, parametric bootstrapping under the single K diversity dependent model also shows that power to detect a diversity dependent process of the magnitude implied by the musteloid data is very low (power = 0.1; Fig. 3b).

Mean net diversification rates inferred from BAMM analyses are broadly congruent across families: Mephitidae = 0.138 lineages/lineage million years (95% HPD, 0.106–0.169 lineages/lineage million years), Procyonidae = 0.138 lineages/lineage million years (95% HPD, 0.106–0.169 lineages/lineage million years), and Mustelidae = 0.143 lineages/lineage million years (95% HPD, 0.114–0.175 lineages/lineage million years). The rate of diversification in Mustelidae is slightly higher than the background musteloid rate, but 99.3% of the samples from the posterior distribution are assigned to just one rate configuration with no indication of a rate shift (Fig. 4a). Contour plots of branch specific diversification rates and plots of clade specific rates through time indicate that diversification rates have tended to increase slightly through the past 31.2 Ma to the present, from 0.101 lineages/lineage million years to 0.145 lineages/lineage million years. Mean net diversification for all of Musteloidea is 0.132 lineages/lineage million years (95% HPD, 0.089–0.174 lineages/lineage million years). Speciation rate and extinction rate for all of Musteloidea are 0.15 lineages/lineage million years (95% HPD, 0.103–0.190 lineages/lineage million years) and 0.014 lineages/lineage million years (95% HPD, 0.001–0.043 lineages/lineage million years), respectively (Fig. 5a). These results are consistent across the pruned-before (Fig. 4) and pruned-after (Supplementary Fig. S3 available on Dryad) trees.

Paleontological estimates of speciation and extinction rates derived from 2168 fossil occurrences indicate a relatively fast net diversification rate for musteloids throughout the Oligocene and the earliest Miocene due to a speciation rate (0.713 lineages/lineage million years, 95% HSD, 0.506–1.001 lineages/lineage million years) that is almost double the extinction rate (0.417 lineages/lineage million years, 95% HSD, 0.259–0.696 lineages/lineage million years) (Fig. 5b). At approximately 19–16 Ma, net diversification rate dramatically decreased to almost 0 lineages/lineage million years (0.020 lineages/lineage million years, 95% HSD, −0.094–0.153 lineages/lineage million years) due to a sudden slowdown in speciation rate just

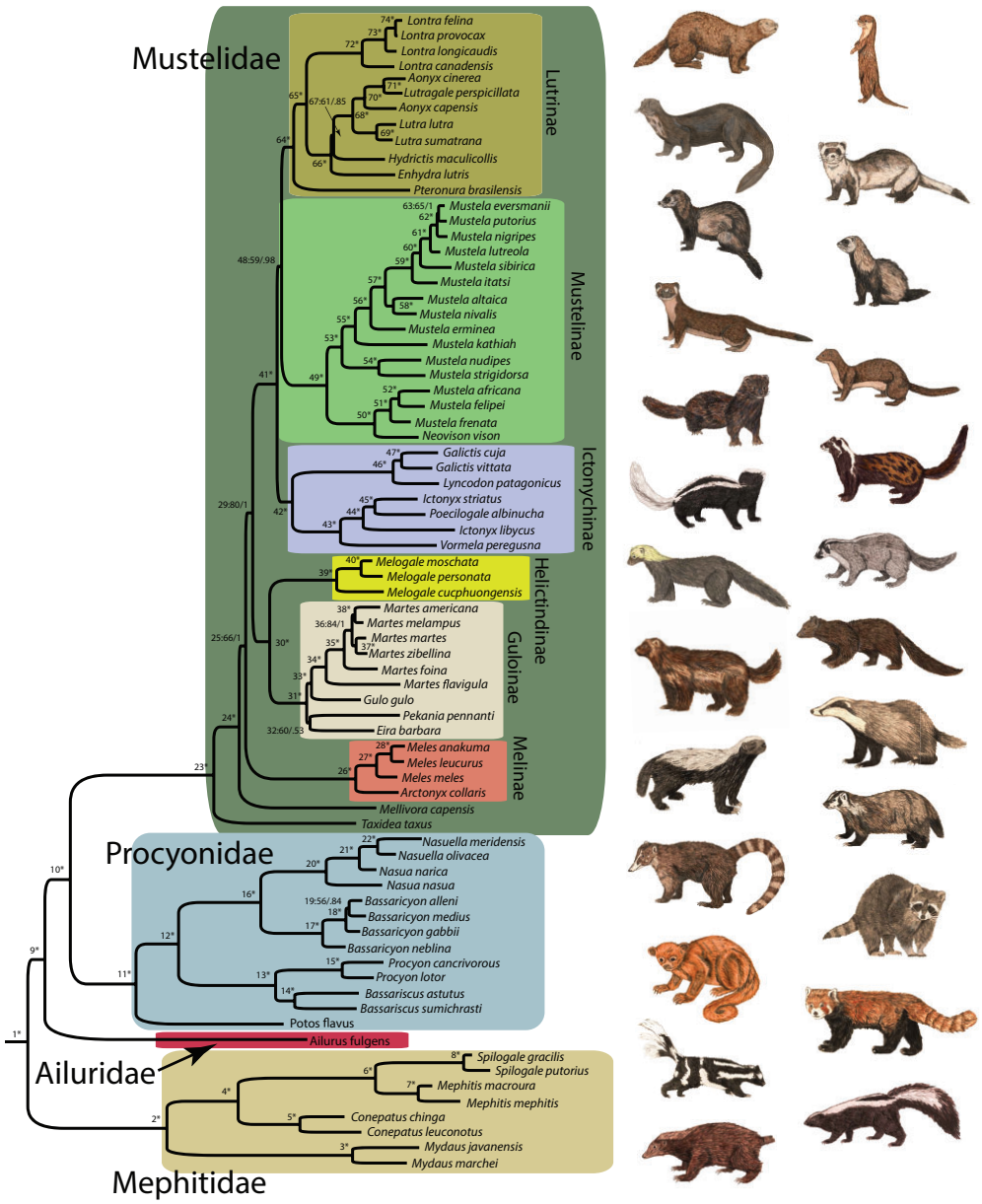

FIGURE 1. Majority rule consensus trees of Musteloidea from Bayesian inference of combined molecular data. Nodes are numbered (1–74), followed by bootstrap support (BS) values from maximum likelihood and posterior probabilities (PP) from Bayesian inference. Support values are in the following order: BS/PP. An asterisk (*) indicates >90% for BS and >0.95 for PP for the node. Nodal support is also presented in Supplementary Table S7 available on Dryad. Outgroup taxa were pruned from the tree.

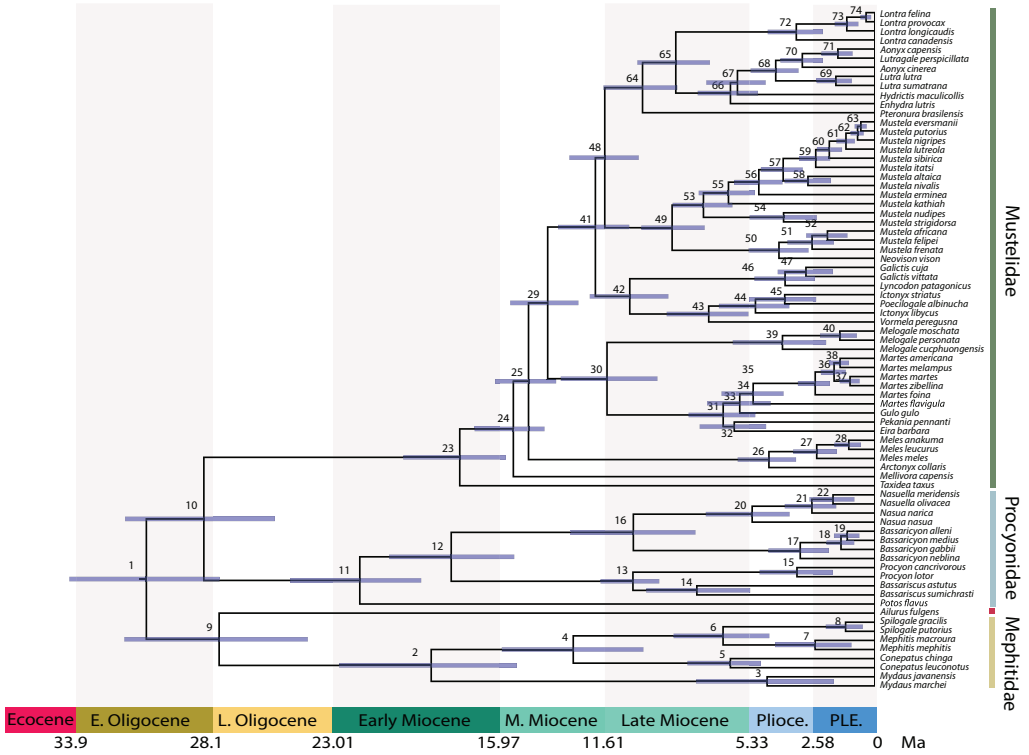

FIGURE 2. Time-calibrated phylogenetic tree of Musteloidea. Mean divergence times estimated using a relaxed molecular clock model on the complete 46 gene dataset with 74 fossil priors. Blue bars across nodes indicate 95% HPD intervals around the mean divergence time estimates. Posterior estimates of mean and 95% HPD of divergence times are presented in Supplementary Table S7 available on Dryad. Nodes are numbered (1–74, same as Fig. 1). Outgroup taxa were pruned from the tree and geological time scale is shown below the tree.

before the onset of the Mid-Miocene Climate Transition. Most of the remaining Miocene is characterized by relatively stable and balanced speciation and extinction rates. Both speciation and extinction rates rapidly increased during the Late Miocene and into the Pliocene, resulting in a brief decrease in net diversification rate. By the late Pliocene, speciation and extinction rates stabilized and net diversification rate returned to near 0 lineages/lineage million years.

Similar to the BAMM results, mean net diversification rates inferred from our PyRate analyses using fossil data are broadly congruent across families: Mephitidae = 0.153 lineages/lineage million years (95% HPD, −0.241 to 0.545 lineages/lineage million years), Ailuridae = 0.009 lineages/lineage million years (95% HPD, −0.223 to 0.232 lineages/lineage million years), Procyonidae = 0.112 lineages/lineage million years (95% HPD, −0.205 to 0.413 lineages/lineage million years), and Neomustelidae = 0.152 lineages/lineage million years (95% HPD, −0.066 to 0.373 lineages/lineage million years). Diversification rates for Mephitidae, Ailuridae, and Procyonidae were relatively constant through time (Fig. 6). Neomustelids, in contrast, exhibited similar diversification rate patterns when compared to diversification patterns of the whole musteloid clade. Net diversification rate dramatically decreased to 0.041 lineages/lineage million years (95% HSD, −0.115 to 0.209 lineages/lineage million years) around 19–16 Ma. Speciation and extinction rates rapidly increased during the Late Miocene and into the Pliocene, resulting in a brief decrease in net diversification rate. Net diversification rate returned to near 0 lineages/lineage million years by the late Pliocene.

Total musteloid species richness continued to increase over the past 37 Ma based on plots offossil diversity through time (Fig. 7). Closer examination of individual musteloid clades reveals that neomustelids have dominated total musteloid species richness since ~20 Ma, when they replaced paleomustelids as the most numerically abundant clade (Fig. 7a). Procyonid richness

TABLE 1. Parameter estimates (speciation rate [λ], extinction rate [μ], clade carrying capacity [K]) and model support (log likelihood [lnL] values, ΔAIC scores, Akaike weights [wA]) for constant rate (CR) and diversity-dependent models with shifts in clade-wide (SR) or clade-specific key innovation related (KI) carry capacities

Model	λ_1	μ_1	K_1	λ_2	μ_2	K_2	t_{shift}	LnL	df	AIC	ΔAIC	w_A
CR0	0.17	0.04	NA	NA	NA	NA	NA	– 218.39	2	440.78	13.60	<0.01
CR1	0.19	0.06	366.24	NA	NA	NA	NA	– 218.35	3	442.7	15.52	<0.01
SR1	0.24	0.04	37.17	λ_1	μ_1	178.95	6.51	– 216.16	5	442.32	15.14	<0.01
SR2	0.18	0.05	54.45	0.48	μ_1	96.38	6.51	– 213.42	6	438.84	11.66	<0.01
SR3	0.47	0.17	27.5	0.47	0.04	97.63	6.51	– 210.94	6	433.88	6.70	0.01
SR4	0.33	0.12	25.04	λ_1	μ_1	111.91	6.51	– 213.08	7	440.16	12.98	<0.01
KI1_M	0.52	0.16	25.71	0.52	μ_1	61.45	17.79	– 210.78	5	431.56	4.38	0.03
KI2_M	1.1	0.17	25.96	λ_1	0.17	61.43	18.15	– 210.38	6	432.76	5.58	0.02
KI3_M	0.47	0.17	26.01	0.47	0.12	63.8	17.83	– 210.54	6	433.08	5.90	0.02
KI4_M	1.16	0.2	26.28	λ_1	μ_1	109.38	18.15	– 209.14	7	432.28	5.10	0.02
KI1_M2	0.55	0.15	31.49	0.55	μ_1	55.89	14.02	– 208.73	5	427.46	0.28	0.27
KI2_M2	0.38	0.14	32.27	λ_1	0.14	55.66	14.03	– 208.33	6	428.66	1.48	0.15
KI3_M2	0.38	0.15	32.56	0.38	0.01	70.16	14.02	– 207.59	6	427.18	0.00	0.31
KI4_M2	0.46	0.17	32.27	λ_1	μ_1	73.32	14.02	– 207.47	7	428.94	1.76	0.13
KI1_IML	0.67	0.21	45.16	0.67	μ_1	38.39	11.98	– 212.56	5	435.12	7.94	0.01
KI2_IML	0.34	0.16	49.2	λ_1	0.16	37.39	11.98	– 210.91	6	433.82	6.64	0.01
KI3_IML	0.39	0.19	47.64	0.39	0	47.76	11.98	– 210.21	6	432.42	5.24	0.02
KI4_IML	0.42	0.19	47.32	0.39	0	47.76	11.98	– 210.2	7	434.4	7.22	0.01

Note: See text for model names.

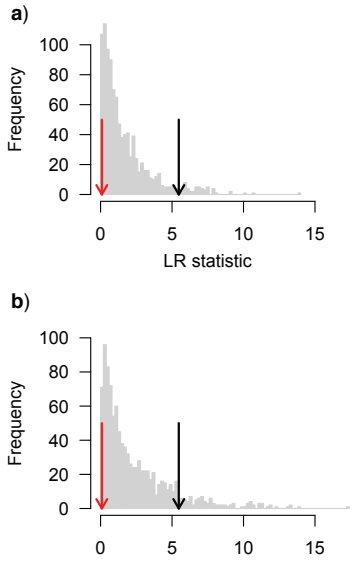

FIGURE 3. Parametric bootstrapping of diversification rate models. (a) The distribution of LR statistics comparing the fit of CR1 to CR0 when CR0 is the true model shows that the critical value for rejecting CR0 at the $\alpha = 0.05$ level is larger than implied by a chi-squared distribution with one degree offreedom, and further increases confidence in rejecting a diversity dependent process. However, (b) shows that power to detect a true diversity dependent process is, in this case, also low. In both plots, the red/dark grey arrow shows the empirically derived LR statistic while the black arrow shows the critical value required to reject the null constant rates model derived from parametric bootstrapping.

has been relatively stable since the Mid-Miocene Climate Transition and mephitid richness leveled off around 10 Ma (Fig. 7b,d). Furthermore, ailurid richness decreased (Fig. 7c) whereas paleomustelids became extinct by 6 Ma (Fig. 7a).

Clade diversity is negatively correlated with speciation rate (– 0.010, 95% HPD – 0.016 to – 0.004) but is not significantly correlated with extinction rate (0.005, 95% HPD – 0.001 to 0.011). Global temperature was also negatively correlated with speciation rate (– 0.0781, 95% HPD – 0.122 to 0.041) and with extinction rate (– 0.129, 95% HPD – 0.170 to – 0.088). Correlations with global temperature are driven by the last 13.65 Ma: from the root age to 13.65 Ma, global temperature is not correlated with speciation rate (– 0.585, 95% HPD – 2.230 to – 0.818) or extinction rate (– 0.965, 95% HPD – 2.571 to – 0.782), whereas from 13.65 Ma to the present, global temperature is negatively correlated with speciation rate (– 2.722, 95% HPD – 4.135 to – 1.526) and extinction rate (– 2.371, 95% HPD – 3.746 to – 1.130). The negative correlation found between clade diversity and speciation rate remains the same in both time periods.

Phenotypic Evolution Rate Through Time

Using BAMM, we recover seven distinct rate shift configurations for body length, of which three configurations account for the majority (f = 0.84) of the posterior probability of the data (Fig. 8b–d). The first shift configuration (f = 0.35) suggests a single rate shift at the node leading to the diversification of Ictonychinae, Mustelinae, and Lutrinae (node 41; Fig. 8b), the second shift configuration (f = 0.33) suggests that there are no significant shifts in phenotypic

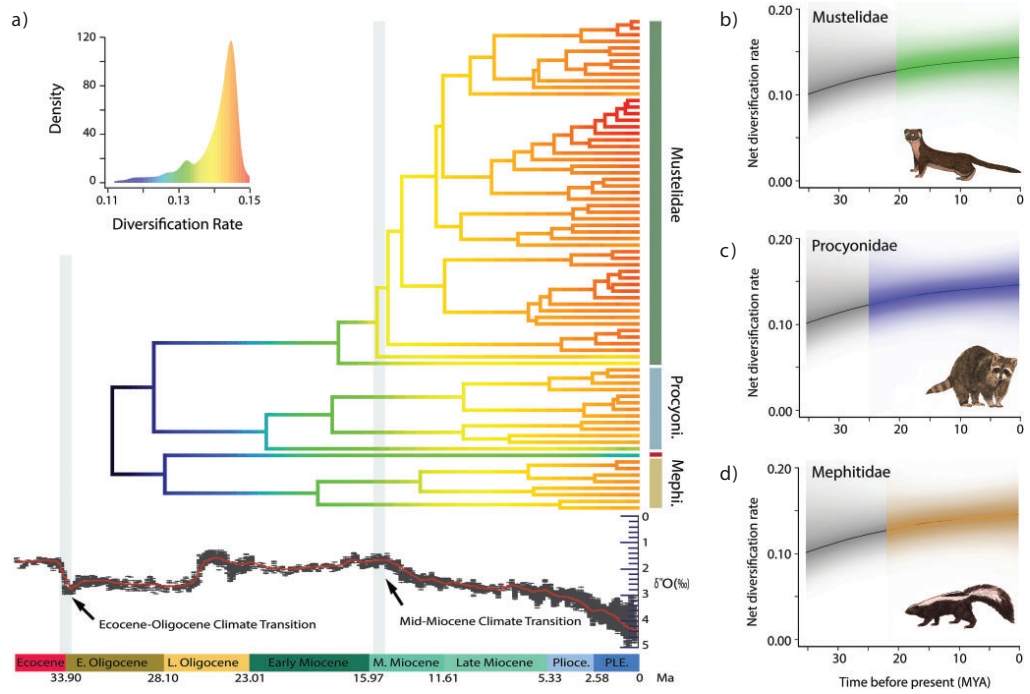

FIGURE 4. Lineage diversification rates through time. a) Phylorate plot oflineage diversification based on the "pruned-before" MCC phylogeny. Colors at each point in time along the branches of the phylorate plot denote instantaneous rate of diversification. Warmer/lighter colors (red) indicate faster rates and cooler/darker colors (blue) indicate slower rates. Below the phylorate plot is the global deep-sea oxygen isotope records (modified from Zachos et al. 2008). These records indicate a rapid decrease in global temperatures following the Eocene–Oligocene Transition and the Mid-Miocene Climate Transition (Zachos et al. 2008), giving rise to more open vegetation habitats such as grasslands and woodlands (Singh 1988; Prothero and Berggren 2014; Leopold et al. 2014). However, the lack of rate shifts suggests that there are no significant increases in diversification rates after these climate events. b–d) Diversification-through-time plots depicting family-specific net diversification trajecto ries computed from the joint posterior density of macroevolutionary rate parameters in BAMM. The black lines denote the background diversification rate (the rate of all musteloids minus the rate of each respective family). Shading intensity of the colored lines indicate the 5% through 95% Bayesian credible regions on the distribution of rates at any point in time for Mustelidae (b), Procyonidae (c), and Mephitidae (d). The black lines denote the mean background diversification rate-through-time (the rate of all musteloids minus the rate of each respective family), and the grayscale shading illustrates the 95% credible interval of the distribution of background rates through time.

evolutionary rate across the entire phylogeny (Fig. 8c), and the third shift configuration (f = 0.16) suggests a single shift ofincreased phenotypic evolutionary rate at the root of Mustelidae (node 23; Fig. 8d). Overall, our BAMM analyses inferred a general pattern ofincreased rates of body length evolution within Mustelidae after the Mid-Miocene Climate Transition followed by a slowdown in evolutionary rates (Figs. 8 and 9a; Supplementary Fig. S4 available on Dryad). Mephitidae and Procyonidae also exhibited a slowdown in evolutionary rates toward to the present but did not exhibit an inferred rate shift.

We found no shifts in rates of body mass evolution (Supplementary Fig. S5 available on Dryad). We did, however, observe a general slowdown in body mass evolutionary rate through time.

DISCUSSION

We compiled a novel time-scaled phylogeny for 88% of extant musteloids and a database of occurrences for fossil musteloids to examine if rates oflineage diversification and phenotypic evolution in this clade followed patterns predicted under adaptive radiation theory. Contrary to expectations linking diversification to ecological opportunity, we found no association between changes in rates oflineage diversification and the Eocene–Oligocene transition or Mid-Miocene Climate Transition as previously hypothesized by Koepfli et al. (2008) and Sato et al. (2009, 2012). Nevertheless, analyses of phenotypic evolutionary rates help to shed some light on musteloid diversification dynamics through time, and explicit modeling of decoupled diversity-dependent dynamics informed by these analyses results in a more

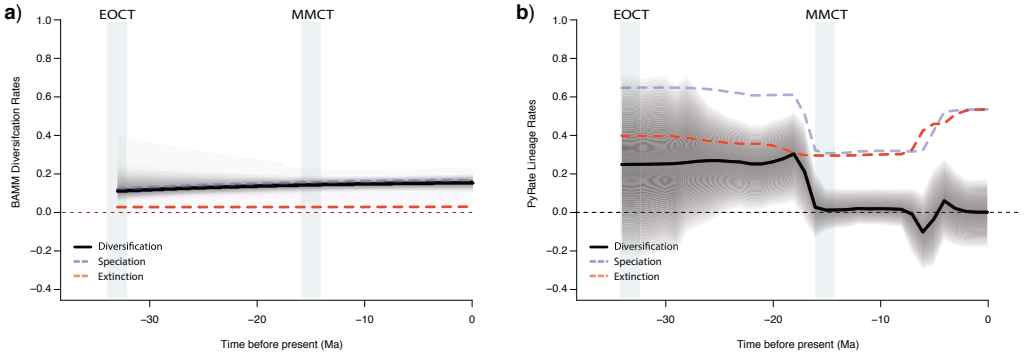

FIGURE 5. Rate-through-time plot in extant musteloids using BAMM (a) and in fossil musteloids using PyRate (b). Net diversification rates are shown in black, speciation rates in blue/light grey, and extinction rates in red/dark grey. The grayscale shading illustrates the 95% credible interval for net diversification. EOCT = Eocene–Oligocene Climate Transition; MMCT = Mid-Miocene Climate Transition.

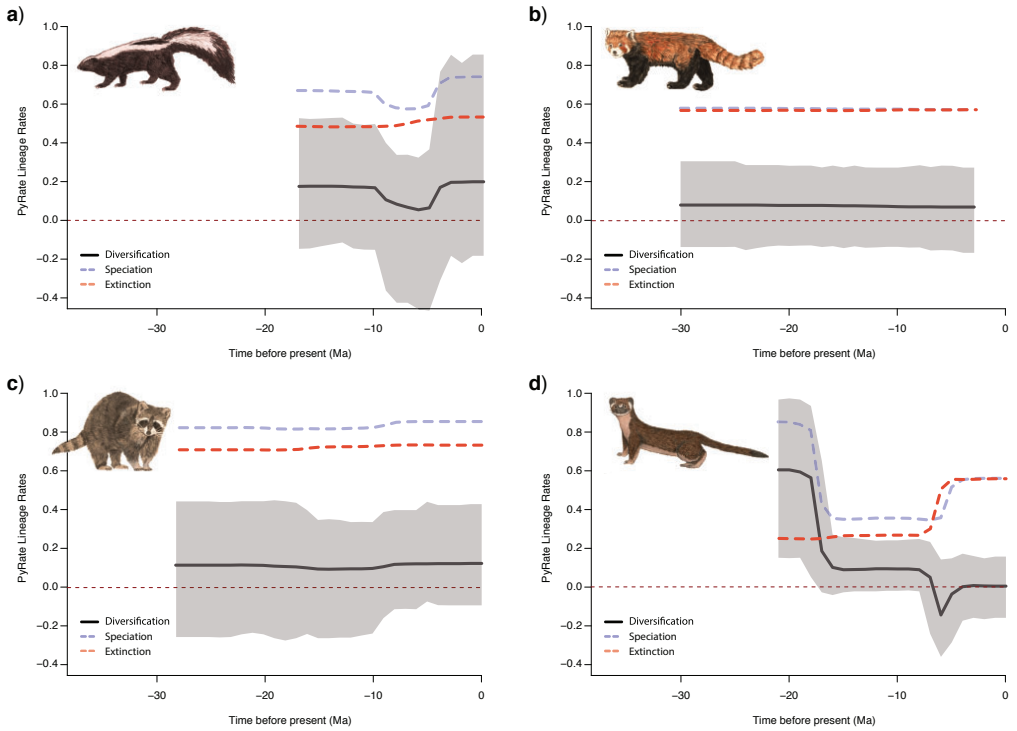

FIGURE 6. Rate-through-time plot in fossil mephitids (a), ailurids (b), procyonids (c), and mustelids (d) from PyRate. Net diversification rates are shown in black, speciation rates in blue/light grey, and extinction rates in red/dark grey. The grayscale shading illustrates the 95% credible interval for net diversification.

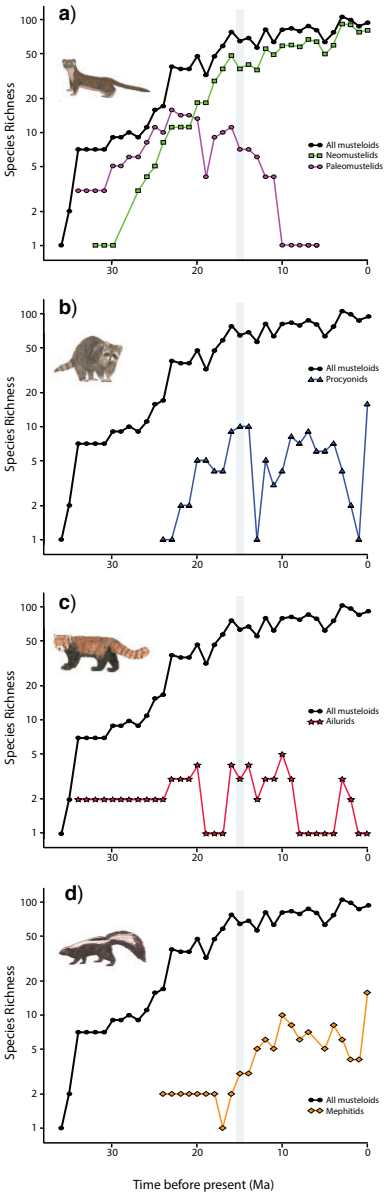

FIGURE 7. Species richness of Mustelidae (a), Procyonidae (b), Ailuridae (c), and Mephitidae (d) across the past 37 Ma. The black curve in each of plot denotes total musteloid richness. The grey bar indicates the Mid-Miocene Climate Transition. Colored curves denote species richness of each respective clade: green squares = neomustelids; pink circles = paleomustelids; blue triangles = procyonids; red stars = ailurids; orange diamonds = mephitids.

nuanced picture of how ecological opportunity has shaped extant diversity and phylogenetic structure of this diverse carnivoran clade. Specifically, our results suggest that body elongation may have served as an innovation that allowed a subclade of mustelids to escape niche competition and rapidly diversify after the onset of ecological opportunity.

Diversification of Musteloidea

The inference of decoupled diversification dynamics with respect to carrying capacity within Mustelidae suggest that ecological opportunity after the onset of the Mid-Miocene Climate Transition played a key role in musteloid diversification, but was phylogenetically restricted in its effects. The DDD analyses, which specifically test for clade-specific shifts in carrying capacity in addition to diversification rates (Etienne and Haegeman 2012), provide support for decoupled dynamics between the mustelid subclade consisting of Helictidinae, Guloninae, Ictonychinae, Mustelinae, and Lutrinae and the remaining musteloid clade (Table 1). This pattern seems to be largely driven by a carrying capacity for the mustelid subclade that is nearly twice as large as that of the main clade, though associated increases in base speciation rate and/or decreases in base extinction rate are also implied. It is important to note that these decoupled diversity-dependent dynamics necessarily imply a pulse of increased diversification in the decoupled clade at its origin, even if there is no increase in basal speciation rate, as speciation rates decline as a function of diversity and the decoupling effectively "resets" them (Sepkoski 1996; Etienne and Haegeman 2012). Within this framework, "early bursts" of net diversification are therefore necessarily implied both at the base of Musteloidea and the decoupled clade, regardless of their magnitude or whether the molecular phylogeny retains a signal. Our ability to reject a null, constant-rates process may be compromised here by the poor performance of AIC as a model selection tool (Etienne et al. 2016) and our parametric bootstraps suggest caution should be taken in interpreting these findings due to slightly elevated type I error rates (Fig. 3a). However, at least heuristically, our parametric bootstrap results are consistent with decoupled dynamics. Etienne et al. (2016) found that power to detect diversity dependent processes declines as extinction rate increases or as intrinsic speciation rate decreases or, alternatively, when clade diversity is low relative to K (Liow et al. 2010). Because decoupled dynamics necessarily imply pulses ofincreased diversification toward the tips of ultrametric phylogenies, we might expect to infer high-carrying capacities, relative to actual clade diversity, when attempting to explain such data under a common diversity dependent regime framework. In our case, the inferred K of ~366 species for the CR1 model is an order of magnitude larger than the background K in our preferred decoupled models (Table 1) and several

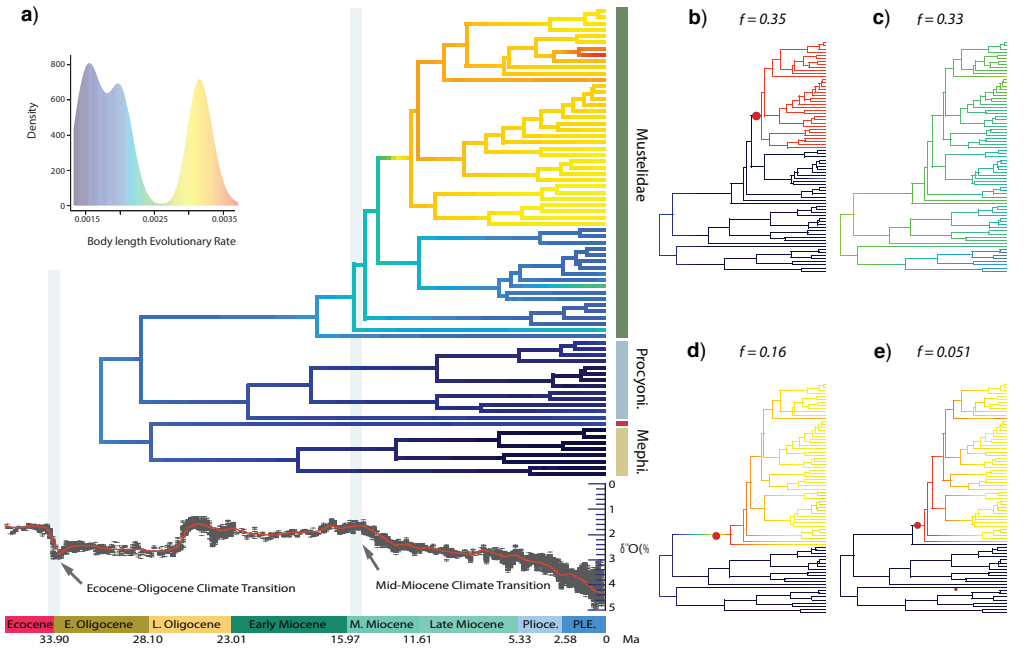

FIGURE 8. Phylorate plot of phenotypic (body length) evolution rates through time a) Phylorate plot of the mean phenotypic evolutionary rate of body length across all shift configurations based the MCC phylogeny. b–d) Phylorate plots offour distinct shift configurations with the highest posterior probability. Rate shifts, shown as red circles with sizes proportional to the marginal probability of the shift, demonstrate significant increase in evolutionary rate. Three distinct shift configurations account for the majority of the posterior probability of the data but result in conflicting rate configurations. The most frequent shift configuration (f = 0.35) signifies no rate shift (b) whereas the second most frequent shift configuration (f = 0.33) indicates an increase in evolutionary rate at the node leading to the divergence of Ictonychinae, Mustelinae, and Lutrinae (c). Conversely, the thirdmost frequent shift configuration (f =0.16) reveals a rate shift at the root of Mustelidae (d).

times larger than the largest K inferred for a decoupled clade. While it is clear that further work is needed to understand and develop appropriate model selection tools for decoupled diversity dependent diversification models, as has recently begun with trait evolutionary models (Ho and Ané 2014), taken at face value our results are consistent with the hypothesis that an elongate mustelid subclade was able to escape niche competition and diversify rapidly after the onset of ecological opportunity in a new niche that could support more species than the ancestral one (Etienne and Haegeman 2012).

Theories linking ecological opportunity to adaptive radiation often invoke the evolution of key innovations as a mechanism to facilitate the exploitation of novel niches (Simpson 1944, 1955; Schluter 2000). Interestingly, many members of the decoupled subclade have been observed to exhibit relatively elongated body plans compared to other carnivorans and even to other musteloids (Brown and Lasiewski 1972; King 1989). Thus, one possible innovation facilitating decoupled diversification dynamics via increased carrying capacity is body elongation, where body lengths are drastically increased relative to body depth. Body elongation in mustelids is often hypothesized to have evolved as a response to the Late Miocene diversification of rodents, permitting mustelid species to enter burrows and confined spaces to capture prey (Brown and Lasiewski 1972; King 1989). In addition, body elongation may have served as a preadaptation that facilitated the exploitation of aquatic habitats by streamlining the body profile and reducing total body drag and energetic demands during high speed swimming (Fish 1996), and semi-aquatic mustelids therefore have a distinct advantage for high speed swimming compared to other nonelongated mammals of similar sizes (Williams 1983, 1989; Fish 1994). A number of authors have noted that mustelid guilds are often particularly diverse in comparison to other carnivore guilds (e.g., Powell et al. 1983), and size-based character displacement appears common (e.g., Dayan et al. 1989; Dayan and Simberloff 1994) though the effects on resource use may be strongest between sexes, rather than among species (McDonald 2002). Significantly, Dayan and Simberloff (1994) found

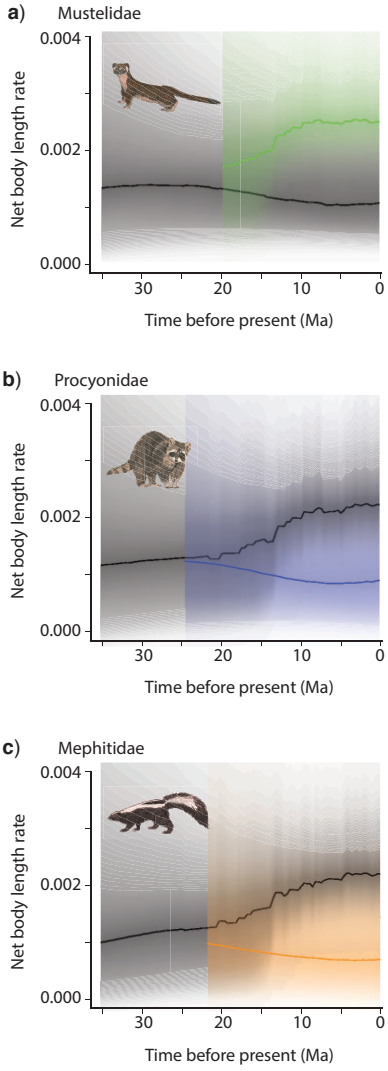

FIGURE 9. Rate-through-time plots depicting net body length evolutionary rate in Mustelidae (a), Procyonidae (b), and Mephitidae (c). Shading intensity of the colored lines indicates the 5% through 95% Bayesian credible regions on the distribution of rates at any point in time for Mustelidae (a), Procyonidae (b), and Mephitidae (c). The black curve in each plot denotes the mean background diversification rate-throughtime (the rate of all musteloids minus the rate of each respective family), and the grayscale shading illustrates the 95% credible interval of the distribution of background rates through time. Mustelids (mean rate, 0.0023; 95% HPD, 0.0016–0.0033) exhibit greater body length evolutionary rates than procyonids (mean rate, 0.0011; 95% HPD, 0.0004–0.0023) and mephitids (mean rate, 0.0011; 95% HPD, 0.0004–0.0023).

that equal-size ratios among British mustelids were only found when the Eurasian badger (*Meles meles*) was excluded. The remaining members of the British mustelid guild (*Martes martes*, *Mustela erminea*, *M. nivalis*, *M. putorius*) all belong to the elongate clade identified in our DDD analyses, suggesting that these taxa may indeed form part of an ecologically discrete community. In line with the observation that many mustelids exhibit relatively elongated bodies for a given mass (Brown and Lasiewski 1972; King 1989; Fish 1994), we found a lack of correspondence in patterns of phenotypic evolutionary rates when examining body mass and length independently (Figs. 7 and 8a; Supplementary Figs. S4 and S5 available on Dryad). This is consistent with Gans (1975) definition of body elongation in which elongate organisms exhibit an increased in relative body length for a given mass. Although not observed in helictidines and gulonines, the discordance of body length and body mass evolutionary rates in ictonychines, mustelines, and lutrines nonetheless suggested that body shape variation may have been partitioned rapidly after the origin of ecological opportunity. Thus, elongate mustelids may have been ideally suited to postMid-Miocene grassland environments and accompanying prey resources, resulting in their diversification whereas other musteloids steadily declined. While this may ultimately suggest that body elongation served as an adaptive trait for this clade, additional investigation is needed to quantify body shape to determine whether body elongation truly conferred adaptation to the ecological opportunity presented by the onset of the Mid-Miocene Climate Transition as well as to further support the decoupling diversification dynamics we found within Mustelidae.

Results from our analyses of diversification rates through time using molecular- and fossil-based methods lead to slightly different interpretations of musteloid diversification dynamics (Fig. 5). Using both BAMM and PyRate, we found no evidence for rapid bursts of musteloid diversification rates during times of hypothesized ecological opportunity near the Eocene–Oligocene transition and Mid-Miocene Climate Transition, contrary to expectations derived from classic adaptive radiation theory (Simpson 1955; Schluter 2000; Harmon et al. 2003; Rabosky and Lovette 2008a). Nevertheless, relative magnitudes of diversification rates throughout the Eocene, Oligocene, and much of the Early Miocene differed substantially between the two sets of analyses (Fig. 5). We inferred low-net diversification rates from the molecular phylogeny throughout this time period, likely due to a lack of extant clades originating at this time (Fig. 5a). In contrast, we found diversification rates inferred from the fossil record were relatively high until just before the Mid-Miocene Climate Transition, when a sudden decrease in origination resulted in net diversification rate of almost 0 lineages/lineage million years for the rest of the Middle Miocene. This pattern is strongly suggestive of equilibrium dynamics (Sepkoski 1978; Rabosky and Lovette 2008b; Etienne et al. 2012;

Etienne and Haegeman 2012); indeed, speciation rate correlated negatively with musteloid paleodiversity over the entire interval examined. Though net diversification rate remained relatively constant, fluctuations in the absolute magnitudes of speciation and extinction rates from the Middle/Late Miocene boundary to the present appear to correlate with global temperature change. The increase in extinction rate observed for the Late Miocene is unsurprising considering that this period is often characterized as a period of high extinction of mammalian taxa hypothesized to be driven by changes in climate and environments (e.g., the Vallesian Crisis; Agusti and Moya-Sola 1990 ; Agustí et al. 2013 ; Fortelius et al. 2014). Concomittant increases in speciation rates further suggest that musetelids experienced high turnover during the Neogene as a result of climate driven environmental change (Baskin 1998).

Similar patterns of sustained diversification have been documented in other clades that were at one time hypothesized to have undergone adaptive radiations, such as Neotropical ovenbirds and woodcreepers (Derryberry et al. 2011), African Synodontis catfish (Day et al. 2013), and Heliconius butterflies (Kozak et al. 2015). These multiple results, including this present study, suggest that the "early burst" model of lineage diversification may be inappropriate for many ecologically diverse clades that otherwise fit within the adaptive radiation paradigm. It is possible that many clades are simply unable to rapidly exploit all suitable niches as soon as they arise, especially across complex and/or large environments such as entire continents (Derryberry et al. 2011 ; Day et al. 2013 ; Kozak et al. 2015; Liedtke et al. 2016). Because mustelids are globally distributed and, presumably, good dispersers, it is possible that ecological opportunity may be less of a limiting factor than it would be in more restrictive settings, such as islands, or for less mobile taxa. It is similarly tempting to infer that the signature of sustained diversification rates recovered from our analyses is an indication that musteloid niche space is not yet fully exploited.

The inconsistency between the BAMM and PyRate results provide a compelling reminder of how extinction can erase the signal of past diversification history in the structure of a molecular phylogeny (Rabosky and Lovette 2008a ; Quental and Marshall 2009 ; Liow et al. 2010) and stress the importance of combining paleontological and neontological data in a unified framework (Slater and Harmon 2013). Such methods are in their infancy at present, but the FBD variant of the skyline model shows some promise in incorporating both datasets in diversification analyses by allowing stepwise rate changes across a FBD tree with extant and extinct species (Stadler et al. 2013 ; Gavryushkina et al. 2014). Using the FBD skyline model implemented in BEAST on a fixed, time-scaled tree including fossil tips, we found little support for distinct diversification rates before and after 19 Ma (see Appendix 3 for full methods and results). However, we found strong support for higher net diversification rate after 13.65 Ma (Mid-Miocene Climate Transition), which corroborates with our findings that global temperature and diversification rates correlate during this timeframe. Nevertheless, the reduced fossil dataset used to date our FBD tree may affect signals of shifts in evolutionary rates; of the 453 fossils used in our PyRate analyses, only 74 of these fossil species had sufficient information required to conservatively place them within a phylogenetic context for the FBD analyses (Appendix 1). Therefore, while the addition of a few fossil taxa to a phylogeny may improve inferences regarding trait evolutionary rates or mode (Slater et al. 2012), more complete sampling may also be necessary for comparable improvements in diversification rate studies.

Body Length or Body Mass?

While the size of an organism has important functional implications for how it utilizes its environment (Schmidt-Nielsen 1984), the question arises of which size metric most thoroughly describes "body size"? Both body length and body mass are readily obtainable in the literature and thus are commonly used as proxies to quantify rates of phenotypic evolution (Gonzalez-Voyer et al. 2009; Slater et al. 2010 ; Derryberry et al. 2011 ; Wilson et al. 2012; Aristide et al. 2015). Because mass and length are normally highly correlated (Schmidt-Nielsen 1984), the majority of studies use just one body size metric, commonly body mass, as a proxy for ecomorphological diversity to test patterns of phenotypic evolution. In this present study, the decoupling of these two body size metrics within Mustelidae illustrates the possibility that rates of phenotypic evolution under a single body size metric may mislead our interpretation of patterns of diversification. Therefore, using both body length and body mass may be a more robust approach for testing patterns of ecomorphological disparity in taxa with derived body plans such as elongation and deeper and/or flatter shapes. Alternatively, future studies interested in characterizing elongation may consider using recent metrics such as elongation ratio (ER) (Ward and Azizi 2004) or the vertebrate shape index (VSI) (Collar et al. 2013). While these metrics require the measurement of character traits that are not readily found in the literature, such as body width or depth for ER or vertebral measurements for VSI, they will provide a more comprehensive view of how clades are changing their body shape. Nevertheless, we recognize that, for several clades, comprehensive ecomorphological datasets are unavailable and we are usually left with body length and/or body mass. We therefore emphasize the importance of using both body size metrics when testing phenotypic evolutionary rates when other more rigorous metrics are unavailable.

Conclusion

Adaptive radiation theory predicts that ecological opportunity promotes rapid lineage diversification

coinciding with increases in phenotypic disparity as colonizing lineages rapidly evolve adaptive traits that are highly correlated to their new resources (Simpson 1955; Schluter 2000). Qualitative inferences derived from time calibrated phylogenies have suggested that Musteloidea, an ecomorphological diverse clade of carnivorans, exhibits two pulses of adaptive radiation, once after the Eocene–Oligocene transition and a second radiation after the Mid-Miocene Climate Transition. Using quantitative phylogenetic methods with both extant and fossil musteloids and a comprehensive time-calibrated phylogeny, we found no evidence an early burst in the rate oflineage diversification throughout the entire phylogeny, including during these climate transitions. Nevertheless, using DDD to specifically test for the effects of key innovations on diversification, we found some support for decoupled diversification dynamics driven by increased clade carrying capacity in the branches leading to a subclade of elongate mustelids. Supporting decoupled diversification dynamics between the mustelid subclade and the remaining musteloids is our finding that there is a lack of correspondence in patterns of body length and body mass evolutionary rates within the decoupled mustelid subclade. The increase in the rate of body length evolution but not body mass evolution suggested that body elongation might be a key innovation for the exploitation of novel Mid-Miocene habitats and resources and subsequent diversification in some musteloids. Additional studies quantifying body shape of both extant and extinct musteloids will further elucidate patterns of ecomorphological diversification within this clade.

Supplementary Material

Data available from the Dryad Digital Repository: http://dx.doi.org/10.5061/dryad.nj1bp .

Author's Contributions

CJL designed the study, collected the sequence, body size, and fossil data, performed the majority of data analyses, and drafted the manuscript. G.J.S helped compile fossil data to date the phylogeny and performed the DDD analyses. R.S.M and G.J.S helped develop the approach, provided crucial insights, and revised the manuscript. All authors read and approved the final manuscript.

Funding

This work was supported by a University of California Santa Cruz Regents Fellowship; a Rebecca and Steve Sooy Graduate Fellowship for Marine Mammals; a Rosemary Grant Graduate Student Research Award from the Society for the Study of Evolution; and a National Foundation of Sciences Graduate Research Fellowship to C.J.L and a Peter Buck postdoctoral fellowship through the National Museum of Natural History to G.J.S.

Acknowledgements

We are grateful to Nancy Hung and Shohei Burns for assisting in the collection of GenBank sequences, Giacomo Bernardi for discussion about phylogenetic methods, Remco Bouckaert and Beth Shapiro for advice with BEAST, Dan Rabosky and Mike Grundler for assistance with BAMM, Daniele Silvestro for advice with PyRate, David Bapst for assistance with Paleotree, Rampal Etienne for advice with DDD, Sasha Gavryushkina for advice with the FBD skyline model, Alan Shabel for insight on Aonyx, and Vikram Baliga for helpful discussions. Lastly, we thank Editor Frank Anderson, Associate Editor Tanja Stadler, Michael Alfaro, Rampal Etienne, and 1 anonymous reviewer for valuable comments that greatly improved previous versions of this manuscript.

Appendix 1. Fossils used to calibrate divergence times estimations using the fossilized birth–death model implemented in BEAST.

Appendix 2. Results of phylogenetic analyses and divergence time estimations.

Appendix 3. Methods and results for FBD skyline model.

References

Adams D.C., Berns C.M., Kozak K.H., Wiens J.J. 2009. Are rates of species diversification correlated with rates of morphological evolution? Proc. R. Soc. B 276:2729–2738.

Agusti J., Moya-Sola S. 1990. Mammal extinctions in the Vallesian (Upper Miocene). In: Kauffman E.G., Walliser O.H., editors. Extinction events in earth history, vol 30. Berlin: Springer. p. 425–432.

Agustí J., Cabrera L., Garcés M. 2013. The Vallesian Mammal Turnover: A Late Miocene record of decoupled land-ocean evolution. Geobios. 46:151–157.

Alfaro M.E., Santini F., Brock C., Alamillo H., Dornburg A., Rabosky D.L., Carnevale G., Harmon L.J. 2009. Nine exceptional radiations plus high turnover explain species diversity in jawed vertebrates. Proc. Natl. Am. Sci. USA 106:13410–13414.

Alroy J. 2014. Accurate and precise estimates of origination and extinction rates. Paleobiology 40:374–397.

Aristide L., Rosenberger A.L., Tejedor M.F., Perez S.I. 2015. Modeling lineage and phenotypic diversification in the New World monkey (Platyrrhini, Primates) radiation. Mol. Phylogenet. Evol. 82:375–385.

Bapst D.W. 2012. paleotree: an R package for paleontological and phylogenetic analyses of evolution. Methods Ecol. Evol. 3:803–807.

Baskin J.A. 1998. Mustelidae. In: Janis C.M., Scott K.M., Jacobs L.L., editors. Evolution of Tertiary Mammals of North America Terrestrial carnivores, ungulates, and ungulatelike mammals. Cambridge, UK: Cambridge University Press. p. 152–173.

Bever G.S., Zakrzewski R.J. 2009. A new species of the Miocene leptarctine Leptarctus (Canivora: Mustelidae) from the early Hemphillian of Kansas. In: Albright III L.B., editor. Papers on geology, vertebrate paleontology, and biostratigraphy in Honor of Michael O. Woodburne. Flagstaff, Arizona, USA: Museum of Northern Arizona Bulletin 65. p. 465–481.

Bouckaert R., Heled J., Kühnert D., Vaughan T., Wu C.-H., Xie D., Suchard M.A., Rambaut A., Drummond A.J. 2014. BEAST 2: a software platform for bayesian evolutionary analysis. PLoS Comput. Biol. 10:e1003537–6.

Brown J.H., Lasiewski R.C. 1972. Metabolism of weasels: the cost of being long and thin. Ecology 53:939.
Calede J.J.M., Hopkins S.S.B., Davis E.B. 2011. Turnover in burrowing rodents: the roles of competition and habitat change. Palaeogeogr. Palaeoclimatol. Palaeoecol. 311:242–255.
Cantalapiedra J.L., Hernández Fernández M., Azanza B., Morales J. 2015. Congruent phylogenetic and fossil signatures of mammalian diversification dynamics driven by Tertiary abiotic change. Evolution 69:2941–2953.
Collar D.C., Reynaga C.M., Ward A.B., Mehta R.S. 2013. A revised metric for quantifying body shape in vertebrates. Zoology 116: 246–257.
Colombo M., Damerau M., Hanel R., Salzburger W., Matschiner M. 2015. Diversity and disparity through time in the adaptive radiation of Antarctic notothenioid fishes. J. Evol. Biol. 28:376–394.
Creevey C.J., McInerney J.O. 2005. Clann: investigating phylogenetic information through supertree analyses. Bioinformatics 21:390–392.
Day J.J., Peart C.R., Brown K.J., Friel J.P., Bills R., Moritz T. 2013. Continental diversification of an African catfish radiation (Mochokidae: Synodontis). Syst. Biol. 62:351–365.
Dayan T., Simberloff D. 1994. Character displacement, sexual dimprphism, and morphological variation among British and Irish mustelids. Ecology 75:1063.
Dayan T., Simberloff D., Tchernov E., Yom-Tov Y. 1989. Inter- and intraspecific character displacement in mustelids. Ecology 70: 1526–1539.
Derryberry E.P., Claramunt S., Derryberry G., Chesser R.T., Cracraft J., Aleixo A., Pérez-Emán J., Remsen J.V. Jr, Brumfield R.T. 2011. Lineage diversification and morphological evolution in a large-scale continental radiation: the neotropical ovenbirds and woodcreepers (Aves: Furnariidae). Evolution 65:2973–2986.
Dumont M., Wall C.E., Botton Divet L., Goswami A., Peigné S., Fabre A.-C. 2015. Do functional demands associated with locomotor habitat, diet, and activity pattern drive skull shape evolution in musteloid carnivorans? Biol. J. Linn. Soc. 117:858–878.
Edgar R.C. 2004. MUSCLE: multiple sequence alignment with high accuracy and high throughput. Nucleic Acids Res. 32:1792–1797.
Eizirik E., Murphy W.J., Koepfli K.-P., Johnson W.E., Dragoo J.W., Wayne R.K., O'Brien S.J. 2010. Pattern and timing of diversification of the mammalian order Carnivora inferred from multiple nuclear gene sequences. Mol. Biol. Evol. 56:49–63.
Estep M.C., McKain M.R., Vela Diaz D., Zhong J., Hodge J.G., Hodkinson T.R., Layton D.J., Malcomber S.T., Pasquet R., Kellogg E.A. 2014. Allopolyploidy, diversification, and the Miocene grassland expansion. Proc. Natl. Acad. Sci. USA 111:15149– 15154.
Etienne R.S., Haegeman B. 2012. A conceptual and statistical framework for adaptive radiations with a key role for diversity dependence. Am. Nat. 180:E75–E89.
Etienne R.S., Haegeman B., Stadler T., Aze T., Pearson P.N., Purvis A., Phillimore A.B. 2012. Diversity-dependence brings molecular phylogenies closer to agreement with the fossil record. Proc. Biol. Sci. 279:1300–1309.
Etienne, Rampal S., Alex L. Pigot, and Albert B. Phillimore. 2016. How reliably can we infer diversity - dependent diversification from phylogenies?. Methods in Ecology and Evolution 7:1092–1099.
Fabre A.-C., Cornette R., Goswami A., Peigné S. 2015. Do constraints associated with the locomotor habitat drive the evolution of forelimb shape? A case study in musteloid carnivorans. J. Anatomy 226:596–610.
Fabre A.C., Cornette R., Slater G., Argot C., Peigné S., Goswami A., Pouydebat E. 2013. Getting a grip on the evolution of grasping in musteloid carnivorans: a three-dimensional analysis offorelimb shape. J. Evol. Biol. 26:1521–1535.
Fabre P.-H., Hautier L., Dimitrov D., Douzery E.J.P. 2012. A glimpse on the pattern of rodent diversification: a phylogenetic approach. BMC Evol Biol. 12:88.
Finarelli J.A. 2008. A total evidence phylogeny of the Arctoidea (Carnivora: Mammalia): relationships among basal taxa. J. Mammal Evol. 15:231–259.
Finarelli J.A., Badgley C. 2010. Diversity dynamics of Miocene mammals in relation to the history of tectonism and climate. Proc. R. Soc. B 277:2721–2726.
Fish F.E. 1994. Association of propulsive swimming mode with behavior in river otters (Lutra canadensis). J. Mammal 75:989–997.
Fish F.E. 1996. Transitions from drag-based to lift-based propulsion in mammalian swimming. Am. Zool. 36:628–641.
Flynn J.J., Finarelli J.A., Zehr S., Hsu J., Nedball M.A. 2005. Molecular phylogeny of the Carnivora (Mammalia): assessing the impact of increased sampling on resolving enigmatic relationships. Syst Biol. 54:317–337.
Fortelius M., Eronen J.T., Kaya F., Tang H., Raia P., Puolamäki K. 2014. Evolution of Neogene mammals in Eurasia: environmental forcing and biotic interactions. Annu. Rev. Earth Planet. Sci. 42:579–604.
Fulton T.L., Strobeck C. 2007. Novel phylogeny of the raccoon family (Procyonidae: Carnivora) based on nuclear and mitochondrial DNA evidence. Mol. Biol. Evol. 43:1171–1177.
Gans C. 1975. Tetrapod limblessness: evolution and functional corollaries. Am. Zool. 15:455–467.
Gavrilets S., Losos J.B. 2009. Adaptive radiation: contrasting theory with data. Science 323:732–737.
Gavryushkina A., Welch D., Stadler T., Drummond A.J. 2014. Bayesian inference of sampled ancestor trees for epidemiology and fossil calibration. PLoS Comput. Biol. 10:e1003919–15.
Gonzalez-Voyer A., Winberg S., Kolm N. 2009. Distinct evolutionary patterns of brain and body size during adaptive radiation. Evolution 63:2266–2274.
Harding L.E., Smith F.A. 2009. Mustela or Vison? Evidence for the taxonomic status of the American mink and a distinct biogeographic radiation of American weasels. Mol. Biol. Evol. 52:632–642.
Harmon L.J., Harmon L.J., Schulte J.A., Larson A., Losos J.B. 2003. Tempo and mode of evolutionary radiation in iguanian lizards. Science 301:961–964.
Heath T.A., Huelsenbeck J.P., Stadler T. 2014. The fossilized birth-death process for coherent calibration of divergence-time estimates. Proc. Natl. Acad. Sci. USA 111:E2957–66.
Ho, L.S.T., Ané, C. 2014. Intrinsic inference difficulties for trait evolution with Ornstein Uhlenbeck models. Methods Ecol. Evol. 5:1133–1146.
Hopkins M.J., Smith A.B. 2015. Dynamic evolutionary change in post-Paleozoic echinoids and the importance of scale when interpreting changes in rates of evolution. Proc. Natl. Acad. Sci. USA 112: 3758–3763.
King C.M. 1989. The advantages and disadvantages of small size to weasels, Mustela species. In: Gittleman J.L., editor. Carnivore behavior, ecology, and evolution. Boston (MA): Springer US. p. 302–334.
Koepfli K.-P., Deere K.A., Slater G.J., Begg C., Begg K., Grassman L., Lucherini M., Veron G., Wayne R.K. 2008. Multigene phylogeny of the Mustelidae: Resolving relationships, tempo and biogeographic history of a mammalian adaptive radiation. BMC Biol. 6:10.
Koepfli K.-P., Gompper M.E., Eizirik E., Ho C.-C., Linden L., Maldonado J.E., Wayne R.K. 2007. Phylogeny of the Procyonidae (Mammalia: Carnivora): Molecules, morphology and the Great American Interchange. Mol. Biol. Evol. 43:1076–1095.
Koepfli K.P., Wayne R.K. 1998. Phylogenetic relationships of otters (Carnivora: Mustelidae) based on mitochondrial cytochrome b sequences. J. Zool. 246:401–416.
Kozak K.M., Wahlberg N., Neild A.F.E., Dasmahapatra K.K., Mallet J., Jiggins C.D. 2015. Multilocus species trees show the recent adaptive radiation of the mimetic heliconius butterflies. Syst. Biol. 64:505–524.
LaBarbera M. 1989. Analyzing body size as a factor in ecology and evolution. Annu. Rev. Ecol. Evol. Syst. 20:97–117.
Lanfear R., Calcott B., Ho S.Y.W., Guindon S. 2012. PartitionFinder: Combined selection of partitioning schemes and substitution models for phylogenetic analyses. Mol. Biol. Evol. 29:1695–1701.
Leopold E.B., Liu G., Clay-Poole S. 2014. 20. Low-biomass vegetation in the Oligocene? In: Prothero D.R., Berggren W.A., editors. Eocene-oligocene climatic and biotic evolution. Princeton (NJ): Princeton University Press. p. 399–419.
Liedtke H.C., Müller H., Rödel M.-O., Menegon M., Gonwouo L.N., Barej M.F., Gvoždík V., Schmitz A., Channing A., Nagel P., Loader S.P. 2016. No ecological opportunity signal on a continental scale? Diversification and life-history evolution of African true toads (Anura: Bufonidae). Evolution 70:1717–1733.

Liow L.H., Quental T.B., Marshall C.R. 2010. When can decreasing diversification rates be detected with molecular phylogenies and the fossil record? Syst. Biol. 59:646–659.
Maddison W., Maddison D. 2011. Mesquite: a modular system for evolutionary analysis. Version 2.75. Available from: URL http://mesquiteproject.org.
Mahler D.L., Ingram T., Revell L.J., Losos J.B. 2013. Exceptional convergence on the macroevolutionary landscape in island lizard radiations. Science 341:292–295.
McDonald R.A. 2002. Resource partitioning among British and Irish mustelids. J Anim Ecol. 71:185–200.
Miller M.A., Pfeiffer W., Schwartz T. 2010. Creating the CIPRES Science Gateway for inference oflarge phylogenetic trees. 2010 Gateway Computing Environments Workshop (GCE). p.1–8.
Mirarab S., Bayzid M.S., Warnow T. 2014. Evaluating summary methods for multilocus species tree estimation in the presence of incomplete lineage sorting. Syst. Biol. 65:366–380.
Moore B.R., Höhna S., May M.R., Rannala B., Huelsenbeck J.P. 2016. Critically evaluating the theory and performance of Bayesian analysis of macroevolutionary mixtures. Proc. Natl. Acad. Sci. USA 113:9569–9574.
Powell R.A., Powell R.A., Zielinski W.J. 1983. Competition and coexistence in mustelid communities. Acta Zool. Fennica 70: 1526–1539.
Prothero D.R., Berggren W.A. 2014. Eocene-oligocene climatic and biotic evolution. Princeton (NJ): Princeton University Press.
R Core Team. 2015. R: A language and environment for statistical computing. Available from: URL http://www.r-project.org/ .
Quental T.B., Marshall C.R. 2009. Extinction during evolutionary radiations: reconciling the fossil record with molecular phylogenies. Evolution 63:3158–3167.
Quental T.B., Marshall C.R. 2010. Diversity dynamics: molecular phylogenies need the fossil record. Trends Ecol Evol. 25:434–441.
Rabosky D.L. 2006. LASER: a maximum likelihood toolkit for detecting temporal shifts in diversification rates from molecular phylogenies. Evol. Bioinform. Online 2:247–250.
Rabosky D.L. 2014. Automatic detection of key innovations, rate shifts, and diversity-dependence on phylogenetic trees. PLoS One 9:e89543–15.
Rabosky D.L., Grundler M., Anderson C., Title P., Shi J.J., Brown J.W., Huang H., Larson J.G. 2014b. BAMMtools: an R package for the analysis of evolutionary dynamics on phylogenetic trees. Methods Ecol Evol. 5:701–707.
Rabosky D.L., Lovette I.J. 2008a. Explosive evolutionary radiations: decreasing speciation or increasing extinction through time? Evolution 62:1866–1875.
Rabosky D.L., Lovette I.J. 2008b. Density-dependent diversification in North American wood warblers. Proc. R. Soc. B 275:2363–2371.
Rabosky D.L., Mitchell J.S., Chang J. 2017. Is BAMM flawed? Theoretical and practical concerns in the analysis of multi-rate diversification models. Syst. Biol. 66:477–498.
Rabosky D.L., Santini F., Eastman J., Smith S.A., Sidlauskas B., Chang J., Alfaro M.E. 2013. Rates of speciation and morphological evolution are correlated across the largest vertebrate radiation. Nat. Commun. 4:1–8.
Ragan M.A. 1992. Matrix representation in reconstructing phylogenetic relationships among the eukaryotes. Biosystems 28:47–55.
Rambaut A., Suchard M.A., Xie D., Drummond A.J. 2014. Tracer v1.6. Available from: URL http://beast.bio.ed.ac.uk/Tracer.
Ronquist F., Teslenko M., van der Mark P., Ayres D.L., Darling A., Hohna S., Larget B., Liu L., Suchard M.A., Huelsenbeck J.P. 2012. MrBayes 3.2: efficient Bayesian phylogenetic inference and model choice across a large model space. Syst Biol. 61:539–542.
Sato J.J., Wolsan M., Minami S., Hosoda T., Sinaga M.H., Hiyama K., Yamaguchi Y., Suzuki H. 2009. Deciphering and dating the red panda's ancestry and early adaptive radiation of Musteloidea. Mol Biol Evol. 53:907–922.
Sato J.J., Wolsan M., Prevosti F.J., D'Elía G., Begg C., Begg K., Hosoda T., Campbell K.L., Suzuki H. 2012. Evolutionary and biogeographic history of weasel-like carnivorans (Musteloidea). Mol Biol Evol. 63:745–757.
Schluter D. 2000. The ecology of adaptive radiation. Oxford (UK): Oxford University Press.
Schmidt-Nielsen K. 1984. Scaling. Cambridge, UK: Cambridge University Press.
Sepkoski J.J. 1978. A kinetic model of Phanerozoic taxonomic diversity I. Analysis of marine orders. Paleobiology 4:223–251.
Silvestro D., Cascales-Miñana B., Bacon C.D., Antonelli A. 2015. Revisiting the origin and diversification of vascular plants through a comprehensive Bayesian analysis of the fossil record. New Phytol. 207:425–436.
Silvestro D., Salamin N., Schnitzler J. 2014a. PyRate: a new program to estimate speciation and extinction rates from incomplete fossil data. Methods Ecol Evol. 5:1126–1131.
Silvestro D., Schnitzler J., Liow L.H., Antonelli A., Salamin N. 2014b. Bayesian estimation of speciation and extinction from incomplete fossil occurrence data. Syst Biol. 63:349–367.
Simpson G.G. 1944. Tempo and mode in evolution. New York: Columbia University Press.
Simpson G.G. 1955. Major features of evolution. New York: Columbia University Press.
Singh G. 1988. History of aridland vegetation and climate: a global perspective. Biol Rev. 63:159–195.
Slater G.J. 2015. Iterative adaptive radiations offossil canids show no evidence for diversity-dependent trait evolution. Proc. Natl. Acad. Sci. USA 112:4897–4902.
Slater G.J., Harmon L.J. 2013. Unifying fossils and phylogenies for comparative analyses of diversification and trait evolution. Methods Ecol Evol. 4:699–702.
Slater G.J., Harmon L.J., Alfaro M.E. 2012. Integrating fossils with molecular phylogenies improves inference of trait evolution. Evolution 66:3931–3944.
Slater G.J., Price S.A., Santini F., Alfaro M.E. 2010. Diversity versus disparity and the radiation of modern cetaceans. Proc. R. Soc. B 277:3097–3104.
Stadler T. 2011. Mammalian phylogeny reveals recent diversification rate shifts. Proc. Natl. Acad. Sci. USA 108:6187–6192.
Stadler T. 2015. TreeSim: simulating phylogenetic trees. R package version 2.2.
Stadler T., Kühnert D., Bonhoeffer S. 2013. Birth–death skyline plot reveals temporal changes of epidemic spread in HIV and hepatitis C virus (HCV). Proc Natl Acad Sci USA 110:228–33.
Stamatakis A. 2014. RAxML version 8: a tool for phylogenetic analysis and post-analysis oflarge phylogenies. Bioinformatics 30:1312–1313.
Swofford D.L. 2003. PAUP*: phylogenetic analysis using parsimony, version 4.0 b10.
Tran L.A.P. 2014. The role of ecological opportunity in shaping disparate diversification trajectories in a bicontinental primate radiation. Proc. Biol. Sci. 281:20131979.
Ward A.B., Azizi E. 2004. Convergent evolution of the head retraction escape response in elongate fishes and amphibians. Zoology 107:205–217.
Williams T.M. 1983. Locomotion in the North American mink, a semi-aquatic mammal. I. Swimming energetics and body drag. J Exp Biol. 103:155–168.
Williams T.M. 1989. Swimming by sea otters: adaptations for low energetic cost locomotion. J. Comp. Physiol. 164:815–824.
Wilson D.E., Mittermeier R.A. 2009. Handbook of the mammals of the world. Barcelona, Spain: Lynx Edicions.
Wilson G.P., Evans A.R., Corfe I.J., Smits P.D., Fortelius M., Jernvall J. 2012. Adaptive radiation of multituberculate mammals before the extinction of dinosaurs. Nature 483:457–460.
Yu L., Peng D., Liu J., Luan P., Liang L., Lee H., Lee M., Ryder O.A., Zhang Y.-P. 2011. On the phylogeny of Mustelidae subfamilies: analysis of seventeen nuclear noncoding loci and mitochondrial complete genomes. BMC Evol Biol. 11:92.
Zachos J.C., Dickens G.R., Zeebe R.E. 2008. An early Cenozoic perspective on greenhouse warming and carbon-cycle dynamics. Nature 451:279–283.

BRIEF COMMUNICATION

doi:10.1111/evo.13514

Carnivory maintains cranial dimorphism between males and females: Evidence for niche divergence in extant Musteloidea

Chris J. Law [1,2] and Rita S. Mehta [1]

[1]Department of Ecology and Evolutionary Biology, University of California, Santa Cruz, Santa Cruz, California 95060

[2]E-mail: cjlaw@ucsc.edu

Received February 27, 2018

Accepted May 23, 2018

The evolution and maintenance of sexual dimorphism has long been attributed to sexual selection. Niche divergence, however, serves as an alternative but rarely tested selective pressure also hypothesized to drive phenotypic disparity between males and females. We reconstructed ancestral social systems and diet and used Ornstein–Uhlenbeck (OU) modeling approaches to test whether niche divergence is stronger than sexual selection in driving the evolution of sexual dimorphism in cranial size and bite force across extant Musteloidea. We found that multipeak OU models favored different dietary regimes over social behavior and that the greatest degree of cranial size and bite force dimorphism were found in terrestrial carnivores. Because competition for terrestrial vertebrate prey is greater than other dietary groups, increased cranial size and bite force dimorphism reduces dietary competition between the sexes. In contrast, neither dietary regime nor social system influenced the evolution of sexual dimorphism in cranial shape. Furthermore, we found that the evolution of sexual dimorphism in bite force is influenced by the evolution of sexual dimorphism in cranial size rather than cranial shape. Overall, our results highlight niche divergence as an important mechanism that maintains the evolution of sexual dimorphism in musteloids.

KEY WORDS: 3D geometric morphometrics, bite force, carnivore, cranial shape, sexual dimorphism, sexual selection.

Divergence between the sexes is a widespread phenomenon observed across the Tree of Life (Fairbairn 2013). Sexual selection has long been evoked as the primary mechanism for both the evolution and maintenance of morphological disparity between males and females (Darwin 1871; Clutton-Brock 2007). Under sexual selection theory, sexually dimorphic traits (e.g., antlers in deer (Clutton-Brock 1982) or increased body sizes in male elephant seals and sea lions (Bartholomew 1970)) evolved as a result of intrasexual competition, providing some individuals greater advantages in contests and/or attracting the opposite sex for breeding opportunities (Clutton-Brock 2007). An alternative hypothesis for the maintenance of sexual dimorphism is intersexual niche divergence (Darwin 1871; Shine 1989; Hedrick and Temeles 1989). Under the niche divergence hypothesis, disparity in phenotypic traits such as trophic morphologies reflect intraspecific differences in resource use, thereby reducing intersexual competition for resources in the environment (Smith 1987; Berwaerts et al. 2006; Butler et al. 2007; Temeles et al. 2010; McGee and Wainwright 2013). Although sexual selection and the niche divergence hypotheses are not mutually exclusive, empirical data supporting the intersexual niche divergence hypothesis are few due to the challenge of directly linking niche divergence and sexual dimorphism (Shine 1989; Hedrick and Temeles 1989). Nevertheless, the large breadth of ecomorphological studies to date (e.g., Dayan and Simberloff 1994; Shetty and Shine 2002; Butler et al. 2007; Temeles et al. 2010; McGee and Wainwright 2013) make a strong argument for the potential role of intersexual niche divergence in expanding the realized niche of a species. Within a clade, intersexual niche divergence could increase the evolution of intersexual differences in dietary composition and trophic morphologies such as the feeding apparatus.

Within carnivoran mammals (Carnivora), the intraspecific divergence of body sizes and craniomandibular morphology between the sexes is often attributed to sexual selection (Gittleman and Van Valkenburgh 1997; Morris and Carrier 2016). Most carnivorans exhibit male-biased sexual dimorphism in which males

are larger than females. Males with larger, stronger bodies and skulls are perceived as more effective in territorial conflicts with male competitors and thus achieve greater reproductive success (Gittleman and Van Valkenburgh 1997; Brunner et al. 2004). Therefore, the greatest degree of sexual size dimorphism is expected to occur in species that are highly territorial and solitary and exhibit polygynous mating systems. However, with the exception of pinnipeds, this pattern between social/mating system and degree of sexual dimorphism is not consistent across all carnivoran clades (Weckerly 1998; Isaac 2005; Lindenfors et al. 2007); the most territorial and solitary carnivorans are not always the most sexually dimorphic, and the least territorial and solitary carnivorans are not always the least sexually dimorphic. This unclear and sometimes conflicting pattern within extant carnivoran clades suggests that additional selective forces also contribute to the evolution and maintenance of sexual dimorphism in carnivorans.

Niche divergence and the partitioning of resources may provide a secondary mechanism that drives the evolution of sexual dimorphism. For example, the divergence of craniomandibular size and shape provides evidence of intersexual niche divergence (Thom and Harrington 2004; Christiansen and Harris 2012; Law et al. 2016b), where phenotypic differentiation in the skull reflects ecological divergence between the sexes and even reduction of intersexual competition for resources and habitat use. It is well documented that males and females of many carnivoran species utilize different dietary resources, often in the form of prey size where males consume larger prey than females (Birks and Dunstone 1985; Funston et al. 2001; McDonald 2002; Radloff and Toit 2004). Furthermore, across carnivorans there is a relationship between the degree of carnivory and the degree of sexual dimorphism in which more carnivorous species exhibit greater size dimorphism between males and females (Gittleman and Van Valkenburgh 1997; Noonan et al. 2016). This pattern is often attributed to the hypothesis that competition for vertebrate prey is likely greater than competition for plant material and nonvertebrate prey (Hairston et al. 1960; Noonan et al. 2015; MacDonald and Johnson 2015). Increased sexual dimorphism in obligate carnivores, therefore, reduces intraspecific dietary competition by reducing competition between males and females. In contrast, increased sexual dimorphism to reduce intraspecific competition is not necessary in species with a lower degree of carnivory (i.e., plant material, nonvertebrate prey) because these prey items are more abundant and easier to obtain (Hairston et al. 1960; Noonan et al. 2015; MacDonald and Johnson 2015).

In this study, we examine how sexual selection and niche divergence influenced the evolution of sexual dimorphism in the crania of musteloid carnivores. Musteloids (e.g., badgers, otters, raccoons, skunks, and weasels) are a speciose and ecologically diverse clade of carnivorans (Fabre et al. 2013, 2015; Dumont et al. 2015; Law et al. 2018). Members of Musteloidea exhibit diverse trophic ecologies, ranging from the generalist diets of raccoons to the specialized diets of the herbivorous red pandas, highly carnivorous weasels, and piscivorous otters. In addition, musteloids exhibit a range of sexual dimorphism from none to highly sexually dimorphic where males are more than twice the size of females (Wilson and Mittermeier 2009). Because almost all musteloid species exhibit polygynous mating systems, sexual selection is often hypothesized to have driven the evolution of sexual dimorphism (Moors 1980). Researchers, however, have also found interspecific differences in the feeding apparatus (Wiig 1986; Thom and Harrington 2004; Law et al. 2016a,b) and diet (Moors 1980; Birks and Dunstone 1985; Zalewski 2007; Elliott Smith et al. 2015), providing evidence that niche divergence may also be an important selective force in the evolution of sexual dimorphism in musteloids.

We use three-dimensional (3D) geometric morphometric and generalized Ornstein-Uhlenbeck (OU) modeling approaches to examine how social systems (a proxy for sexual selection) and diet (a proxy for natural selection via niche divergence) correspond with the evolution of sexual dimorphism in cranial shape, cranial size, and bite force across Musteloidea. We use social system as a proxy of mating system (Noonan et al. 2016) because the degree of polygyny for the majority of musteloids is unknown. Musteloids have varied social systems ranging from highly solitary musteloids that exhibit intrasexual territoriality in which one male defends a territory that may contain multiple female territories to highly social musteloids that tend to be monogamous or promiscuous (Johnson et al. 2000; Macdonald and Newman 2018). If sexual selection is the primary force driving sexual dimorphism, the degree of cranial sexual dimorphism should be greatest in solitary species and lowest in social species, suggesting that sexual dimorphism evolved as a response to male–male competition. Alternatively, if niche divergence is the primary force driving sexual dimorphism, the degree of cranial sexual dimorphism should be greatest in obligate carnivorous species that feed on less abundant vertebrate prey whereas the degree of cranial sexual dimorphism should be lowest in omnivorous and herbivorous musteloids that feed on nonvertebrate prey and plant material that more abundant and easier to obtain. This would suggest that intraspecific competition for less abundant resources facilitates the evolution of sexual dimorphism. Lastly, if both sexual selection and niche divergence are important drivers of sexual dimorphism in extant musteloids, the degree of cranial sexual dimorphism should be greatest in solitary, obligate carnivorous species.

Material and Methods

MORPHOLOGICAL DATA

We obtained 910 skull specimens across 63 musteloid species, sampling between one and 12 individuals per sex per species

(median = seven females and seven males per species) from 20 natural history museums (see Table A1 for list of specimens and museums). We 3D scanned each specimen using a Next Engine 3D Ultra HD surface scanner. All specimens were fully mature, determined by the closure of exoccipital–basioccipital and basisphenoid–basioccipital sutures on the cranium.

We quantified cranial size and shape using 3D geometric morphometrics (Rohlf and Slice 1990; Zelditch et al. 2012). Fifty-two landmarks and 85 semi-landmarks were digitized on the 3D scans using Stratovan Checkpoint and superimposed by Generalized Procrustes analysis (Rohlf and Slice 1990) to remove variation in position, size, and orientation (Fig. 1; Table A2). In addition, the Procrustes algorithm allowed semilandmarks on the curves to slide along their tangent vectors until their positions minimized bending energy (Bookstein 1997; Zelditch et al. 2012). After superimposition, bilaterally homologous landmarks on the ventral cranium were reflected across the midline and averaged using the geomorph function bilat.symmetry. We then quantified cranial size of each specimen by calculating the centroid size of each configuration of landmarks, that is the square root of the sum of the squared distances from each landmark to the geometric center of the shape (Bookstein 1996). All Procrustes superimposition was performed in the R package geomorph 3.0.5 (Adams and Otárola-Castillo 2013).

We used Thomason's (1991) dry skull method to estimate carnassial bite forces by estimating cross-sectional areas for the major jaw adductors and treating the jaw as a third class lever. We photographed each specimen in three views: (1) the cranium in posterodorsal view, photographed by orienting the cranium so that the plane between the orbital processes and posterior most points of the zygomatic arches is parallel to the photographic plane; (2) the cranium in ventral view, photographed by orienting the palate plane parallel to the photographic plane; and (3) the mandible in lateral view, photographed by orienting the long axis of the dentary parallel to the photographic plane. We then estimated cross-sectional areas (CSA) of the temporalis and masseter-pterygoid complex by outlining the left and right infratemporal fossae from the posterodorsal cranial and ventral cranial views, respectively (Fig. A1). The resulting areas were then multiplied by a muscle stress value 30 N/cm^2 to estimate forces of the temporalis (*T*) and masseter-pterygoid (*M*) complex. Each muscle force was modeled as a single force vector (*T* and *M*) and assumed to act through their centroids perpendicular to the plane of the muscle CSA. We then measured the moment arms (in-levers) of the temporalis (MAT) and masseter-pterygoid complex (MAM) as the distance from centroid to the temporomandibular joint (TMJ) using the lateral and ventral views of the cranium as well as the out-lever (O_M) as the distance from the bite point to the TMJ joint (Fig. A1). We estimated bite force at the carnassial by dividing the total moment

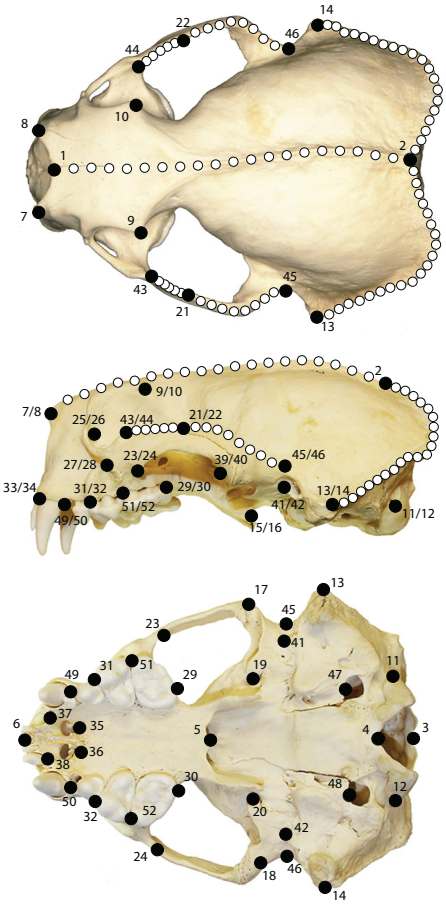

Figure 1. Landmarks (large black circles) and semi-landmarks (small white circles) used for geometric morphometric analysis of skull shape and size. Landmark descriptions are in Table A2.

by the out-lever and multiplied it by 2 to account for bilateral biting:

$$BF = 2\left(\frac{T \quad MAT + \quad M \quad MAM}{O_M}\right)$$

We measured bite forces at the carnassial rather than the canine because food processing occurs at the carnassial in all musteloids across different dietary groups. All cross sectional areas and linear measurements were taken digitally using ImageJ v. 1.48 (Schneider et al. 2012).

DEGREE OF SEXUAL DIMORPHISM

We assessed the degree of sexual dimorphism in cranial size and bite force using the size dimorphism index (SDI) (Lovich and Gibbons 1992). We first determined the mean cranial size and bite force of males and females in each species and quantified SDI: $SDI = (\pm 1(\frac{S_M}{S_F} - 1))\ \ 100$, where S_M and S_F are the mean centroid sizes or mean bite forces of males and females, respectively. A positive sign is assigned if the male trait is larger whereas a negative sign is assigned if the female trait is larger. There is no sexual dimorphism if $SDI = 0\%$. In contrast, the degree of sexual dimorphism in cranial shape cannot be quantified with SDI. Therefore, we quantified the degree of cranial shape dimorphism of each species by measuring the shape differences via Procrustes distance (P_D) between the mean female shape and mean male shape of each species with the permudist function in the R package Morpho 2.5.1 (Schlager 2016).

We examined the relationship between the degree of cranial size dimorphism, cranial shape dimorphism, and bite force dimorphism using phylogenetic generalized least-squares (PGLS) regression with R package caper (Orme 2013). All regression parameters were simultaneously estimated with phylogenetic signal in the residual error as Pagel's (Pagel 1999) lambda (Revell 2010). We also calculated the correlation coefficient between each of the relationships. We used the function phyl.vcv in the R package phytools (Revell 2011) to compute the phylogenetic trait variance-covariance matrix between the traits and used this matrix to calculate the correlation coefficient (r) of each relationship. PGLS regressions were performed using a recently constructed time-calibrated phylogeny of Musteloidea (Law et al. 2018).

ANCESTRAL RECONSTRUCTION OF SOCIAL SYSTEM AND DIETARY REGIMES

We used Johnson et al.'s (2000) categorical scheme to classify the 63 musteloids into one of four social systems: solitary, pair-living, group-living, and variable groups. Some species range from solitary to living in groups across different populations and the variable category captures this geographic difference in social systems. The data in the variable category reflect variation in social systems, which are not due to increased number of studies for these particular species.

We obtained dietary data primarily from *Mammalian Species* accounts (see Table A3 for references) and classified the 63 musteloids into one of four dietary categories: herbivory with diets consisting of > 90% plant material, omnivory (hypocarnivory) with diets consisting of > 70% nonplant and nonvertebrates (e.g., insects, earthworms), terrestrial carnivory with diets consisting of > 50% terrestrial vertebrates (e.g. rodents, amphibians, reptiles), and aquatic carnivory with diets consisting of > 90% aquatic prey (e.g., fish, crustaceans, molluscs). Our four dietary categories roughly follow Van Valkenburgh's (2007) classification deviating by the addition of the herbivorous and aquatic carnivorous categories and the combination of hypercarnivorous and mesocarnivorous as terrestrial carnivorous. We separated aquatic diets from terrestrial diets for two reasons. First, aquatic mammals exhibit unique morphological and behavioral adaptations that allow them to target aquatic prey (Hocking et al. 2017; Kienle et al. 2017). Second, the aquatic environment can influence shifts in the degree of sexual size dimorphism in mammals (Ralls and Mesnick 2002; Lindenfors et al. 2002).

We examined the evolution of social systems, dietary regimes, and social system dietary regimes independently by performing ancestral state reconstructions using 1000 stochastic character mapping simulations (Nielsen 2002; Huelsenbeck et al. 2003; Bollback 2006) with the make.simmap function in the phytools R package (Revell 2011).

GENERALIZED ORNSTEIN–UHLENBECK MODELING

We assessed the fit of eight evolutionary models to our three metrics of sexual dimorphism (SDI for cranial size dimorphism, Procrustes distances for cranial shape dimorphism, and SDI for bite force dimorphism) to determine the influence of social system and diet on the evolution of sexual dimorphism. The two simplest models, a single-rate Brownian (BM1) model that assumes trait variance accumulates proportional to evolutionary time under a random walk (Felsenstein 1985) and a single-optimum Ornstein–Uhlenbeck (OU1) model that constrains traits to evolve toward one optimum, allow the degree of sexual dimorphism to evolve independently of dietary and social system regimes. The remaining six models are multi-peak OU models that allow social system/dietary regimes to exhibit different strengths of attraction (α) and/or rates of stochastic motion of trait evolution ($\sigma 2$) toward separate trait optima (θ). The OUM multipeak model allows for separate θ but does not permit $\sigma 2$ and α to vary between regimes. In contrast, the OUMA multipeak model estimates separate α parameters for each θ, whereas the OUMV multipeak model estimates separate $\sigma 2$ parameters for each θ. Lastly, the full OUMVA multipeak model allows both parameters (α and $\sigma 2$) to vary with each θ. Support for any of these multipeak models would suggest that social system, diet, or the combination of social system and diet influences the evolution of sexual dimorphism. We performed our OU modeling across all 1000 stochastically mapped trees to take into account uncertainty in the ancestral character states with the function OUwie in the R package OUwie (Beaulieu et al. 2012). We evaluated the best-fitting model for each dimorphism metric using corrected Aikaike Information Criterion (AICc) weights. We then generated a 95% confidence interval for all model parameters (θ, α, and $\sigma 2$) of the best-fit model. Bootstrapping was performed for 1000 replicates using the function OUwie.boot.

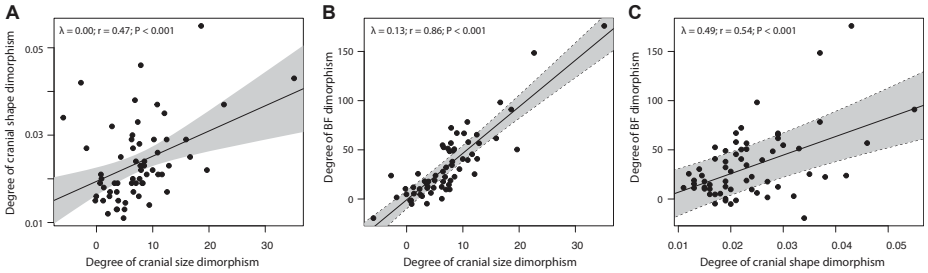

Figure 2. PGLS regressions between (A) the degree of cranial size dimorphism and cranial shape dimorphism, (B) the degree of cranial size dimorphism and bite force dimorphism, and (C) the degree of cranial shape dimorphism and bite force dimorphism with 95% confidence intervals (shaded polygons).

Additional processes aside from niche divergence and sexual selection may also drive the evolution of sexual dimorphism in the cranium and bite force. These hidden processes are not captured by our OUwie analyses under our hypothesis-testing framework of niche divergence and sexual selection. Therefore, we also used bayou (Uyeda and Harmon 2014) to determine if additional shifts of sexual dimorphism occur on branches not predicted by niche divergence or sexual selection. Bayou uses a reversible-jump Bayesian approach that fits multioptimum OU models to estimate the placement and magnitude of regime shifts without a priori designation of dietary ecology and social systems. Using the *make.prior* function in bayou, we placed a Poisson prior with lambda = 15 on the number of shifts between adaptive regimes. Additionally, we allowed only one shift per branch with equal probability that each branch has a shift. We ran two independent MCMC analyses with one million generations each and examined if the two chains converged using Gelman and Rubin's R statistic. All effective sample sizes were > 200 after discarding the first 30% of samples as burn-in. We then examined the posterior probabilities (pp) for regime shift locations and magnitudes.

Results

SEXUAL DIMORPHISM IN MUSTELOID CRANIA

We found extensive variation in the degree of sexual dimorphism across Musteloidea in each of our three dimorphic metrics (Fig. A2 A–C). Our PGLS regressions indicated significant positive relationships between the degree of cranial size dimorphism, cranial shape dimorphism, and bite force dimorphism (Fig. 2). Phylogenetic correlation tests reveal strong correlations between the degree of cranial size dimorphism and bite force dimorphism ($r = 0.86$) but weaker correlations between the degree of cranial shape dimorphism with cranial size dimorphism ($r = 0.47$) and bite force dimorphism ($r = 0.54$).

ANCESTRAL RECONSTRUCTION OF SOCIAL SYSTEM AND DIETARY REGIMES

Ancestral reconstructions of social systems across 1000 simulations revealed that solitary-living is the ancestral state of musteloids (Fig. 3A). Group-living evolved on average 7.80 times—kinkajou (*Potus flavus*), coatis (*Nasua* spp.), *Meles* badgers, and four independent evolutions in otters. Pair-living evolved on average 2.06 times—Sunda stink-badger (*Mydaus javanensis*) and yellow-throated marten (*Martes flavigula*). Variable social systems evolved on average 5.39 times—raccoons (*Procyon* spp.), tayra (*Eira barbara*), grisons (*Galictis* spp.), Eurasian otter (*Lutra lutra*), and African clawless otter (*Aonyx capensis*).

For dietary regimes, omnivory is the ancestral state of musteloids (Fig. 3B). Across our 1000 simmap simulations, herbivory evolved on average 3.01 times—red panda (*Ailurus fulgens*), kinkajou (*Potos flavus*), and olingos (*Bassaricyon* spp.)—and carnivory evolved on average 3.51 times—spotted skunks (*Spilogale* spp.), ringtail (*Bassariscus astutus*), and Mustelidae. Within carnivory, omnivory reevolved on average 2.62 times—meline badgers and ferret-badgers (*Melogale* spp.)—and aquatic carnivory evolved on average 1.042 times in otters.

GENERALIZED ORNSTEIN-UHLENBECK (OU) MODELING OF SOCIAL SYSTEMS AND DIET

Multipeak OU models (OUM and OUMV) with separate optima under dietary regimes were strongly favored for cranial size dimorphism and bite force dimorphism ($w_A > 0.99$; Table 1). These results indicate that diet rather than social system influence the evolution of cranial size and bite force dimorphism in musteloids. Specifically, the OUM and OUMV models along with parametric bootstrapping revealed that the four dietary regimes exhibited separate optima for the degree of male-biased cranial size dimorphism (terrestrial carnivory $\theta = 10.39\%$ [7.93%, 12.95%]; omnivory $\theta = 7.40\%$ [4.97%, 9.61%]; aquatic carnivory $\theta = 3.80\%$ [1.79%,

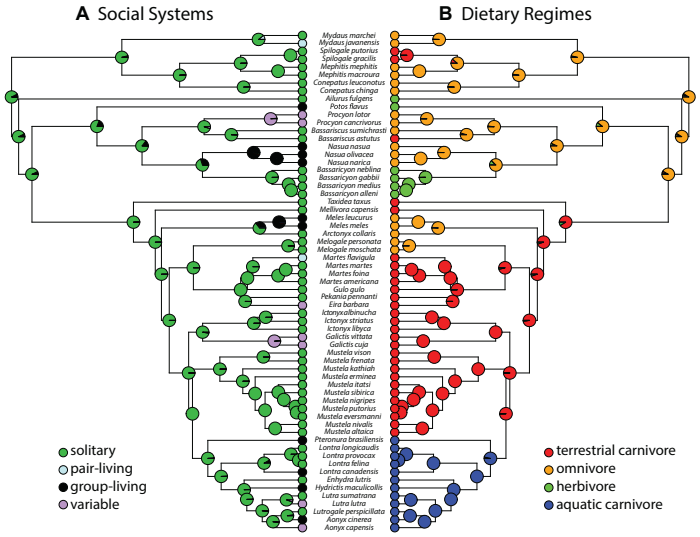

Figure 3. Ancestral state reconstruction of (A) social systems and (B) dietary regimes mapped onto a pruned time-calibrated phylogeny of 63 musteloid species. Pie charts on each node show the relative Bayesian posterior probability of each character state across 1000 simulations.

5.71%]; herbivory θ = –0.09% [–4.42%, 2.74%]) and male-biased bite force dimorphism (terrestrial carnivory θ = 50.45% [34.75%, 66.53%]; omnivory θ = 33.92% [22.63%, 45.98%]; aquatic carnivory θ = 12.49% [5.71%, 18.61%]; herbivory θ = –2.74% [–12.24%, 5.91%]). These results reveal that terrestrial carnivorous musteloids exhibited the greatest degree of male-biased sexual dimorphism in cranial size and bite force whereas herbivorous musteloids exhibited the lowest degree of male-biased sexual dimorphism (Fig. 4). The OUMV model (w_A = 0.73) was supported over the OUM model (w_A = 0.26) for cranial size dimorphism, suggesting that the evolutionary rates of cranial size dimorphism also differed between the four dietary regimes (Table 1). However, parametric bootstrapping revealed that these evolutionary rates were largely overlapping, cautioning any interpretation. OU modeling approaches are sensitive to sample sizes; therefore, these overlapping rate estimates may be due to the low number of species (63 species) (Beaulieu et al. 2012). Multipeak OU models under the social system and social system dietary regimes were not well supported and exhibited ΔAICc scores less than a single peak OU model (Table 1).

In contrast, a single peak OU model was favored over multipeak OU models for cranial shape dimorphism (w_A = 0.86; Table 1). This suggests that neither diet nor social system strongly influences the evolution of cranial shape dimorphism.

EVOLUTIONARY SHIFTS IN SEXUAL DIMORPHISM

With bayou, we found that significant regime shifts (posterior probability > 0.3) primarily occurred closer to the species tips (Fig. A3). We found evolutionary shifts toward lower size dimorphism in herbivorous olingos, hypocarnivorous ferret-badgers, and some aquatic carnivorous otters whereas only a single evolutionary shift toward greater sexual size dimorphism in the hypercarnivorous Japanese weasel (Fig. A3A). In contrast, we found one significant shift in shape dimorphism—within the hypercarnivorous fisher (Fig. A3B). Lastly, evolutionary shifts toward lower bite force dimorphism occurs in herbivorous olingos and a clade comprising of hypercarnivorous, hypocarnivorous, and aquatic carnivorous mustelids with a subsequent evolutionary shift toward higher bite force dimorphism in hypercarnivorous weasels (Fig. A3C).

Discussion

We found evidence that niche divergence is stronger than sexual selection in driving the evolution of sexual dimorphism in Musteloidea. Specifically, multipeak OU models under dietary regimes were strongly favored for cranial size and bite force dimorphism, suggesting that niche divergence maintains the evolution of sexual dimorphism in cranial size and bite force across

Table 1. Comparisons of evolutionary model fits for cranial size, cranial shape, and bite force. Mean Akaike information criterion (AICc) is the averaged AICc over 1000 replications and ΔAICc is the model's mean AICc minus the minimum AICc between models.

model	Optimal regimes	loglik	AICc	ΔAICc	w_A
Cranial size Dimorphism					
BM	NA	−218.98	442.16	37.42	0.00
OU	NA	−203.32	413.04	8.30	0.01
OUM	Diet	−196.65	406.79	2.05	0.26
OUMV	**Diet**	**−191.67**	**404.74**	**0.00**	**0.73**
OUM	Social system	−202.30	418.10	13.36	0.00
OUMV	Social system	−198.38	418.16	13.43	0.00
OUM	Social system diet	−193.28	423.30	18.56	0.00
OUMV	Social system diet	–	–	–	–
Cranial shape Dimorphism					
BM	NA	178.55	−352.89	36.08	0.00
OU	**NA**	**197.69**	**−388.97**	**0.00**	**0.86**
OUM	Diet	198.22	−382.94	6.03	0.04
OUMV	Diet	200.38	−379.37	9.60	0.01
OUM	Social system	199.01	−384.51	4.46	0.09
OUMV	Social system	–	–	–	–
OUM	Social system diet	200.41	−378.92	10.05	0.01
OUMV	Social system diet	–	–	–	–
Bite force Dimorphism					
BM	NA	−319.42	643.05	48.63	0.00
OU	NA	−307.26	620.93	26.51	0.00
OUM	Diet	−302.54	618.58	24.16	0.00
OUMV	**Diet**	**−286.51**	**594.42**	**0.00**	**1.00**
OUM	Social system	−306.33	626.16	31.74	0.00
OUMV	Social system	−302.12	625.64	31.22	0.00
OUM	Social system diet	−298.19	633.13	38.71	0.00
OUMV	Social system diet	–	–	–	–

Bolded rows represent the best-fit model as indicated by Akaike weights (w_A). Indicate models that were unable to converge. OUMA and OUMVA models did not converge for all sexual dimorphism metrics.

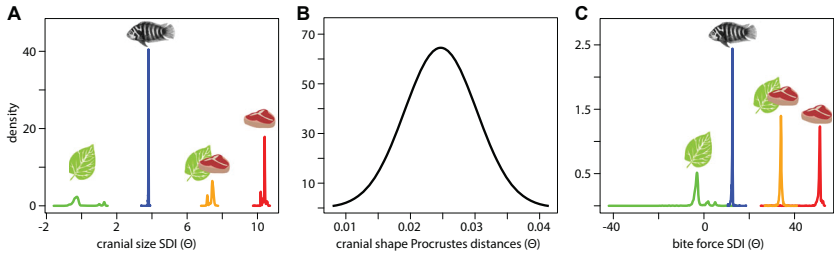

Figure 4. Density plots of the estimated optima from the best-fitting generalized Ornstein–Uhlenbeck (OU) model of (A) cranial size dimorphism, (B) cranial shape dimorphism, and (C) bite force dimorphism. Multi-peak OU models with separate optima under dietary regimes (herbivory, green; aquatic carnivory, blue; omnivory, orange; and terrestrial carnivory, red) were the best-fitting models for cranial size dimorphism and bite force dimorphism. A single peak OU model was the best-fitting model for cranial shape dimorphism.

extant musteloids. Carnivorous musteloids exhibit the greatest degree of sexual dimorphism in cranial size and bite force, whereas herbivorous musteloids exhibit the lowest degree of sexual dimorphism. These results support previous findings (Noonan et al. 2016) that the degree of sexual dimorphism in body size is related to the degree of carnivory on terrestrial vertebrates. Because competition for terrestrial vertebrate prey is greater than for plant material, nonvertebrate prey (Hairston et al. 1960; Noonan et al. 2015; MacDonald and Johnson 2015), and aquatic vertebrate prey, increased sexual dimorphism is thought to reduce dietary competition between male and female carnivores under niche divergence. Field observations and dietary analyses support this scenario, finding that males of many carnivorous musteloids (e.g., martens, minks, and weasels) target different, and often larger, prey items than females (Moors 1980; Birks and Dunstone 1985; Zalewski 2007). Following predictions of niche divergence, omnivorous and herbivorous musteloids exhibit reduced degrees of sexual dimorphism as nonvertebrate prey and plant material are more abundant and easier to obtain therefore reducing intraspecific competition (Hairston et al. 1960; Noonan et al. 2015; MacDonald and Johnson 2015). Aquatic carnivorous musteloids (e.g., otters) also exhibit reduced degrees of sexual size dimorphism. Otters specialize on a variety of prey from hard-shelled invertebrates to fish, and further examination of each individual species confirmed reduced degree of cranial size and bite force dimorphism compared to terrestrial carnivorous musteloids.

Although our results indicate that dietary regimes influenced the evolution of sexual dimorphism in musteloid crania, social systems may nevertheless have confounding effects on sexual dimorphism. It has been noted that carnivorous musteloids tend to be territorial and solitary and exhibit the greatest sexual size dimorphism, whereas omnivorous musteloids tend to form group systems and display a decrease in sexual size dimorphism (Johnson et al. 2000; Johnson and Macdonald 2001; MacDonald and Johnson 2015). Noonan et al. (2016) speculated that these different dietary regimes, herbivory to carnivory, could have facilitated different social and mating systems, which in turn could have led to different degrees of sexual dimorphism across Musteloidea. That is, carnivores exhibit great intraspecific competition for prey and mates and therefore remain solitary and territorial (Powell 1979; Newman et al. 2011). Sexual dimorphism in body size is then maintained under sexual selection in which males compete for females under a polygynous mating system (Moors 1980). Omnivores and herbivores, in contrast, are hypothesized to form group systems because of the reduced intraspecific competition for food items (Johnson et al. 2000; MacDonald and Johnson 2015; Noonan et al. 2015). The formation of these groups is thought to lead to reduced sexual selection of increased male body sizes because members of both sexes exhibit a promiscuous mating system and individuals mate with multiple partners (Johnson et al. 2000; Johnson and Macdonald 2001; MacDonald and Johnson 2015; Noonan et al. 2016). However, our ancestral state reconstructions of extant social system and dietary regimes reveal that there is no clear pattern between the degree of carnivory and the degree of social system (Fig. 3). Solitary-living is the ancestral condition in musteloids during the Early Oligocene whereas carnivorous diets did not appear until the Early Miocene near the base of Mustelidae. Similarly, the majority of omnivorous musteloids do not exhibit a group social system as suggested by Noonan et al. (Noonan et al. 2016). Rather, our data support the hypothesis that sexual selection may have been the original mechanism for the evolution of sexual dimorphism in Musteloidea (Moors 1980) but that niche divergence maintains the divergence between the sexes. The subsequent evolution of different dietary regimes contributed to further evolution of sexual dimorphism across extant musteloid clades, specifically through the intensification and relaxation of the degree of sexual dimorphism of the crania in carnivorous musteloids and noncarnivorous musteloids, respectively. We encourage future efforts of gathering higher resolution dietary data to better understand how prey size relates to male/female predator size and to help detect subtle differences in polygynous mating systems and its potential effects on sexual dimorphism.

We found that neither social system nor dietary regimes had strong influences on the evolution of sexual dimorphism of cranial shape. Cranial shape, instead, evolved toward the same dimorphism optimum under a single rate OU model across the entire clade. Many musteloid species exhibit cranial shape dimorphism, driven particularly by relatively wider zygomatic arches, larger canines, robust mastoid breadth, and more pronounced sagittal crests in males (Wiig 1985, 1989; Lynch and O'Sullivan 1993; Abramov and Tumanov 2003; Thom and Harrington 2004; Law et al. 2016b, 2017). Relatively larger craniomandibular traits translate to relative increases in jaw adductor muscle attachment sites (Radinsky 1981a,b but see Law et al. 2016a), thereby facilitating stronger biting ability and heavier heads that can be used in territorial conflicts with male competitors or for capturing and processing larger prey items. We find that species with the highest degree of cranial shape dimorphism exhibit relatively larger sagittal crests (e.g., male fishers, *Pekania pennanti*; coatis, *Nasua* and *Nasuella* spp.; and hog badgers, *Arctonyx collaris*), relatively broader zygomatic arches (e.g., male cacomistles, *Bassariscus sumichrasti*), and relatively flattened crania (e.g., male weasels, *Mustela* spp). However, we did not find a pattern between social system, dietary regimes, and the presence of these different shape dimorphisms. For example, fishers, coatis, and hog badgers all have pronounced sagittal crests but do not share the same social system or dietary regime: fishers are carnivorous and solitary, coatis are omnivorous and gregarious, and hog badgers are omnivorous and solitary (Fig. 3).

A possible explanation for the lack of relationship between cranial shape dimorphism and social system/dietary regimes is that changes in cranial shape may not be necessary to increase bite forces when species can simply increase their overall size. Size alone can drive ecomorphological diversification between species (Zelditch et al. 2017). Furthermore, size is the primary mechanism for increased cranial disparity in mammals and serves as a constraint for disparity in cranial shape (Cardini and Polly 2013; Cardini et al. 2015; Tamagnini 2017). Because the mammalian skull consists of few evolutionary modules that are highly integrated and selected to maintain peak performance (Goswami 2006; Porto et al. 2008), selective pressures may constrain the evolution of extreme cranial shape. Instead, bite force, like many performance traits, tends to scale positively with size across evolutionary ontogeny; therefore, size is a strong predictor of bite performance (Christiansen and Wroe 2007; Hartstone-Rose et al. 2012; Santana and Miller 2016). Alternatively, there may be multiple compensatory changes in cranial shape that may lead to the same bite force (i.e., many to one mapping); that is, evolutionary changes in cranial shape across different species can all lead to the same bite force output. Therefore, different degrees of sexual shape dimorphism can all lead to the same degree of bite force dimorphism. Consequently, there may not be an optimal shape dimorphism associated with different social system and/or dietary regime.

Consistent with these studies, we found a much stronger relationship between the degree of cranial size dimorphism and bite force dimorphism compared to relationships between the degree of cranial shape dimorphism and the degree of cranial size dimorphism as well as the degree of bite force dimorphism (Fig. 2). These results support the hypothesis that cranial size plays a larger role in facilitating bite force generation over cranial shape. Therefore, the evolution of diet maintains the evolution of sexual dimorphism in cranial size, which in turns shapes the performance disparities in the musteloid crania.

Additional processes aside from niche divergence and sexual selection may also drive the evolution of sexual dimorphism of the cranium and bite force. However, we did not observe unexpected shifts in the three metrics of sexual dimorphism with our bayou analyses. Although there was not a perfect correspondence between shifts in bayou and the lineages that form peaks with the OUwie analyses, the evolutionary shifts in bayou are consistent with what we predicted under niche divergence theory: reduced degree of sexual dimorphism in size and bite force were found in herbivorous and aquatic carnivorous musteloids whereas increased degree of sexual dimorphism in size and bite force were found in carnivorous musteloids (Fig. A3). We found only a single shift—on a branch toward fishers (*Pekania pennanti*)—in sexual shape dimorphism. These results confirm three major points. First, dietary ecology has the strongest effect on the evolution of sexual dimorphism in crania size and bite force. Second, neither niche divergence nor sexual selection strongly affects the evolution of sexual shape dimorphism in the crania. Third, hidden processes do not appear to strongly influence the evolution of crania and bite force dimorphism.

Conclusion

The evolution and maintenance of sexual dimorphism has long been attributed to sexual selection (Darwin 1871; Clutton-Brock 2007). Alternatively, niche divergence, a nonmutually exclusive mechanism for the evolution of sexual dimorphism (Darwin 1871; Shine 1989; Temeles et al. 2000) is rarely tested. Here, OU modeling of social system and diet support the hypothesis that niche divergence rather than sexual selection maintain the evolution of sexual dimorphism in cranial size and bite force across Musteloidea. We found greater degrees of sexual dimorphism in cranial size and bite force in terrestrial carnivores and that the degrees of cranial size and bite force dimorphism are highly correlated. In contrast, neither dietary regime nor social system influenced the evolution of sexual dimorphism in cranial shape. Overall, our results demonstrate the importance of diet in reducing intraspecific competition for resources as an important mechanism that maintains the evolution of sexual dimorphism in extant musteloids.

AUTHOR CONTRIBUTIONS

C.J.L. designed the study, collected geometric morphometric data, carried out data analysis, and drafted the manuscript; R.S.M. helped develop the approach, provided crucial insight, and revised the manuscript. Both authors read and approved the final manuscript.

ACKNOWLEDGMENTS

We thank Nancy Hung, Ekai Richards, Emma Duran, and Issac Santillan for helping collect bite force data; Abby Vander Lidden for helpful discussions about sexual dimorphism; Sarah Friedman, Sam Price, and Vikram Baliga for valuable R codes with our OUwie analyses; Kat Dale, Sarah Kienle, Sam Gartner, Kelley Voss, and Ben Higgins for helpful comments on earlier versions of this manuscripts; and Andrea Ward for motivation to write this article. We are grateful to the following natural history museums and their collection managers and curators for allowing us to visit and/or loan specimens: the American Museum of Natural History (AMNH), Academy of Natural Sciences of Drexel University (ANSP), Burke Museum (UWBM), California Academy of Sciences (CAS), Cornell University Museum of Vertebrates (CUMV), Denver Museum of Nature & Science (DMNS), Field Museum (FM), Florida Museum of Natural History (UF), KU Natural History Museum (KU), Natural History Museum of Los Angeles County (LACM), Louisiana Museum of Natural History (LSUMZ), Museum of Comparative Zoology (MCZ), Moore Laboratory of Zoology (MLZ), Muséum national d'Histoire naturelle (MNHN), Museum of Southwestern Biology (MSB), Museum of Vertebrate Zoology (MVZ), National Museum of Natural History (USNM), Texas Cooperative Wildlife Collection (TCWC), University of Arkansas Collections Facility (UAFMC), and University of Michigan Museum of Zoology

(UMMZ). C.J.L. also thanks Mimi Zelditch and Don Swiderski for the training and advice in geometric morphometric methods during the 2016 UC Berkeley geometric morphometric workshop and all the instructors for comparative methods training at the 2017 Bodega Bay Workshop. We also thank Mimi Zelditch and two anonymous reviewers for their helpful reviews. Funding for this project was provided by a National Science Foundation (NSF) Graduate Research Fellowship, a NSF Doctoral Dissertation Improvement Grant, a Collection Study Grant through the American Museum of Natural History, a Visiting Scholarship through the Field Museum, a James L. Patton Award through the American Society of Mammalogists, a Rosemary Grant Student Research Award through the Society for the Study of Evolution, and a Fellowship of Graduate Student Travel through the Society of Integrative and Comparative Biology.

The authors have declared no conflict of interests.

DATA ARCHIVING

The doi for our data is https://doi.org/10.5061/dryad.62517nb.

LITERATURE CITED

Abramov, A. V., and I. L. Tumanov. 2003. Sexual dimorphism in the skull of the European mink *Mustela lutreola* from NW part of Russia. Acta Theriol. 48:239–246.

Adams, D. C., and E. Otárola-Castillo. 2013. geomorph: an r package for the collection and analysis of geometric morphometric shape data. Methods Ecol. Evol. 4:393–399.

Bartholomew, G. A. 1970. A model for the evolution of pinniped polygyny. Evolution 24:546–559.

Beaulieu, J. M., D.-C. Jhwueng, C. Boettiger, and B. C. O'Meara. 2012. Modeling stabilizing selection: expanding the Ornstein–Uhlenbeck model of adaptive evolution. Evolution 66:2369–2383.

Berwaerts, K., P. Aerts, and H. Van Dyck. 2006. On the sex-specific mechanisms of butterfly flight: flight performance relative to flight morphology, wing kinematics, and sex in *Pararge aegeria*. Biol. J. Linn. Soc. 89:675–687.

Birks, J. D. S., and N. Dunstone. 1985. Sex-related differences in the diet of the mink *Mustela vison*. Holarctic Ecol. 8:245–252.

Bollback, J. 2006. SIMMAP: stochastic character mapping of discrete traits on phylogenies. BMC Bioinformatics 7:88–7.

Bookstein, F. L. 1996. Combining the tools of geometric morphometrics. Pp. 131–151 *in* L. F. Marcus, M. Corti, A. Loy, G. J. P. Naylor, and D. E. Slice, eds. Advances in morphometrics. Springer US, Boston, MA.

Bookstein, F. L. 1997. Landmark methods for forms without landmarks: morphometrics of group differences in outline shape. Med. Image Anal. 1:225–243.

Brunner, S., M. M. Bryden, and P. D. Shaughnessy. 2004. Cranial ontogeny of otariid seals. Syst. Biodiv. 2:83–110.

Butler, M. A., S. A. Sawyer, and J. B. Losos. 2007. Sexual dimorphism and adaptive radiation in *Anolis* lizards. Nature 447:202–205.

Cardini, A., and P. D. Polly. 2013. Larger mammals have longer faces because of size-related constraints on skull form. Nat. Comm. 4:2458.

Cardini, A., D. Polly, R. Dawson, and N. Milne. 2015. Why the long face? Kangaroos and wallabies follow the same "rule" of cranial evolutionary allometry (CREA) as placentals. Evol. Biol. 42:169–176.

Christiansen, P., and J. M. Harris. 2012. Variation in craniomandibular morphology and sexual dimorphism in pantherines and the sabercat *Smilodon fatalis*. PLoS ONE 7:e48352.

Christiansen, P., and S. Wroe. 2007. Bite forces and evolutionary adaptations to feeding ecology in carnivores. Ecology 88:347–358.

Clutton-Brock, T. 2007. Sexual selection in males and females. Science 318:1882–1885.

Clutton-Brock, T. H. 1982. The functions of antlers. Behaviour 79:108–124.

Darwin, C. 1871. The descent of man and selection in relation to sex. John Murray, London.

Dayan, T., and D. Simberloff. 1994. Character displacement, sexual dimorphism, and morphological variation among British and Irish mustelids. Ecology 75:1063–1073.

Dumont, M., C. E. Wall, L. Botton Divet, A. Goswami, S. Peigné, and A.-C. Fabre. 2015. Do functional demands associated with locomotor habitat, diet, and activity pattern drive skull shape evolution in musteloid carnivorans? Biol. J. Linn. Soc. 117:858–878.

Elliott Smith, E. A., S. D. Newsome, J. A. Estes, and M. T. Tinker. 2015. The cost of reproduction: differential resource specialization in female and male California sea otters. Oecologia 178:17–29.

Fabre, A. C., R. Cornette, G. Slater, C. Argot, S. Peigné, A. Goswami, and E. Pouydebat. 2013. Getting a grip on the evolution of grasping in musteloid carnivorans: a three-dimensional analysis of forelimb shape. J. Evol. Biol. 26:1521–1535.

Fabre, A.-C., R. Cornette, A. Goswami, and S. Peigné. 2015. Do constraints associated with the locomotor habitat drive the evolution of forelimb shape? A case study in musteloid carnivorans. J. Anatomy 226:596–610.

Fairbairn, D. J. 2013. Odd couples: extraordinary differences between the sexes in the animal kingdom. Princeton Univ. Press, Princeton, New Jersey.

Felsenstein, J. 1985. Phylogenies and the comparative method. Am. Nat. 125:1–15.

Funston, P. J., M. Mills, and H. C. Biggs. 2001. Factors affecting the hunting success of male and female lions in the Kruger National Park. J. Zool. 253:419–431.

Gittleman, J. L., and B. Van Valkenburgh. 1997. Sexual dimorphism in the canines and skulls of carnivores: effects of size, phylogency, and behavioural ecology. J. Zool. 242:97–117.

Goswami, A. 2006. Cranial modularity shifts during mammalian evolution. Am. Nat. 168:270–280.

Hairston, N. G., F. E. Smith, and L. B. Slobodkin. 1960. Community structure, population control, and competition. Am. Nat. 94:421–425.

Hartstone-Rose, A., J. M. G. Perry, and C. J. Morrow. 2012. Bite force estimation and the fiber architecture of felid masticatory muscles. Anat. Rec. 295:1336–1351.

Hedrick, A. V., and E. J. Temeles. 1989. The evolution of sexual dimorphism in animals: hypotheses and tests. Trends Ecol. Evolut. 4:136–138.

Hocking, D. P., F. G. Marx, T. Park, E. M. G. Fitzgerald, and A. R. Evans. 2017. A behavioural framework for the evolution of feeding in predatory aquatic mammals. Proc. R Soc. B 284:20162750.

Huelsenbeck, J. P., R. Nielsen, and J. P. Bollback. 2003. Stochastic mapping of morphological characters. Syst. Biol. 52:131–158.

Isaac, J. L. 2005. Potential causes and life-history consequences of sexual size dimorphism in mammals. Mammal Rev. 35:1–15.

Johnson, D. D. P., and D. W. Macdonald. 2001. Why are group-living badgers (*Meles meles*) sexually dimorphic? J. Zool. 255:199–204.

Johnson, D. D. P., D. W. Macdonald, and A. J. Dickman. 2000. An analysis and review of models of the sociobiology of the Mustelidae. Mammal Rev. 30:171–196.

Kienle, S. S., C. J. Law, D. P. Costa, A. Berta, and R. S. Mehta. 2017. Revisiting the behavioural framework of feeding in predatory aquatic mammals. Proc. R Soc. B 284:20171035.

Law, C. J., C. Young, and R. S. Mehta. 2016a. Ontogenetic scaling of theoretical bite force in southern sea otters (*Enhydra lutris nereis*). Physiol. Biochem. Zool. 89:347–363.

Law, C. J., G. J. Slater, and R. S. Mehta. 2018. Lineage diversity and size disparity in Musteloidea: testing patterns of adaptive radiation using molecular and fossil-based methods. Syst. Biol. 67:127–144.

Law, C. J., V. B. Baliga, M. T. Tinker, and R. S. Mehta. 2017. Asynchrony in craniomandibular development and growth in *Enhydra lutris nereis* (Carnivora: Mustelidae): are southern sea otters born to bite? Biol. J. Linn. Soc. 121:420–438.

Law, C. J., V. Venkatram, and R. S. Mehta. 2016b. Sexual dimorphism in craniomandibular morphology of southern sea otters (*Enhydra lutris nereis*). J. Mammal 97:1764–1773.

Lindenfors, P., B. Tullberg, and M. Biuw. 2002. Phylogenetic analyses of sexual selection and sexual size dimorphism in pinnipeds. Behav. Ecol. Sociobiol. 52:188–193.

Lindenfors, P., J. L. Gittleman, and K. E. Jones. 2007. Sexual size dimorphism in mammals. Pp. 16–26 *in* D. J. Fairbairn, W. U. Blanckenhorn, and T. Székely, eds. Sex, size and gender roles evolutionary studies of sexual size dimorphism. Oxford Univ. Press, Oxford.

Lovich, J. E., and J. W. Gibbons. 1992. A review of techniques for quantifying sexual size dimorphism. Growth Dev. Aging 56:269–281.

Lynch, J. M., and W. M. O'Sullivan. 1993. Cranial form and sexual dimorphism in the Irish otter *Lutra lutra L.* Biol. Environ. Proc. R Irish Acad. 93B:97–105.

Macdonald, D. W., and C. Newman. 2018. Musteloid sociality: the grass-roots of society. *in* D. W. Macdonald, C. Newman, and L. A. Harrington, eds. Biology and conservation of musteloids. Oxford Univ. Press, Oxford.

MacDonald, D. W., and D. D. P. Johnson. 2015. Patchwork planet: the resource dispersion hypothesis, society, and the ecology of life. J. Zool. 295:75–107.

McDonald, R. A. 2002. Resource partitioning among British and Irish mustelids. J. Anim. Ecol. 71:185–200.

McGee, M. D., and P. C. Wainwright. 2013. Sexual dimorphism in the feeding mechanism of threespine stickleback. J. Exp. Biol. 216:835–840.

Moors, P. J. 1980. Sexual dimorphism in the body size of mustelids (Carnivora): the roles of food habits and breeding systems. Oikos 34:147–158.

Morris, J. S., and D. R. Carrier. 2016. Sexual selection on skeletal shape in Carnivora. Evolution 70:767–780.

Newman, C., Y.-B. Zhou, C. D. Buesching, and Y. Kaneko. 2011. Contrasting sociality in two widespread, generalist, mustelid genera, *Meles* and *Martes*. Mammal Study 36:169–188.

Nielsen, R. 2002. Mapping mutations on phylogenies. Syst. Biol. 51:729–739.

Noonan, M. J., C. Newman, C. D. Buesching, and D. W. Macdonald. 2015. Evolution and function of fossoriality in the Carnivora: implications for group-living. Front. Ecol. Evol. 3:726–814.

Noonan, M. J., P. J. Johnson, A. C. Kitchener, L. A. Harrington, C. Newman, and D. W. Macdonald. 2016. Sexual size dimorphism in musteloids: an anomalous allometric pattern is explained by feeding ecology. Ecol. Evol. 6:8495–8501.

Orme, D. 2013. The caper package: comparative analysis of phylogenetics and evolution in R. R package version.

Pagel, M. 1999. Inferring the historical patterns of biological evolution. Nature 401:877–884.

Porto, A., F. B. de Oliveira, L. T. Shirai, V. De Conto, and G. Marroig. 2008. The evolution of modularity in the mammalian skull i: morphological integration patterns and magnitudes. Evol. Biol. 36:118–135.

Powell, R. A. 1979. Mustelid spacing patterns—variations on a theme by *Mustela*. Ethology 50:153–165.

Radinsky, L. B. 1981a. Evolution of skull shape in Carnivores. 1. Representative modern Carnivores. Biol. J. Linn. Soc. 15:369–388.

———. 1981b. Evolution of skull shape in carnivores: 2. Additional modern carnivores. Biol. J. Linn. Soc. 16:337–355.

Radloff, F., and J. T. Du Toit. 2004. Large predators and their prey in a southern African savanna: a predator's size determines its prey size range. J. Anim. Ecol. 73:410–423.

Ralls, K., and S. L. Mesnick. 2002. Sexual dimorphism. Pp. 1071–1078 *in* W. F. Perrin, B. Würsig, and J. G. M. Thewissen, eds. Academic Press, San Diego.

Revell, L. J. 2010. Phylogenetic signal and linear regression on species data. Methods Ecol. Evol. 1:319–329.

———. 2011. phytools: an R package for phylogenetic comparative biology (and other things). Methods Ecol. Evol. 3:217–223.

Rohlf, F. J., and D. Slice. 1990. Extensions of the procrustes method for the optimal superimposition of landmarks. Syst. Zool. 39:40–59.

Santana, S. E., and K. E. Miller. 2016. Extreme postnatal scaling in bat feeding performance: a view of ecomorphology from ontogenetic and macroevolutionary perspectives. Integr. Comp. Biol. 56:459–568.

Schlager, S. 2016. Morpho: calculations and visualisations related to geometric morphometrics. R-package version 2.4.

Schneider, C. A., W. S. Rasband, and K. W. Eliceiri. 2012. NIH Image to ImageJ: 25 years of image analysis. Nat. Meth. 9:671–675.

Shetty, S., and R. Shine. 2002. Sexual divergence in diets and morphology in Fijian sea snakes *Laticauda colubrina* (Laticaudinae). Austral. Ecol. 27:77–84.

Shine, R. 1989. Ecological causes for the evolution of sexual dimorphism—a review of the evidence. Q Rev. Biol. 64:419–461.

Smith, T. B. 1987. Bill size polymorphism and intraspecific niche utilization in an African finch. Nature 329:717–719.

Tamagnini, D. 2017. Anyone with a long-face? Craniofacial evolutionary allometry (CREA) in a family of short-faced mammals, the felidae. Evol. Biol. 44:476–495.

Temeles, E. J., I. L. Pan, J. L. Brennan, and J. N. Horwitt. 2000. Evidence for ecological causation of sexual dimorphism in a hummingbird. Science 289:441–443.

Temeles, E. J., J. S. Miller, and J. L. Rifkin. 2010. Evolution of sexual dimorphism in bill size and shape of hermit hummingbirds (Phaethornithinae): a role for ecological causation. Phil. Trans. R Soc. B 365:1053–1063.

Thom, M. D., and L. A. Harrington. 2004. Why are American mink sexually dimorphic? A role for niche separation. Oikos 105:525–535.

Thomason, J. J. 1991. Cranial strength in relation to estimated biting forces in some mammals. Can. J. Zool. 69:2326–2333.

Uyeda, J. C., and L. J. Harmon. 2014. A novel Bayesian method for inferring and interpreting the dynamics of adaptive landscapes from phylogenetic comparative data. Syst. Biol. 63:902–918.

Van Valkenburgh, B. 2007. Deja vu: the evolution of feeding morphologies in the Carnivora. Am. Zool. 47:147–163.

Weckerly, F. W. 1998. Sexual-size dimorphism: influence of mass and mating systems in the most dimorphic mammals. J. Mammal 79:33–52.

Wiig, Ø. 1985. Morphometric variation in the Hooded seal (Cystophora cristata). J. Zool. 206:497–508.

———. 1986. Sexual dimorphism in the skull of minks *Mustela vison*, badgers *Meles meles* and otters *Lutra lutra*. Zool. J. Linn. Soc. 87:163–179.

———. 1989. Craniometric variation in Norwegian wolverines *Gulo gulo L.* Zool. J. Linn Soc. 95:177–204.

Wilson, D. E., and R. A. Mittermeier. 2009. Handbook of the mammals of the world. Lynx Edicions, Spain.

Zalewski, A. 2007. Does size dimorphism reduce competition between sexes? The diet of male and female pine martens at local and wider geographical scales. Acta Theriol. 52:237–250.

Zelditch, M. L., D. L. Swiderski, and H. D. Sheets. 2012. Geometric morphometrics for biologists: A primer. Academic Press, Cambridge, Massachusetts.

Zelditch, M. L., J. Ye, J. S. Mitchell, and D. L. Swiderski. 2017. Rare ecomorphological convergence on a complex adaptive landscape: body size and diet mediate evolution of jaw shape in squirrels (Sciuridae). Evolution 71:633–649.

Associate Editor: M. Zelditch
Handling Editor: P. Tiffin

Supporting Information

Additional supporting information may be found online in the Supporting Information section at the end of the article.

Figure S1. Photographs of the cranium in A) posterodorsal, B) lateral, and C) ventral views used to estimate cross sectional areas (CSAs) and in-lever lengths of the temporalis and masseter-pterygoid complex.
Table S1. Museum catalog numbers for each specimen used in this study.
Table S2. Landmarks for Geometric Morphometrics.
Table S3. Dietary references.

BRIEF COMMUNICATION

doi:10.1111/evo.13514

Carnivory maintains cranial dimorphism between males and females: Evidence for niche divergence in extant Musteloidea

Chris J. Law [1,2] and Rita S. Mehta [1]

[1]Department of Ecology and Evolutionary Biology, University of California, Santa Cruz, Santa Cruz, California 95060

[2]E-mail: cjlaw@ucsc.edu

Received February 27, 2018

Accepted May 23, 2018

The evolution and maintenance of sexual dimorphism has long been attributed to sexual selection. Niche divergence, however, serves as an alternative but rarely tested selective pressure also hypothesized to drive phenotypic disparity between males and females. We reconstructed ancestral social systems and diet and used Ornstein–Uhlenbeck (OU) modeling approaches to test whether niche divergence is stronger than sexual selection in driving the evolution of sexual dimorphism in cranial size and bite force across extant Musteloidea. We found that multipeak OU models favored different dietary regimes over social behavior and that the greatest degree of cranial size and bite force dimorphism were found in terrestrial carnivores. Because competition for terrestrial vertebrate prey is greater than other dietary groups, increased cranial size and bite force dimorphism reduces dietary competition between the sexes. In contrast, neither dietary regime nor social system influenced the evolution of sexual dimorphism in cranial shape. Furthermore, we found that the evolution of sexual dimorphism in bite force is influenced by the evolution of sexual dimorphism in cranial size rather than cranial shape. Overall, our results highlight niche divergence as an important mechanism that maintains the evolution of sexual dimorphism in musteloids.

KEY WORDS: 3D geometric morphometrics, bite force, carnivore, cranial shape, sexual dimorphism, sexual selection.

Divergence between the sexes is a widespread phenomenon observed across the Tree of Life (Fairbairn 2013). Sexual selection has long been evoked as the primary mechanism for both the evolution and maintenance of morphological disparity between males and females (Darwin 1871; Clutton-Brock 2007). Under sexual selection theory, sexually dimorphic traits (e.g., antlers in deer (Clutton-Brock 1982) or increased body sizes in male elephant seals and sea lions (Bartholomew 1970)) evolved as a result of intrasexual competition, providing some individuals greater advantages in contests and/or attracting the opposite sex for breeding opportunities (Clutton-Brock 2007). An alternative hypothesis for the maintenance of sexual dimorphism is intersexual niche divergence (Darwin 1871; Shine 1989; Hedrick and Temeles 1989). Under the niche divergence hypothesis, disparity in phenotypic traits such as trophic morphologies reflect intraspecific differences in resource use, thereby reducing intersexual competition for resources in the environment (Smith 1987; Berwaerts et al. 2006; Butler et al. 2007; Temeles et al. 2010; McGee and Wainwright 2013). Although sexual selection and the niche divergence hypotheses are not mutually exclusive, empirical data supporting the intersexual niche divergence hypothesis are few due to the challenge of directly linking niche divergence and sexual dimorphism (Shine 1989; Hedrick and Temeles 1989). Nevertheless, the large breadth of ecomorphological studies to date (e.g., Dayan and Simberloff 1994; Shetty and Shine 2002; Butler et al. 2007; Temeles et al. 2010; McGee and Wainwright 2013) make a strong argument for the potential role of intersexual niche divergence in expanding the realized niche of a species. Within a clade, intersexual niche divergence could increase the evolution of intersexual differences in dietary composition and trophic morphologies such as the feeding apparatus.

Within carnivoran mammals (Carnivora), the intraspecific divergence of body sizes and craniomandibular morphology between the sexes is often attributed to sexual selection (Gittleman and Van Valkenburgh 1997; Morris and Carrier 2016). Most carnivorans exhibit male-biased sexual dimorphism in which males

are larger than females. Males with larger, stronger bodies and skulls are perceived as more effective in territorial conflicts with male competitors and thus achieve greater reproductive success (Gittleman and Van Valkenburgh 1997; Brunner et al. 2004). Therefore, the greatest degree of sexual size dimorphism is expected to occur in species that are highly territorial and solitary and exhibit polygynous mating systems. However, with the exception of pinnipeds, this pattern between social/mating system and degree of sexual dimorphism is not consistent across all carnivoran clades (Weckerly 1998; Isaac 2005; Lindenfors et al. 2007); the most territorial and solitary carnivorans are not always the most sexually dimorphic, and the least territorial and solitary carnivorans are not always the least sexually dimorphic. This unclear and sometimes conflicting pattern within extant carnivoran clades suggests that additional selective forces also contribute to the evolution and maintenance of sexual dimorphism in carnivorans.

Niche divergence and the partitioning of resources may provide a secondary mechanism that drives the evolution of sexual dimorphism. For example, the divergence of craniomandibular size and shape provides evidence of intersexual niche divergence (Thom and Harrington 2004; Christiansen and Harris 2012; Law et al. 2016b), where phenotypic differentiation in the skull reflects ecological divergence between the sexes and even reduction of intersexual competition for resources and habitat use. It is well documented that males and females of many carnivoran species utilize different dietary resources, often in the form of prey size where males consume larger prey than females (Birks and Dunstone 1985; Funston et al. 2001; McDonald 2002; Radloff and Toit 2004). Furthermore, across carnivorans there is a relationship between the degree of carnivory and the degree of sexual dimorphism in which more carnivorous species exhibit greater size dimorphism between males and females (Gittleman and Van Valkenburgh 1997; Noonan et al. 2016). This pattern is often attributed to the hypothesis that competition for vertebrate prey is likely greater than competition for plant material and nonvertebrate prey (Hairston et al. 1960; Noonan et al. 2015; MacDonald and Johnson 2015). Increased sexual dimorphism in obligate carnivores, therefore, reduces intraspecific dietary competition by reducing competition between males and females. In contrast, increased sexual dimorphism to reduce intraspecific competition is not necessary in species with a lower degree of carnivory (i.e., plant material, nonvertebrate prey) because these prey items are more abundant and easier to obtain (Hairston et al. 1960; Noonan et al. 2015; MacDonald and Johnson 2015).

In this study, we examine how sexual selection and niche divergence influenced the evolution of sexual dimorphism in the crania of musteloid carnivores. Musteloids (e.g., badgers, otters, raccoons, skunks, and weasels) are a speciose and ecologically diverse clade of carnivorans (Fabre et al. 2013, 2015; Dumont et al. 2015; Law et al. 2018). Members of Musteloidea exhibit diverse trophic ecologies, ranging from the generalist diets of raccoons to the specialized diets of the herbivorous red pandas, highly carnivorous weasels, and piscivorous otters. In addition, musteloids exhibit a range of sexual dimorphism from none to highly sexually dimorphic where males are more than twice the size of females (Wilson and Mittermeier 2009). Because almost all musteloid species exhibit polygynous mating systems, sexual selection is often hypothesized to have driven the evolution of sexual dimorphism (Moors 1980). Researchers, however, have also found interspecific differences in the feeding apparatus (Wiig 1986; Thom and Harrington 2004; Law et al. 2016a,b) and diet (Moors 1980; Birks and Dunstone 1985; Zalewski 2007; Elliott Smith et al. 2015), providing evidence that niche divergence may also be an important selective force in the evolution of sexual dimorphism in musteloids.

We use three-dimensional (3D) geometric morphometric and generalized Ornstein-Uhlenbeck (OU) modeling approaches to examine how social systems (a proxy for sexual selection) and diet (a proxy for natural selection via niche divergence) correspond with the evolution of sexual dimorphism in cranial shape, cranial size, and bite force across Musteloidea. We use social system as a proxy of mating system (Noonan et al. 2016) because the degree of polygyny for the majority of musteloids is unknown. Musteloids have varied social systems ranging from highly solitary musteloids that exhibit intrasexual territoriality in which one male defends a territory that may contain multiple female territories to highly social musteloids that tend to be monogamous or promiscuous (Johnson et al. 2000; Macdonald and Newman 2018). If sexual selection is the primary force driving sexual dimorphism, the degree of cranial sexual dimorphism should be greatest in solitary species and lowest in social species, suggesting that sexual dimorphism evolved as a response to male–male competition. Alternatively, if niche divergence is the primary force driving sexual dimorphism, the degree of cranial sexual dimorphism should be greatest in obligate carnivorous species that feed on less abundant vertebrate prey whereas the degree of cranial sexual dimorphism should be lowest in omnivorous and herbivorous musteloids that feed on nonvertebrate prey and plant material that more abundant and easier to obtain. This would suggest that intraspecific competition for less abundant resources facilitates the evolution of sexual dimorphism. Lastly, if both sexual selection and niche divergence are important drivers of sexual dimorphism in extant musteloids, the degree of cranial sexual dimorphism should be greatest in solitary, obligate carnivorous species.

Material and Methods

MORPHOLOGICAL DATA

We obtained 910 skull specimens across 63 musteloid species, sampling between one and 12 individuals per sex per species

(median = seven females and seven males per species) from 20 natural history museums (see Table A1 for list of specimens and museums). We 3D scanned each specimen using a Next Engine 3D Ultra HD surface scanner. All specimens were fully mature, determined by the closure of exoccipital–basioccipital and basisphenoid–basioccipital sutures on the cranium.

We quantified cranial size and shape using 3D geometric morphometrics (Rohlf and Slice 1990; Zelditch et al. 2012). Fifty-two landmarks and 85 semi-landmarks were digitized on the 3D scans using Stratovan Checkpoint and superimposed by Generalized Procrustes analysis (Rohlf and Slice 1990) to remove variation in position, size, and orientation (Fig. 1; Table A2). In addition, the Procrustes algorithm allowed semilandmarks on the curves to slide along their tangent vectors until their positions minimized bending energy (Bookstein 1997; Zelditch et al. 2012). After superimposition, bilaterally homologous landmarks on the ventral cranium were reflected across the midline and averaged using the geomorph function bilat.symmetry. We then quantified cranial size of each specimen by calculating the centroid size of each configuration of landmarks, that is the square root of the sum of the squared distances from each landmark to the geometric center of the shape (Bookstein 1996). All Procrustes superimposition was performed in the R package geomorph 3.0.5 (Adams and Otárola-Castillo 2013).

We used Thomason's (1991) dry skull method to estimate carnassial bite forces by estimating cross-sectional areas for the major jaw adductors and treating the jaw as a third class lever. We photographed each specimen in three views: (1) the cranium in posterodorsal view, photographed by orienting the cranium so that the plane between the orbital processes and posterior most points of the zygomatic arches is parallel to the photographic plane; (2) the cranium in ventral view, photographed by orienting the palate plane parallel to the photographic plane; and (3) the mandible in lateral view, photographed by orienting the long axis of the dentary parallel to the photographic plane. We then estimated cross-sectional areas (CSA) of the temporalis and masseter-pterygoid complex by outlining the left and right infratemporal fossae from the posterodorsal cranial and ventral cranial views, respectively (Fig. A1). The resulting areas were then multiplied by a muscle stress value 30 N/cm^2 to estimate forces of the temporalis (*T*) and masseter-pterygoid (*M*) complex. Each muscle force was modeled as a single force vector (*T* and *M*) and assumed to act through their centroids perpendicular to the plane of the muscle CSA. We then measured the moment arms (in-levers) of the temporalis (MAT) and masseter-pterygoid complex (MAM) as the distance from centroid to the temporomandibular joint (TMJ) using the lateral and ventral views of the cranium as well as the out-lever (O_M) as the distance from the bite point to the TMJ joint (Fig. A1). We estimated bite force at the carnassial by dividing the total moment

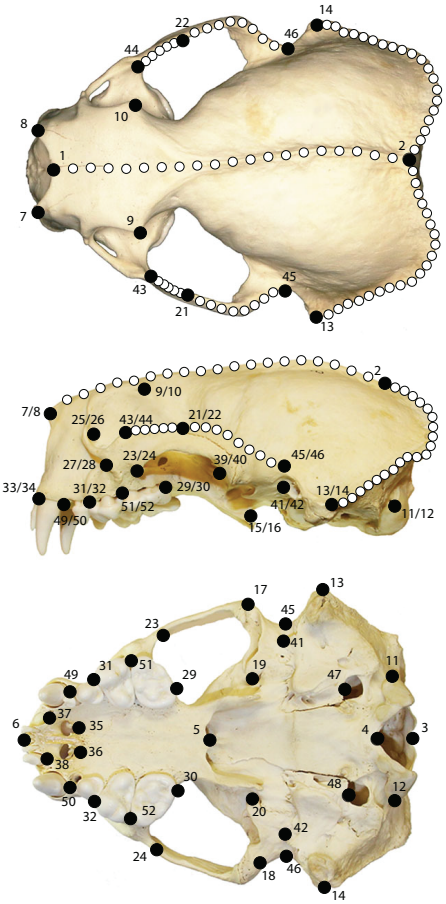

Figure 1. Landmarks (large black circles) and semi-landmarks (small white circles) used for geometric morphometric analysis of skull shape and size. Landmark descriptions are in Table A2.

by the out-lever and multiplied it by 2 to account for bilateral biting:

$$BF = 2\left(\frac{T \quad MAT + M \quad MAM}{O_M}\right)$$

We measured bite forces at the carnassial rather than the canine because food processing occurs at the carnassial in all musteloids across different dietary groups. All cross sectional areas and linear measurements were taken digitally using ImageJ v. 1.48 (Schneider et al. 2012).

DEGREE OF SEXUAL DIMORPHISM

We assessed the degree of sexual dimorphism in cranial size and bite force using the size dimorphism index (SDI) (Lovich and Gibbons 1992). We first determined the mean cranial size and bite force of males and females in each species and quantified SDI: $SDI = (\pm 1(\frac{S_M}{S_F} - 1))$ 100, where S_M and S_F are the mean centroid sizes or mean bite forces of males and females, respectively. A positive sign is assigned if the male trait is larger whereas a negative sign is assigned if the female trait is larger. There is no sexual dimorphism if $SDI = 0\%$. In contrast, the degree of sexual dimorphism in cranial shape cannot be quantified with SDI. Therefore, we quantified the degree of cranial shape dimorphism of each species by measuring the shape differences via Procrustes distance (P_D) between the mean female shape and mean male shape of each species with the permudist function in the R package Morpho 2.5.1 (Schlager 2016).

We examined the relationship between the degree of cranial size dimorphism, cranial shape dimorphism, and bite force dimorphism using phylogenetic generalized least-squares (PGLS) regression with R package caper (Orme 2013). All regression parameters were simultaneously estimated with phylogenetic signal in the residual error as Pagel's (Pagel 1999) lambda (Revell 2010). We also calculated the correlation coefficient between each of the relationships. We used the function phyl.vcv in the R package phytools (Revell 2011) to compute the phylogenetic trait variance-covariance matrix between the traits and used this matrix to calculate the correlation coefficient (r) of each relationship. PGLS regressions were performed using a recently constructed time-calibrated phylogeny of Musteloidea (Law et al. 2018).

ANCESTRAL RECONSTRUCTION OF SOCIAL SYSTEM AND DIETARY REGIMES

We used Johnson et al.'s (2000) categorical scheme to classify the 63 musteloids into one of four social systems: solitary, pair-living, group-living, and variable groups. Some species range from solitary to living in groups across different populations and the variable category captures this geographic difference in social systems. The data in the variable category reflect variation in social systems, which are not due to increased number of studies for these particular species.

We obtained dietary data primarily from *Mammalian Species* accounts (see Table A3 for references) and classified the 63 musteloids into one of four dietary categories: herbivory with diets consisting of > 90% plant material, omnivory (hypocarnivory) with diets consisting of > 70% nonplant and nonvertebrates (e.g., insects, earthworms), terrestrial carnivory with diets consisting of > 50% terrestrial vertebrates (e.g. rodents, amphibians, reptiles), and aquatic carnivory with diets consisting of > 90% aquatic prey (e.g., fish, crustaceans, molluscs). Our four dietary categories roughly follow Van Valkenburgh's (2007) classification deviating by the addition of the herbivorous and aquatic carnivorous categories and the combination of hypercarnivorous and mesocarnivorous as terrestrial carnivorous. We separated aquatic diets from terrestrial diets for two reasons. First, aquatic mammals exhibit unique morphological and behavioral adaptations that allow them to target aquatic prey (Hocking et al. 2017; Kienle et al. 2017). Second, the aquatic environment can influence shifts in the degree of sexual size dimorphism in mammals (Ralls and Mesnick 2002; Lindenfors et al. 2002).

We examined the evolution of social systems, dietary regimes, and social system dietary regimes independently by performing ancestral state reconstructions using 1000 stochastic character mapping simulations (Nielsen 2002; Huelsenbeck et al. 2003; Bollback 2006) with the make.simmap function in the phytools R package (Revell 2011).

GENERALIZED ORNSTEIN–UHLENBECK MODELING

We assessed the fit of eight evolutionary models to our three metrics of sexual dimorphism (SDI for cranial size dimorphism, Procrustes distances for cranial shape dimorphism, and SDI for bite force dimorphism) to determine the influence of social system and diet on the evolution of sexual dimorphism. The two simplest models, a single-rate Brownian (BM1) model that assumes trait variance accumulates proportional to evolutionary time under a random walk (Felsenstein 1985) and a single-optimum Ornstein–Uhlenbeck (OU1) model that constrains traits to evolve toward one optimum, allow the degree of sexual dimorphism to evolve independently of dietary and social system regimes. The remaining six models are multi-peak OU models that allow social system/dietary regimes to exhibit different strengths of attraction (α) and/or rates of stochastic motion of trait evolution ($\sigma 2$) toward separate trait optima (θ). The OUM multipeak model allows for separate θ but does not permit $\sigma 2$ and α to vary between regimes. In contrast, the OUMA multipeak model estimates separate α parameters for each θ, whereas the OUMV multipeak model estimates separate $\sigma 2$ parameters for each θ. Lastly, the full OUMVA multipeak model allows both parameters (α and $\sigma 2$) to vary with each θ. Support for any of these multipeak models would suggest that social system, diet, or the combination of social system and diet influences the evolution of sexual dimorphism. We performed our OU modeling across all 1000 stochastically mapped trees to take into account uncertainty in the ancestral character states with the function OUwie in the R package OUwie (Beaulieu et al. 2012). We evaluated the best-fitting model for each dimorphism metric using corrected Aikaike Information Criterion (AICc) weights. We then generated a 95% confidence interval for all model parameters (θ, α, and $\sigma 2$) of the best-fit model. Bootstrapping was performed for 1000 replicates using the function OUwie.boot.

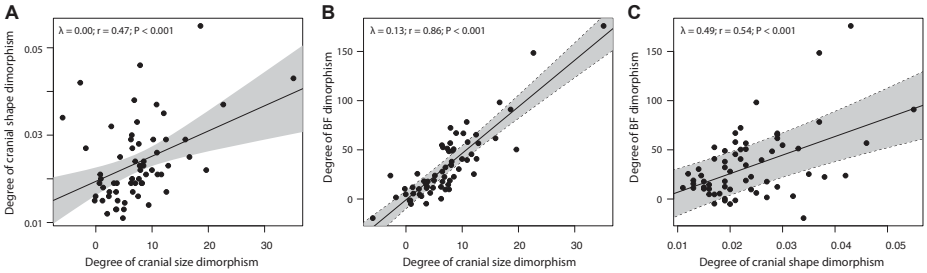

Figure 2. PGLS regressions between (A) the degree of cranial size dimorphism and cranial shape dimorphism, (B) the degree of cranial size dimorphism and bite force dimorphism, and (C) the degree of cranial shape dimorphism and bite force dimorphism with 95% confidence intervals (shaded polygons).

Additional processes aside from niche divergence and sexual selection may also drive the evolution of sexual dimorphism in the cranium and bite force. These hidden processes are not captured by our OUwie analyses under our hypothesis-testing framework of niche divergence and sexual selection. Therefore, we also used bayou (Uyeda and Harmon 2014) to determine if additional shifts of sexual dimorphism occur on branches not predicted by niche divergence or sexual selection. Bayou uses a reversible-jump Bayesian approach that fits multioptimum OU models to estimate the placement and magnitude of regime shifts without a priori designation of dietary ecology and social systems. Using the *make.prior* function in bayou, we placed a Poisson prior with lambda = 15 on the number of shifts between adaptive regimes. Additionally, we allowed only one shift per branch with equal probability that each branch has a shift. We ran two independent MCMC analyses with one million generations each and examined if the two chains converged using Gelman and Rubin's R statistic. All effective sample sizes were > 200 after discarding the first 30% of samples as burn-in. We then examined the posterior probabilities (pp) for regime shift locations and magnitudes.

Results

SEXUAL DIMORPHISM IN MUSTELOID CRANIA

We found extensive variation in the degree of sexual dimorphism across Musteloidea in each of our three dimorphic metrics (Fig. A2 A–C). Our PGLS regressions indicated significant positive relationships between the degree of cranial size dimorphism, cranial shape dimorphism, and bite force dimorphism (Fig. 2). Phylogenetic correlation tests reveal strong correlations between the degree of cranial size dimorphism and bite force dimorphism ($r = 0.86$) but weaker correlations between the degree of cranial shape dimorphism with cranial size dimorphism ($r = 0.47$) and bite force dimorphism ($r = 0.54$).

ANCESTRAL RECONSTRUCTION OF SOCIAL SYSTEM AND DIETARY REGIMES

Ancestral reconstructions of social systems across 1000 simulations revealed that solitary-living is the ancestral state of musteloids (Fig. 3A). Group-living evolved on average 7.80 times—kinkajou (*Potus flavus*), coatis (*Nasua* spp.), *Meles* badgers, and four independent evolutions in otters. Pair-living evolved on average 2.06 times—Sunda stink-badger (*Mydaus javanensis*) and yellow-throated marten (*Martes flavigula*). Variable social systems evolved on average 5.39 times—raccoons (*Procyon* spp.), tayra (*Eira barbara*), grisons (*Galictis* spp.), Eurasian otter (*Lutra lutra*), and African clawless otter (*Aonyx capensis*).

For dietary regimes, omnivory is the ancestral state of musteloids (Fig. 3B). Across our 1000 simmap simulations, herbivory evolved on average 3.01 times—red panda (*Ailurus fulgens*), kinkajou (*Potos flavus*), and olingos (*Bassaricyon* spp.)—and carnivory evolved on average 3.51 times—spotted skunks (*Spilogale* spp.), ringtail (*Bassariscus astutus*), and Mustelidae. Within carnivory, omnivory reevolved on average 2.62 times—meline badgers and ferret-badgers (*Melogale* spp.)—and aquatic carnivory evolved on average 1.042 times in otters.

GENERALIZED ORNSTEIN-UHLENBECK (OU) MODELING OF SOCIAL SYSTEMS AND DIET

Multipeak OU models (OUM and OUMV) with separate optima under dietary regimes were strongly favored for cranial size dimorphism and bite force dimorphism ($w_A > 0.99$; Table 1). These results indicate that diet rather than social system influence the evolution of cranial size and bite force dimorphism in musteloids. Specifically, the OUM and OUMV models along with parametric bootstrapping revealed that the four dietary regimes exhibited separate optima for the degree of male-biased cranial size dimorphism (terrestrial carnivory $\theta = 10.39\%$ [7.93%, 12.95%]; omnivory $\theta = 7.40\%$ [4.97%, 9.61%]; aquatic carnivory $\theta = 3.80\%$ [1.79%,

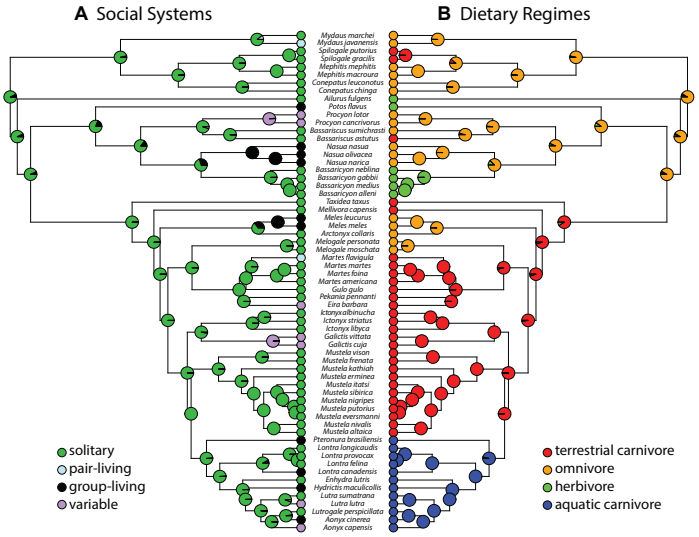

Figure 3. Ancestral state reconstruction of (A) social systems and (B) dietary regimes mapped onto a pruned time-calibrated phylogeny of 63 musteloid species. Pie charts on each node show the relative Bayesian posterior probability of each character state across 1000 simulations.

5.71%]; herbivory θ = –0.09% [–4.42%, 2.74%]) and male-biased bite force dimorphism (terrestrial carnivory θ = 50.45% [34.75%, 66.53%]; omnivory θ = 33.92% [22.63%, 45.98%]; aquatic carnivory θ = 12.49% [5.71%, 18.61%]; herbivory θ = –2.74% [–12.24%, 5.91%]). These results reveal that terrestrial carnivorous musteloids exhibited the greatest degree of male-biased sexual dimorphism in cranial size and bite force whereas herbivorous musteloids exhibited the lowest degree of male-biased sexual dimorphism (Fig. 4). The OUMV model (w_A = 0.73) was supported over the OUM model (w_A = 0.26) for cranial size dimorphism, suggesting that the evolutionary rates of cranial size dimorphism also differed between the four dietary regimes (Table 1). However, parametric bootstrapping revealed that these evolutionary rates were largely overlapping, cautioning any interpretation. OU modeling approaches are sensitive to sample sizes; therefore, these overlapping rate estimates may be due to the low number of species (63 species) (Beaulieu et al. 2012). Multipeak OU models under the social system and social system dietary regimes were not well supported and exhibited ΔAICc scores less than a single peak OU model (Table 1).

In contrast, a single peak OU model was favored over multipeak OU models for cranial shape dimorphism (w_A = 0.86; Table 1). This suggests that neither diet nor social system strongly influences the evolution of cranial shape dimorphism.

EVOLUTIONARY SHIFTS IN SEXUAL DIMORPHISM

With bayou, we found that significant regime shifts (posterior probability > 0.3) primarily occurred closer to the species tips (Fig. A3). We found evolutionary shifts toward lower size dimorphism in herbivorous olingos, hypocarnivorous ferret-badgers, and some aquatic carnivorous otters whereas only a single evolutionary shift toward greater sexual size dimorphism in the hypercarnivorous Japanese weasel (Fig. A3A). In contrast, we found one significant shift in shape dimorphism—within the hypercarnivorous fisher (Fig. A3B). Lastly, evolutionary shifts toward lower bite force dimorphism occurs in herbivorous olingos and a clade comprising of hypercarnivorous, hypocarnivorous, and aquatic carnivorous mustelids with a subsequent evolutionary shift toward higher bite force dimorphism in hypercarnivorous weasels (Fig. A3C).

Discussion

We found evidence that niche divergence is stronger than sexual selection in driving the evolution of sexual dimorphism in Musteloidea. Specifically, multipeak OU models under dietary regimes were strongly favored for cranial size and bite force dimorphism, suggesting that niche divergence maintains the evolution of sexual dimorphism in cranial size and bite force across

Table 1. Comparisons of evolutionary model fits for cranial size, cranial shape, and bite force. Mean Akaike information criterion (AICc) is the averaged AICc over 1000 replications and ΔAICc is the model's mean AICc minus the minimum AICc between models.

model	Optimal regimes	loglik	AICc	ΔAICc	w_A
Cranial size Dimorphism					
BM	NA	−218.98	442.16	37.42	0.00
OU	NA	−203.32	413.04	8.30	0.01
OUM	Diet	−196.65	406.79	2.05	0.26
OUMV	**Diet**	**−191.67**	**404.74**	**0.00**	**0.73**
OUM	Social system	−202.30	418.10	13.36	0.00
OUMV	Social system	−198.38	418.16	13.43	0.00
OUM	Social system diet	−193.28	423.30	18.56	0.00
OUMV	Social system diet	–	–	–	–
Cranial shape Dimorphism					
BM	NA	178.55	−352.89	36.08	0.00
OU	**NA**	**197.69**	**−388.97**	**0.00**	**0.86**
OUM	Diet	198.22	−382.94	6.03	0.04
OUMV	Diet	200.38	−379.37	9.60	0.01
OUM	Social system	199.01	−384.51	4.46	0.09
OUMV	Social system	–	–	–	–
OUM	Social system diet	200.41	−378.92	10.05	0.01
OUMV	Social system diet	–	–	–	–
Bite force Dimorphism					
BM	NA	−319.42	643.05	48.63	0.00
OU	NA	−307.26	620.93	26.51	0.00
OUM	Diet	−302.54	618.58	24.16	0.00
OUMV	**Diet**	**−286.51**	**594.42**	**0.00**	**1.00**
OUM	Social system	−306.33	626.16	31.74	0.00
OUMV	Social system	−302.12	625.64	31.22	0.00
OUM	Social system diet	−298.19	633.13	38.71	0.00
OUMV	Social system diet	–	–	–	–

Bolded rows represent the best-fit model as indicated by Akaike weights (w_A). Indicate models that were unable to converge. OUMA and OUMVA models did not converge for all sexual dimorphism metrics.

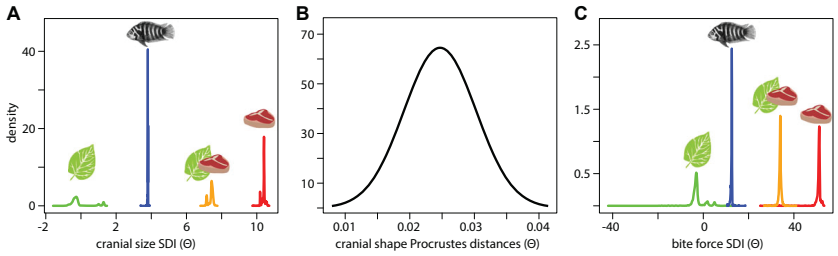

Figure 4. Density plots of the estimated optima from the best-fitting generalized Ornstein–Uhlenbeck (OU) model of (A) cranial size dimorphism, (B) cranial shape dimorphism, and (C) bite force dimorphism. Multi-peak OU models with separate optima under dietary regimes (herbivory, green; aquatic carnivory, blue; omnivory, orange; and terrestrial carnivory, red) were the best-fitting models for cranial size dimorphism and bite force dimorphism. A single peak OU model was the best-fitting model for cranial shape dimorphism.

extant musteloids. Carnivorous musteloids exhibit the greatest degree of sexual dimorphism in cranial size and bite force, whereas herbivorous musteloids exhibit the lowest degree of sexual dimorphism. These results support previous findings (Noonan et al. 2016) that the degree of sexual dimorphism in body size is related to the degree of carnivory on terrestrial vertebrates. Because competition for terrestrial vertebrate prey is greater than for plant material, nonvertebrate prey (Hairston et al. 1960; Noonan et al. 2015; MacDonald and Johnson 2015), and aquatic vertebrate prey, increased sexual dimorphism is thought to reduce dietary competition between male and female carnivores under niche divergence. Field observations and dietary analyses support this scenario, finding that males of many carnivorous musteloids (e.g., martens, minks, and weasels) target different, and often larger, prey items than females (Moors 1980; Birks and Dunstone 1985; Zalewski 2007). Following predictions of niche divergence, omnivorous and herbivorous musteloids exhibit reduced degrees of sexual dimorphism as nonvertebrate prey and plant material are more abundant and easier to obtain therefore reducing intraspecific competition (Hairston et al. 1960; Noonan et al. 2015; MacDonald and Johnson 2015). Aquatic carnivorous musteloids (e.g., otters) also exhibit reduced degrees of sexual size dimorphism. Otters specialize on a variety of prey from hard-shelled invertebrates to fish, and further examination of each individual species confirmed reduced degree of cranial size and bite force dimorphism compared to terrestrial carnivorous musteloids.

Although our results indicate that dietary regimes influenced the evolution of sexual dimorphism in musteloid crania, social systems may nevertheless have confounding effects on sexual dimorphism. It has been noted that carnivorous musteloids tend to be territorial and solitary and exhibit the greatest sexual size dimorphism, whereas omnivorous musteloids tend to form group systems and display a decrease in sexual size dimorphism (Johnson et al. 2000; Johnson and Macdonald 2001; MacDonald and Johnson 2015). Noonan et al. (2016) speculated that these different dietary regimes, herbivory to carnivory, could have facilitated different social and mating systems, which in turn could have led to different degrees of sexual dimorphism across Musteloidea. That is, carnivores exhibit great intraspecific competition for prey and mates and therefore remain solitary and territorial (Powell 1979; Newman et al. 2011). Sexual dimorphism in body size is then maintained under sexual selection in which males compete for females under a polygynous mating system (Moors 1980). Omnivores and herbivores, in contrast, are hypothesized to form group systems because of the reduced intraspecific competition for food items (Johnson et al. 2000; MacDonald and Johnson 2015; Noonan et al. 2015). The formation of these groups is thought to lead to reduced sexual selection of increased male body sizes because members of both sexes exhibit a promiscuous mating system and individuals mate with multiple partners (Johnson et al. 2000; Johnson and Macdonald 2001; MacDonald and Johnson 2015; Noonan et al. 2016). However, our ancestral state reconstructions of extant social system and dietary regimes reveal that there is no clear pattern between the degree of carnivory and the degree of social system (Fig. 3). Solitary-living is the ancestral condition in musteloids during the Early Oligocene whereas carnivorous diets did not appear until the Early Miocene near the base of Mustelidae. Similarly, the majority of omnivorous musteloids do not exhibit a group social system as suggested by Noonan et al. (Noonan et al. 2016). Rather, our data support the hypothesis that sexual selection may have been the original mechanism for the evolution of sexual dimorphism in Musteloidea (Moors 1980) but that niche divergence maintains the divergence between the sexes. The subsequent evolution of different dietary regimes contributed to further evolution of sexual dimorphism across extant musteloid clades, specifically through the intensification and relaxation of the degree of sexual dimorphism of the crania in carnivorous musteloids and noncarnivorous musteloids, respectively. We encourage future efforts of gathering higher resolution dietary data to better understand how prey size relates to male/female predator size and to help detect subtle differences in polygynous mating systems and its potential effects on sexual dimorphism.

We found that neither social system nor dietary regimes had strong influences on the evolution of sexual dimorphism of cranial shape. Cranial shape, instead, evolved toward the same dimorphism optimum under a single rate OU model across the entire clade. Many musteloid species exhibit cranial shape dimorphism, driven particularly by relatively wider zygomatic arches, larger canines, robust mastoid breadth, and more pronounced sagittal crests in males (Wiig 1985, 1989; Lynch and O'Sullivan 1993; Abramov and Tumanov 2003; Thom and Harrington 2004; Law et al. 2016b, 2017). Relatively larger craniomandibular traits translate to relative increases in jaw adductor muscle attachment sites (Radinsky 1981a,b but see Law et al. 2016a), thereby facilitating stronger biting ability and heavier heads that can be used in territorial conflicts with male competitors or for capturing and processing larger prey items. We find that species with the highest degree of cranial shape dimorphism exhibit relatively larger sagittal crests (e.g., male fishers, *Pekania pennanti*; coatis, *Nasua* and *Nasuella* spp.; and hog badgers, *Arctonyx collaris*), relatively broader zygomatic arches (e.g., male cacomistles, *Bassariscus sumichrasti*), and relatively flattened crania (e.g., male weasels, *Mustela* spp). However, we did not find a pattern between social system, dietary regimes, and the presence of these different shape dimorphisms. For example, fishers, coatis, and hog badgers all have pronounced sagittal crests but do not share the same social system or dietary regime: fishers are carnivorous and solitary, coatis are omnivorous and gregarious, and hog badgers are omnivorous and solitary (Fig. 3).

A possible explanation for the lack of relationship between cranial shape dimorphism and social system/dietary regimes is that changes in cranial shape may not be necessary to increase bite forces when species can simply increase their overall size. Size alone can drive ecomorphological diversification between species (Zelditch et al. 2017). Furthermore, size is the primary mechanism for increased cranial disparity in mammals and serves as a constraint for disparity in cranial shape (Cardini and Polly 2013; Cardini et al. 2015; Tamagnini 2017). Because the mammalian skull consists of few evolutionary modules that are highly integrated and selected to maintain peak performance (Goswami 2006; Porto et al. 2008), selective pressures may constrain the evolution of extreme cranial shape. Instead, bite force, like many performance traits, tends to scale positively with size across evolutionary ontogeny; therefore, size is a strong predictor of bite performance (Christiansen and Wroe 2007; Hartstone-Rose et al. 2012; Santana and Miller 2016). Alternatively, there may be multiple compensatory changes in cranial shape that may lead to the same bite force (i.e., many to one mapping); that is, evolutionary changes in cranial shape across different species can all lead to the same bite force output. Therefore, different degrees of sexual shape dimorphism can all lead to the same degree of bite force dimorphism. Consequently, there may not be an optimal shape dimorphism associated with different social system and/or dietary regime.

Consistent with these studies, we found a much stronger relationship between the degree of cranial size dimorphism and bite force dimorphism compared to relationships between the degree of cranial shape dimorphism and the degree of cranial size dimorphism as well as the degree of bite force dimorphism (Fig. 2). These results support the hypothesis that cranial size plays a larger role in facilitating bite force generation over cranial shape. Therefore, the evolution of diet maintains the evolution of sexual dimorphism in cranial size, which in turns shapes the performance disparities in the musteloid crania.

Additional processes aside from niche divergence and sexual selection may also drive the evolution of sexual dimorphism of the cranium and bite force. However, we did not observe unexpected shifts in the three metrics of sexual dimorphism with our bayou analyses. Although there was not a perfect correspondence between shifts in bayou and the lineages that form peaks with the OUwie analyses, the evolutionary shifts in bayou are consistent with what we predicted under niche divergence theory: reduced degree of sexual dimorphism in size and bite force were found in herbivorous and aquatic carnivorous musteloids whereas increased degree of sexual dimorphism in size and bite force were found in carnivorous musteloids (Fig. A3). We found only a single shift—on a branch toward fishers (*Pekania pennanti*)—in sexual shape dimorphism. These results confirm three major points. First, dietary ecology has the strongest effect on the evolution of sexual dimorphism in crania size and bite force. Second, neither niche divergence nor sexual selection strongly affects the evolution of sexual shape dimorphism in the crania. Third, hidden processes do not appear to strongly influence the evolution of crania and bite force dimorphism.

Conclusion

The evolution and maintenance of sexual dimorphism has long been attributed to sexual selection (Darwin 1871; Clutton-Brock 2007). Alternatively, niche divergence, a nonmutually exclusive mechanism for the evolution of sexual dimorphism (Darwin 1871; Shine 1989; Temeles et al. 2000) is rarely tested. Here, OU modeling of social system and diet support the hypothesis that niche divergence rather than sexual selection maintain the evolution of sexual dimorphism in cranial size and bite force across Musteloidea. We found greater degrees of sexual dimorphism in cranial size and bite force in terrestrial carnivores and that the degrees of cranial size and bite force dimorphism are highly correlated. In contrast, neither dietary regime nor social system influenced the evolution of sexual dimorphism in cranial shape. Overall, our results demonstrate the importance of diet in reducing intraspecific competition for resources as an important mechanism that maintains the evolution of sexual dimorphism in extant musteloids.

AUTHOR CONTRIBUTIONS

C.J.L. designed the study, collected geometric morphometric data, carried out data analysis, and drafted the manuscript; R.S.M. helped develop the approach, provided crucial insight, and revised the manuscript. Both authors read and approved the final manuscript.

ACKNOWLEDGMENTS

We thank Nancy Hung, Ekai Richards, Emma Duran, and Issac Santillan for helping collect bite force data; Abby Vander Lidden for helpful discussions about sexual dimorphism; Sarah Friedman, Sam Price, and Vikram Baliga for valuable R codes with our OUwie analyses; Kat Dale, Sarah Kienle, Sam Gartner, Kelley Voss, and Ben Higgins for helpful comments on earlier versions of this manuscripts; and Andrea Ward for motivation to write this article. We are grateful to the following natural history museums and their collection managers and curators for allowing us to visit and/or loan specimens: the American Museum of Natural History (AMNH), Academy of Natural Sciences of Drexel University (ANSP), Burke Museum (UWBM), California Academy of Sciences (CAS), Cornell University Museum of Vertebrates (CUMV), Denver Museum of Nature & Science (DMNS), Field Museum (FM), Florida Museum of Natural History (UF), KU Natural History Museum (KU), Natural History Museum of Los Angeles County (LACM), Louisiana Museum of Natural History (LSUMZ), Museum of Comparative Zoology (MCZ), Moore Laboratory of Zoology (MLZ), Muséum national d'Histoire naturelle (MNHN), Museum of Southwestern Biology (MSB), Museum of Vertebrate Zoology (MVZ), National Museum of Natural History (USNM), Texas Cooperative Wildlife Collection (TCWC), University of Arkansas Collections Facility (UAFMC), and University of Michigan Museum of Zoology

(UMMZ). C.J.L. also thanks Mimi Zelditch and Don Swiderski for the training and advice in geometric morphometric methods during the 2016 UC Berkeley geometric morphometric workshop and all the instructors for comparative methods training at the 2017 Bodega Bay Workshop. We also thank Mimi Zelditch and two anonymous reviewers for their helpful reviews. Funding for this project was provided by a National Science Foundation (NSF) Graduate Research Fellowship, a NSF Doctoral Dissertation Improvement Grant, a Collection Study Grant through the American Museum of Natural History, a Visiting Scholarship through the Field Museum, a James L. Patton Award through the American Society of Mammalogists, a Rosemary Grant Student Research Award through the Society for the Study of Evolution, and a Fellowship of Graduate Student Travel through the Society of Integrative and Comparative Biology.

The authors have declared no conflict of interests.

DATA ARCHIVING

The doi for our data is https://doi.org/10.5061/dryad.62517nb.

LITERATURE CITED

Abramov, A. V., and I. L. Tumanov. 2003. Sexual dimorphism in the skull of the European mink *Mustela lutreola* from NW part of Russia. Acta Theriol. 48:239–246.

Adams, D. C., and E. Otárola-Castillo. 2013. geomorph: an r package for the collection and analysis of geometric morphometric shape data. Methods Ecol. Evol. 4:393–399.

Bartholomew, G. A. 1970. A model for the evolution of pinniped polygyny. Evolution 24:546–559.

Beaulieu, J. M., D.-C. Jhwueng, C. Boettiger, and B. C. O'Meara. 2012. Modeling stabilizing selection: expanding the Ornstein–Uhlenbeck model of adaptive evolution. Evolution 66:2369–2383.

Berwaerts, K., P. Aerts, and H. Van Dyck. 2006. On the sex-specific mechanisms of butterfly flight: flight performance relative to flight morphology, wing kinematics, and sex in *Pararge aegeria*. Biol. J. Linn. Soc. 89:675–687.

Birks, J. D. S., and N. Dunstone. 1985. Sex-related differences in the diet of the mink *Mustela vison*. Holarctic Ecol. 8:245–252.

Bollback, J. 2006. SIMMAP: stochastic character mapping of discrete traits on phylogenies. BMC Bioinformatics 7:88–7.

Bookstein, F. L. 1996. Combining the tools of geometric morphometrics. Pp. 131–151 *in* L. F. Marcus, M. Corti, A. Loy, G. J. P. Naylor, and D. E. Slice, eds. Advances in morphometrics. Springer US, Boston, MA.

Bookstein, F. L. 1997. Landmark methods for forms without landmarks: morphometrics of group differences in outline shape. Med. Image Anal. 1:225–243.

Brunner, S., M. M. Bryden, and P. D. Shaughnessy. 2004. Cranial ontogeny of otariid seals. Syst. Biodiv. 2:83–110.

Butler, M. A., S. A. Sawyer, and J. B. Losos. 2007. Sexual dimorphism and adaptive radiation in *Anolis* lizards. Nature 447:202–205.

Cardini, A., and P. D. Polly. 2013. Larger mammals have longer faces because of size-related constraints on skull form. Nat. Comm. 4:2458.

Cardini, A., D. Polly, R. Dawson, and N. Milne. 2015. Why the long face? Kangaroos and wallabies follow the same "rule" of cranial evolutionary allometry (CREA) as placentals. Evol. Biol. 42:169–176.

Christiansen, P., and J. M. Harris. 2012. Variation in craniomandibular morphology and sexual dimorphism in pantherines and the sabercat *Smilodon fatalis*. PLoS ONE 7:e48352.

Christiansen, P., and S. Wroe. 2007. Bite forces and evolutionary adaptations to feeding ecology in carnivores. Ecology 88:347–358.

Clutton-Brock, T. 2007. Sexual selection in males and females. Science 318:1882–1885.

Clutton-Brock, T. H. 1982. The functions of antlers. Behaviour 79:108–124.

Darwin, C. 1871. The descent of man and selection in relation to sex. John Murray, London.

Dayan, T., and D. Simberloff. 1994. Character displacement, sexual dimorphism, and morphological variation among British and Irish mustelids. Ecology 75:1063–1073.

Dumont, M., C. E. Wall, L. Botton Divet, A. Goswami, S. Peigné, and A.-C. Fabre. 2015. Do functional demands associated with locomotor habitat, diet, and activity pattern drive skull shape evolution in musteloid carnivorans? Biol. J. Linn. Soc. 117:858–878.

Elliott Smith, E. A., S. D. Newsome, J. A. Estes, and M. T. Tinker. 2015. The cost of reproduction: differential resource specialization in female and male California sea otters. Oecologia 178:17–29.

Fabre, A. C., R. Cornette, G. Slater, C. Argot, S. Peigné, A. Goswami, and E. Pouydebat. 2013. Getting a grip on the evolution of grasping in musteloid carnivorans: a three-dimensional analysis of forelimb shape. J. Evol. Biol. 26:1521–1535.

Fabre, A.-C., R. Cornette, A. Goswami, and S. Peigné. 2015. Do constraints associated with the locomotor habitat drive the evolution of forelimb shape? A case study in musteloid carnivorans. J. Anatomy 226:596–610.

Fairbairn, D. J. 2013. Odd couples: extraordinary differences between the sexes in the animal kingdom. Princeton Univ. Press, Princeton, New Jersey.

Felsenstein, J. 1985. Phylogenies and the comparative method. Am. Nat. 125:1–15.

Funston, P. J., M. Mills, and H. C. Biggs. 2001. Factors affecting the hunting success of male and female lions in the Kruger National Park. J. Zool. 253:419–431.

Gittleman, J. L., and B. Van Valkenburgh. 1997. Sexual dimorphism in the canines and skulls of carnivores: effects of size, phylogency, and behavioural ecology. J. Zool. 242:97–117.

Goswami, A. 2006. Cranial modularity shifts during mammalian evolution. Am. Nat. 168:270–280.

Hairston, N. G., F. E. Smith, and L. B. Slobodkin. 1960. Community structure, population control, and competition. Am. Nat. 94:421–425.

Hartstone-Rose, A., J. M. G. Perry, and C. J. Morrow. 2012. Bite force estimation and the fiber architecture of felid masticatory muscles. Anat. Rec. 295:1336–1351.

Hedrick, A. V., and E. J. Temeles. 1989. The evolution of sexual dimorphism in animals: hypotheses and tests. Trends Ecol. Evolut. 4:136–138.

Hocking, D. P., F. G. Marx, T. Park, E. M. G. Fitzgerald, and A. R. Evans. 2017. A behavioural framework for the evolution of feeding in predatory aquatic mammals. Proc. R Soc. B 284:20162750.

Huelsenbeck, J. P., R. Nielsen, and J. P. Bollback. 2003. Stochastic mapping of morphological characters. Syst. Biol. 52:131–158.

Isaac, J. L. 2005. Potential causes and life-history consequences of sexual size dimorphism in mammals. Mammal Rev. 35:1–15.

Johnson, D. D. P., and D. W. Macdonald. 2001. Why are group-living badgers (*Meles meles*) sexually dimorphic? J. Zool. 255:199–204.

Johnson, D. D. P., D. W. Macdonald, and A. J. Dickman. 2000. An analysis and review of models of the sociobiology of the Mustelidae. Mammal Rev. 30:171–196.

Kienle, S. S., C. J. Law, D. P. Costa, A. Berta, and R. S. Mehta. 2017. Revisiting the behavioural framework of feeding in predatory aquatic mammals. Proc. R Soc. B 284:20171035.

Law, C. J., C. Young, and R. S. Mehta. 2016a. Ontogenetic scaling of theoretical bite force in southern sea otters (*Enhydra lutris nereis*). Physiol. Biochem. Zool. 89:347–363.

Law, C. J., G. J. Slater, and R. S. Mehta. 2018. Lineage diversity and size disparity in Musteloidea: testing patterns of adaptive radiation using molecular and fossil-based methods. Syst. Biol. 67:127–144.

Law, C. J., V. B. Baliga, M. T. Tinker, and R. S. Mehta. 2017. Asynchrony in craniomandibular development and growth in *Enhydra lutris nereis* (Carnivora: Mustelidae): are southern sea otters born to bite? Biol. J. Linn. Soc. 121:420–438.

Law, C. J., V. Venkatram, and R. S. Mehta. 2016b. Sexual dimorphism in craniomandibular morphology of southern sea otters (*Enhydra lutris nereis*). J. Mammal 97:1764–1773.

Lindenfors, P., B. Tullberg, and M. Biuw. 2002. Phylogenetic analyses of sexual selection and sexual size dimorphism in pinnipeds. Behav. Ecol. Sociobiol. 52:188–193.

Lindenfors, P., J. L. Gittleman, and K. E. Jones. 2007. Sexual size dimorphism in mammals. Pp. 16–26 *in* D. J. Fairbairn, W. U. Blanckenhorn, and T. Székely, eds. Sex, size and gender roles evolutionary studies of sexual size dimorphism. Oxford Univ. Press, Oxford.

Lovich, J. E., and J. W. Gibbons. 1992. A review of techniques for quantifying sexual size dimorphism. Growth Dev. Aging 56:269–281.

Lynch, J. M., and W. M. O'Sullivan. 1993. Cranial form and sexual dimorphism in the Irish otter *Lutra lutra L.* Biol. Environ. Proc. R Irish Acad. 93B:97–105.

Macdonald, D. W., and C. Newman. 2018. Musteloid sociality: the grass-roots of society. *in* D. W. Macdonald, C. Newman, and L. A. Harrington, eds. Biology and conservation of musteloids. Oxford Univ. Press, Oxford.

MacDonald, D. W., and D. D. P. Johnson. 2015. Patchwork planet: the resource dispersion hypothesis, society, and the ecology of life. J. Zool. 295:75–107.

McDonald, R. A. 2002. Resource partitioning among British and Irish mustelids. J. Anim. Ecol. 71:185–200.

McGee, M. D., and P. C. Wainwright. 2013. Sexual dimorphism in the feeding mechanism of threespine stickleback. J. Exp. Biol. 216:835–840.

Moors, P. J. 1980. Sexual dimorphism in the body size of mustelids (Carnivora): the roles of food habits and breeding systems. Oikos 34:147–158.

Morris, J. S., and D. R. Carrier. 2016. Sexual selection on skeletal shape in Carnivora. Evolution 70:767–780.

Newman, C., Y.-B. Zhou, C. D. Buesching, and Y. Kaneko. 2011. Contrasting sociality in two widespread, generalist, mustelid genera, *Meles* and *Martes*. Mammal Study 36:169–188.

Nielsen, R. 2002. Mapping mutations on phylogenies. Syst. Biol. 51:729–739.

Noonan, M. J., C. Newman, C. D. Buesching, and D. W. Macdonald. 2015. Evolution and function of fossoriality in the Carnivora: implications for group-living. Front. Ecol. Evol. 3:726–814.

Noonan, M. J., P. J. Johnson, A. C. Kitchener, L. A. Harrington, C. Newman, and D. W. Macdonald. 2016. Sexual size dimorphism in musteloids: an anomalous allometric pattern is explained by feeding ecology. Ecol. Evol. 6:8495–8501.

Orme, D. 2013. The caper package: comparative analysis of phylogenetics and evolution in R. R package version.

Pagel, M. 1999. Inferring the historical patterns of biological evolution. Nature 401:877–884.

Porto, A., F. B. de Oliveira, L. T. Shirai, V. De Conto, and G. Marroig. 2008. The evolution of modularity in the mammalian skull i: morphological integration patterns and magnitudes. Evol. Biol. 36:118–135.

Powell, R. A. 1979. Mustelid spacing patterns—variations on a theme by *Mustela*. Ethology 50:153–165.

Radinsky, L. B. 1981a. Evolution of skull shape in Carnivores. 1. Representative modern Carnivores. Biol. J. Linn. Soc. 15:369–388.

———. 1981b. Evolution of skull shape in carnivores: 2. Additional modern carnivores. Biol. J. Linn. Soc. 16:337–355.

Radloff, F., and J. T. Du Toit. 2004. Large predators and their prey in a southern African savanna: a predator's size determines its prey size range. J. Anim. Ecol. 73:410–423.

Ralls, K., and S. L. Mesnick. 2002. Sexual dimorphism. Pp. 1071–1078 *in* W. F. Perrin, B. Würsig, and J. G. M. Thewissen, eds. Academic Press, San Diego.

Revell, L. J. 2010. Phylogenetic signal and linear regression on species data. Methods Ecol. Evol. 1:319–329.

———. 2011. phytools: an R package for phylogenetic comparative biology (and other things). Methods Ecol. Evol. 3:217–223.

Rohlf, F. J., and D. Slice. 1990. Extensions of the procrustes method for the optimal superimposition of landmarks. Syst. Zool. 39:40–59.

Santana, S. E., and K. E. Miller. 2016. Extreme postnatal scaling in bat feeding performance: a view of ecomorphology from ontogenetic and macroevolutionary perspectives. Integr. Comp. Biol. 56:459–568.

Schlager, S. 2016. Morpho: calculations and visualisations related to geometric morphometrics. R-package version 2.4.

Schneider, C. A., W. S. Rasband, and K. W. Eliceiri. 2012. NIH Image to ImageJ: 25 years of image analysis. Nat. Meth. 9:671–675.

Shetty, S., and R. Shine. 2002. Sexual divergence in diets and morphology in Fijian sea snakes *Laticauda colubrina* (Laticaudinae). Austral. Ecol. 27:77–84.

Shine, R. 1989. Ecological causes for the evolution of sexual dimorphism—a review of the evidence. Q Rev. Biol. 64:419–461.

Smith, T. B. 1987. Bill size polymorphism and intraspecific niche utilization in an African finch. Nature 329:717–719.

Tamagnini, D. 2017. Anyone with a long-face? Craniofacial evolutionary allometry (CREA) in a family of short-faced mammals, the felidae. Evol. Biol. 44:476–495.

Temeles, E. J., I. L. Pan, J. L. Brennan, and J. N. Horwitt. 2000. Evidence for ecological causation of sexual dimorphism in a hummingbird. Science 289:441–443.

Temeles, E. J., J. S. Miller, and J. L. Rifkin. 2010. Evolution of sexual dimorphism in bill size and shape of hermit hummingbirds (Phaethornithinae): a role for ecological causation. Phil. Trans. R Soc. B 365:1053–1063.

Thom, M. D., and L. A. Harrington. 2004. Why are American mink sexually dimorphic? A role for niche separation. Oikos 105:525–535.

Thomason, J. J. 1991. Cranial strength in relation to estimated biting forces in some mammals. Can. J. Zool. 69:2326–2333.

Uyeda, J. C., and L. J. Harmon. 2014. A novel Bayesian method for inferring and interpreting the dynamics of adaptive landscapes from phylogenetic comparative data. Syst. Biol. 63:902–918.

Van Valkenburgh, B. 2007. Deja vu: the evolution of feeding morphologies in the Carnivora. Am. Zool. 47:147–163.

Weckerly, F. W. 1998. Sexual-size dimorphism: influence of mass and mating systems in the most dimorphic mammals. J. Mammal 79:33–52.

Wiig, Ø. 1985. Morphometric variation in the Hooded seal (Cystophora cristata). J. Zool. 206:497–508.

———. 1986. Sexual dimorphism in the skull of minks *Mustela vison*, badgers *Meles meles* and otters *Lutra lutra*. Zool. J. Linn. Soc. 87:163–179.

———. 1989. Craniometric variation in Norwegian wolverines *Gulo gulo L.* Zool. J. Linn Soc. 95:177–204.

Wilson, D. E., and R. A. Mittermeier. 2009. Handbook of the mammals of the world. Lynx Edicions, Spain.

Zalewski, A. 2007. Does size dimorphism reduce competition between sexes? The diet of male and female pine martens at local and wider geographical scales. Acta Theriol. 52:237–250.

Zelditch, M. L., D. L. Swiderski, and H. D. Sheets. 2012. Geometric morphometrics for biologists: A primer. Academic Press, Cambridge, Massachusetts.

Zelditch, M. L., J. Ye, J. S. Mitchell, and D. L. Swiderski. 2017. Rare ecomorphological convergence on a complex adaptive landscape: body size and diet mediate evolution of jaw shape in squirrels (Sciuridae). Evolution 71:633–649.

Associate Editor: M. Zelditch
Handling Editor: P. Tiffin

Supporting Information

Additional supporting information may be found online in the Supporting Information section at the end of the article.

Figure S1. Photographs of the cranium in A) posterodorsal, B) lateral, and C) ventral views used to estimate cross sectional areas (CSAs) and in-lever lengths of the temporalis and masseter-pterygoid complex.
Table S1. Museum catalog numbers for each specimen used in this study.
Table S2. Landmarks for Geometric Morphometrics.
Table S3. Dietary references.

Biological Journal of the Linnean Society , 2017, 121 , 420–438. With 10 figures.

Asynchrony in craniomandibular development and growth in Enhydra lutris nereis (Carnivora: Mustelidae): are southern sea otters born to bite?

CHRIS J. LAW [1*], VIKRAM B. BALIGA [1], M. TIM TINKER [2] and RITA S. MEHTA [1]

[1]Department of Ecology and Evolutionary Biology, Long Marine Laboratory, University of California, Santa Cruz, 100 Shaffer Road, Santa Cruz, CA 95060, USA
[2]U.S. Geological Survey, Western Ecological Research Center, Long Marine Lab, 100 Shaffer Road, Santa Cruz, CA 95060, USA

Received 17 November 2016; revised 18 December 2016; accepted for publication 22 December 2016

Weaning represents a major ontogenetic dietary shift in southern sea otters (Enhydra lutris nereis), as juveniles must transition from depending on mother's milk to independently processing hard-shelled invertebrates. When the skulls of juveniles have reached sufficient maturity to transition to a durophagous diet remains to be investigated. Here, we conducted a comprehensive analysis of skull development and growth and sexual dimorphism using geometric morphometric approaches in 204 southern sea otter skulls. We found that southern sea otters of both sexes exhibit dramatic changes in cranial and mandibular shape and size over ontogeny. Although the majority of these changes occur in the pup stage, full development and growth of the skull does not occur until well after weaning. We hypothesize that the slower maturation of the crania of newly weaned juveniles serves as a handicap by constraining jaw adductor muscle size, biting ability and feeding on hard-shelled prey. In our analysis of sexual dimorphism, we found significant sexual shape and size dimorphism in adult craniomandibular morphology that arose through differences in developmental and growth rates and duration. We postulate that males are selected to attain mature crania faster to presumably reach adult biting ability sooner, gaining a competitive advantage in obtaining food and in male–male agonistic interactions.

ADDITIONAL KEYWORDS: Carnivora – geometric morphometrics – growth curves – mechanical advantage – Mustelidae – ontogeny – sea otter – sexual dimorphism – skull morphology.

INTRODUCTION

The development and growth of the feeding apparatus are among the most important changes across an organism's ontogeny as they affect the procurement of resources (Herrel & Gibb, 2006 ; Gignac & Santana, 2016). In many vertebrates, these ontogenetic changes correspond to major ontogenetic shifts in diet and resource use (e.g. Herrel & O'Reilly, 2006 ; Baliga & Mehta, 2014 ; Gignac & Erickson, 2014 ; Santana & Miller, 2016). In mammals, weaning represents a major ontogenetic shift in diet, as juveniles must transition from dependence on mother's milk to independently obtaining and processing adult foods for survival. The transition from a liquid food source (milk) to solid food may be particularly challenging for mammals with highly specialized diets such as hypercarnivores, that must actively capture, kill and consume prey, or durophagous carnivores, that must first break into hard, tough material to feed. Within the mammalian order Carnivora, the skull is the primary feeding apparatus used to process prey across most hypercarnivorous and durophagous specialists (Wilson & Mittermeier, 2009). Although adults typically exhibit large craniomandibular traits and strong biting ability for specialization on large prey or hard material such as bones or calcified prey (Radinsky, 1981a , b; Christiansen & Wroe, 2007), these traits are often not fully developed in the skulls of juveniles. Juveniles exhibit smaller sizes and less developed morphologies compared to adults (Tanner, Zelditch &

*Corresponding author. E-mail: cjlaw@ucsc.edu

Lundrigan, 2010 ; La Croix et al. , 2011). Unsurprisingly, the carnivoran feeding apparatus undergoes tremendous changes in both size and shape through ontogeny (Tanner et al. , 2010 ; La Croix et al. , 2011 ; Tarnawski, Cassini & Flores, 2014 ; Segura, 2015), where selection is expected to favour individuals that minimize the length of development and growth and thus more quickly become efficient foragers (Herrel & Gibb, 2006 ; Gignac & Santana, 2016).

A complete understanding of the development and growth of the feeding apparatus, however, is not possible without knowledge of the effects of sex (Wiley, 1974 ; Shea, 1986 ; Badyaev, 2002). Selective pressures underlying sexual dimorphism (i.e. sexual selection, fecundity selection and natural selection) act not only on adult morphology but also on the development and growth of traits throughout ontogeny (Badyaev, 2002). Male-biased sexual dimorphism in body size is widespread across almost all major carnivoran clades (Moors, 1980 ; Weckerly, 1998 ; Lindenfors, Tullberg & Biuw, 2002 ; Lindenfors, Gittleman & Jones, 2007). Sexual dimorphism also occurs in the skull (Gittleman & Van Valkenburgh, 1997 ; Brunner, Bryden & Shaughnessy, 2004 ; Christiansen & Harris, 2012). These intersexual differences in craniomandibular morphologies can arise through multiple developmental and growth processes such as differences in birth sizes, developmental and growth duration, or developmental and growth rates (Brunner et al. , 2004 ; Thom & Harrington, 2004 ; Sanfelice & De Freitas, 2008). In addition, some male carnivorans also exhibit biphasic growth in the skull, whereby some craniomandibular traits exhibit secondary development and growth after the rest of the skull is fully mature (Brunner et al. , 2004 ; Tarnawski, Cassini & Flores, 2013 ; Tarnawski et al. , 2014). Sex-based differences in skull morphology may have multiple fitness consequences, affecting both foraging performance and intrasexual competitive ability (Moors, 1980 ; Ralls & Harvey, 1985 Gittleman & Van Valkenburgh, 1997); therefore, the rate of ontogenetic changes may be under different selective pressures between males and females.

Here, we investigate the growth and development of the feeding apparatus for the southern sea otter (Enhydra lutris nereis) to examine when the skulls of juveniles have reached sufficient maturity to transition to a durophagous diet and if these ontogenetic patterns differ between the sexes. As one of the smallest marine mammals, sea otters exhibit the highest known mass-specific metabolic rates of marine mammals (Morrison, Rosenmann & Estes, 1974 ; Costa & Kooyman, 1984 ; Yeates, Williams & Fink, 2007) and consequently must consume 20–30% of their body mass in food per day (Morrison et al. , 1974 ; Costa & Kooyman, 1982). Sea otters are durophagous, spending 20–50% of the day foraging on a variety of hard-shelled invertebrates such as chitinous crabs and calcifying bivalves and gastropods (Estes, Underwood & Karmann, 1986 ; Riedman & Estes, 1990 ; Ralls & Siniff, 1990 ; Thometz et al. , 2016). The craniomandibular adaptations that facilitate durophagy have been well characterized and studied in adult sea otters, and traits include short, blunt skulls (Riley, 1985); taller and wider mandibular rami (Timm-Davis, DeWitt & Marshall, 2015); bunodont dentition (Fisher, 1941 ; Constantino et al. , 2011); fracture-resistant dental enamel (Ziscovici et al. , 2014) and positive allometric increases in jaw adductor musculature and bite force (Law, Young & Mehta, 2016b). Furthermore, southern sea otters exhibit sexual dimorphism, and adults exhibit intersexual differences in skull size and shape, jaw adductor musculature and absolute bite forces (Wilson et al. , 1991 ; Law et al. , 2016b ; Law, Venkatram & Mehta, 2016a).

In contrast, the craniomandibular adaptations to durophagy have not been characterized in pre-weaned and juvenile sea otters, and little work has examined the rate and duration of craniomandibular development and growth across ontogeny (but see Hattori et al. , 2003). Dependent pups, who exhibit even greater mass-specific energetic demands than adult otters (Thometz et al. , 2014), rely on a combination of milk provided by the mother as well as an increasing amount of hard-shelled invertebrates to meet their metabolic demands as they grow. During the first month, pups obtain the majority of their nourishment from nursing and rarely eat solid food (Payne & Jameson, 1984). However, by 6 weeks of age, pups begin soliciting food from their mothers, manipulating small pieces of food with the mouth and forepaws and chewing very slowly (Payne & Jameson, 1984). The frequency of eating solid food along with the size of the prey items rapidly increase as pups age and begin to dive. By 8.9 weeks of age, pups are able to catch and consume their own prey (Staedler, 2011). By 9.5 weeks of age, pups are given solid food after nearly every successful foraging dive made by the mothers, and by 14–20 weeks, pups are able to break open hard-shelled prey items (Payne & Jameson, 1984). By 6–8 months of age, sea otter pups are weaned and completely independent (Jameson & Johnson, 1993). Although newly weaned juveniles incur the highest daily energy demands of all developmental stages and exhibit mass-specific energetic demands similar to adults (Thometz et al. , 2014), these juveniles no longer have the benefit of obtaining food from their mothers and must forage independently. Furthermore, because of their extremely high metabolic rate (Costa & Kooyman, 1984 ; Yeates et al. , 2007 ; Thometz et al. , 2014), their restricted foraging depths in nearshore habitats (Thometz et al. , 2016), and their very high site fidelity (Tarjan & Tinker, 2016), sea otters have the capacity to greatly

deplete the abundance of their most preferred prey taxa (including abalones and large urchins); therefore, populations are ultimately limited by food abundance (Riedman & Estes, 1990). Thus, in established populations that are at carrying capacity, juveniles must compete with conspecific adults in an environment already characterized by low prey resources and intense resource competition (Tinker, Bentall & Estes, 2008; Newsome et al., 2015; Tinker & Hatfield, 2015), suggesting that selection should be strong on the rapid development and growth of morphological traits critical for foraging success.

The point at which the skulls of juveniles reach sufficient maturity required for durophagy and whether these ontogenetic changes differ between the sexes remains to be investigated. We recently found that southern sea otters exhibit positive allometric increases in bite force with respect to body size and condylobasal length (Law et al., 2016b), suggesting that feeding ability may be limited by the smaller, less developed morphology. Thus, the primary goal of this study was to conduct a comprehensive analysis of ontogenetic changes in the feeding apparatus of the southern sea otter. Our second goal was to examine if these ontogenetic patterns differed between the sexes, given the sexual dimorphism observed in adult skull morphology. To accomplish our goals, we used geometric morphometric approaches and nonlinear modelling to quantify ontogenetic changes in skull shape and size as well as measured the rate and duration of development and growth.

MATERIAL AND METHODS

Samples and geometric morphometric procedure

We obtained 204 southern sea otters skulls (106 females and 98 males; Supporting Information, Table S1) from the California Department of Fish and Wildlife Marine Wildlife Veterinary Care and Research Center (CDFW-MWVCRC) and the California Academy of Sciences (CAS) across five age classes (Fig. 1). Skulls were obtained from naturally deceased southern sea otters (1992–2015) as part of the CDFW Sea Otter Necropsy Program. The age class - pup, immature, subadult, adult and aged adult - of each specimen was determined using a suite of morphological characteristics including total body length, tooth wear and closure of cranial sutures (age classes defined in Supporting Information, Table S2). Each specimen was then assigned an estimated age based on the relative total length within that age class, dentition condition and characteristics of the pelt following CDFW protocol (Hatfield, 2006). Ages estimated using this protocol correlated well with age estimations obtained by measuring tooth cementum layers (Laidre et al., 2006). All specimens originated from the central California coast, from Half Moon Bay to San Luis Obispo. Skull transfer from the CDFW-MWVCRC was conducted under a U.S. Fish and Wildlife Service Letter of Authorization to CJL.

We quantified ontogenetic changes in cranial and mandibular development (shape) and growth (size) by analyzing three views of the skull with 2D landmark-based geometric morphometrics (Rohlf & Slice, 1990; Zelditch, Swiderski & Sheets, 2012): (1) the cranium in ventral view, photographed by orienting the palate

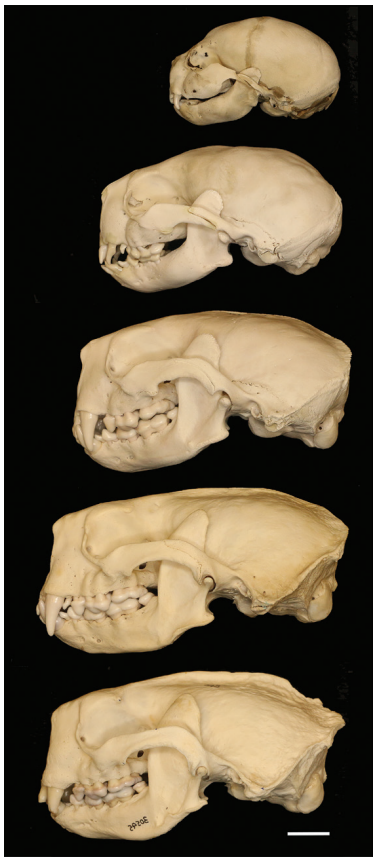

Figure 1. Photographs of male sea otter skulls illustrating changes in size and shape throughout development at 1 month (pup), 7 months (immature), 2.5 years (subadult), 4.5 years (adult) and 10 years (aged adult). Scale bar represents 2 cm.

plane parallel to the photographic plane; (2) the cranium in lateral view, photographed by orienting the mid-sagittal plane parallel to the photographic plane and (3) the mandible in lateral view, photographed by orienting the long axis of the dentary parallel to the photographic plane. We used 19 landmarks on the ventral view of the cranium, 15 landmarks on the lateral view of the cranium and 9 landmarks on the mandible to describe skull shape (Supporting Information, Fig. S1 and Table S3). Since cranial sutures are completely fused in adult sea otters resulting in few homologous landmarks and because landmarks cannot effectively capture curves, an additional 14 semilandmarks and 22 semilandmarks were selected for the lateral views of the cranium (Supporting Information, Fig. S1B) and mandible (Supporting Information, Fig. S1C), respectively. Landmarks and semilandmarks were digitized using TPSDIG 2.10 (Rohlf, 2010) and subsequently superimposed by Generalized Procrustes analysis to remove variation in position, size and orientation (Gower, 1975; Rohlf & Slice, 1990) with GEOMORPH 3.0.1 (Adams & Otárola-Castillo, 2013) in R 3.2.1 (R Core Team, 2015). During the Procrustes superimposition, semilandmarks on the curves were allowed to slide along their tangent vectors until their positions minimized bending energy (Bookstein, 1997; Zelditch et al., 2012). After superimposition, bilaterally homologous landmarks on the ventral cranium were reflected across the midline and averaged using the geomorph function bilat.symmetry. We obtained 38 Procrustes shape coordinates for the ventral cranium, 58 for the lateral cranium and 62 for the lateral mandible.

Ontogenetic change in skull shape and size

We performed a Procrustes ANOVA (Goodall, 1991; Anderson, 2001) with a factorial design on each of the skull view datasets to determine (1) if there were significant changes in skull shape through ontogeny and (2) if ontogenetic shape changes differed between male and female sea otters. For each skull view, we used shape as the dependent variable, sex as the main factor and the natural log (ln) of estimated age as a covariate. Procrustes ANOVAs were performed with the procD.lm function in the R package geomorph 3.0.1 (Adams & Otárola-Castillo, 2013). We then used a pairwise permutation test in the R package MORPHO 2.4 (Schlager, 2016) to quantify ontogenetic shape differences (Procrustes distances) in both sexes and to determine if these ontogenetic differences were significant. Procrustes ANOVAs and pairwise permutation tests were also used to assess and quantify the ontogeny of skull shape and sexual shape dimorphism between the mean youngest individual and the mean oldest individual within each of our five age classes - pup, immature, subadult, adult and aged adult.

Similarly, we determined if changes in skull size were significantly different through ontogeny and between sexes by using analyses of covariance (ANCOVAs) on each skull view. To quantify cranial and mandibular size, we calculated the centroid size of each configuration of landmarks, that is, the square root of the sum of the squared distances from each landmark to the geometric center of the shape (Bookstein, 1996). Centroid size was then used as the dependent variable, and the interaction between sex and ln estimated age was assessed to determine whether males and females exhibited significantly different slopes. We also determined the extent of sexual size dimorphism within each age class using separate ANCOVAs and assessed the magnitude of sexual size dimorphism for each trait using Lovich & Gibbons' (1992) size dimorphism index (SDI) (Lovich & Gibbons, 1992; Smith, 1999; Fairbairn, 2007):

$$SDI = \pm 1\left(\frac{S_L}{S_S} - 1\right)$$

where S_L and S_S are the mean trait measurements of the larger and smaller sexes, respectively. A negative sign is assigned if the male trait is larger whereas a positive sign is assigned if the female trait is larger. There is no intersexual difference if SDI = 0%.

Rates and timing of skull development, growth and mechanical advantage

We determined the rate and the age at which skull development and growth reached maturity using a series of nonlinear growth models. To assess rates and time of development, we used the Procrustes distance (P_D) between each specimen and the mean shape of the youngest female and male specimens as our index of shape (Zelditch et al., 2003). To assess rate and timing of growth, we used centroid size as our measure of size.

We also quantified the mechanical advantage (MA) of jaw closing to infer how changes in mandibular shape over ontogeny might affect feeding performance. We modelled the lower jaw as a lever and calculated MA of the primary masticatory muscles - the temporalis (TMA: mechanical advantage of the temporalis) and the masseter (MMA: mechanical advantage of the masseter) (Radinsky, 1981a; Timm-Davis et al., 2015). MA is calculated as the ratio between the in-lever length (the distance between the mandibular condyle and the muscle insertion point) and the out-lever length (the distance from the mandibular condyle to the bite point). We defined the temporalis insertion point as the dorsal tip of the coronoid process and the masseter insertion point as the anterior point of the masseteric fossa. We calculated MA at two bite points, the canine (TMA_{can} and MMA_{can}) and the lower third premolar (TMA_{pre} and MMA_{pre}). These two bite points

represent important bite positions in prey processing for sea otters; biting at the canine is used to pry open hard-shelled invertebrates such as bivalves and crabs whereas the molars are used to crush items prior to consumption. We were unable to calculate MA at the carnassial because many of the younger specimens (< 1 years of age) did not have erupted first molars.

We then fit growth models to each measurement separately for each sex. Seven models - Brody (mono - molecular), Gompertz, 4-parameter Gompertz, linear, logistic, quadratic and Richard - were fitted and eval - uated for their relative goodness-of-fit based on cor - rected Akaike Information Criterion (AICc) weights. The residuals of each selected growth model were checked to ensure that there were no significant serial autocorrelations. We determined whether the parame - ter estimates of development and growth significantly differed between the sexes by comparing the mean values of one sex with the 95% confidence intervals of the mean with the other sex. Following previous work, we report the age of maturity as the estimated age at which the measurement reached the lower limit of the 95% confidence interval for the asymptote estimate (Zelditch et al. , 2003).

In order to provide context for growth models based on skull development, we also analyzed ontogenetic changes in body size by fitting growth models to mass-at-age and length-at-age data from wild sea otters. Previously conducted research studies on southern sea otters (Tinker et al. , 2016) have resulted in extensive morphometric data from throughout the sea otter's range in California. As described elsewhere (Tinker et al. , 2006), sea otters were anesthetized after capture (using scuba-based methods), weighed using a digital scale and measured for nose-to-tail length while prone. Age for each animal was estimated based on tooth wear patterns and age-dependent fur colora - tion (grizzle). Following established methods (Laidre et al. , 2006), we used nonlinear least squares to fit Von Bertlanffy growth models to the data on age-spe - cific mass and length for each sex. We plotted best-fit functions and 95% confidence intervals for males and females, and report the age of maturity for each sex as the age at which the functions reached 95% (in the case of mass) and 99% (in the case of length) of the asymptote values.

RESULTS

Significant ontogenetic changes in skull shape between males and females occurred in all three cranial views (Table 1). The lateral cranium and mandible exhibited a significant interaction effect between sex and ln esti - mated age, indicating that the trajectories (slopes) of

Table 1. Results from Procrustes ANOVAs for ontogenetic changes and sex differences in cranial and mandibular shape across the entire lifespan

	SS	MS	R^2	$F_{1,203}$	P-value
A. Ventral cranium					
ln(estimated age)	0.062073	0.062073	0.229497	61.161	0.001
Sex	0.004224	0.004224	0.015617	4.162	0.001
ln(estimated age):sex	0.001196	0.001196	0.004422	1.178	0.272
Residuals	0.202981	0.001015			
Total	0.270473				
B. Lateral cranium					
ln(estimated age)	0.12234	0.122343	0.242088	66.289	0.001
Sex	0.00754	0.007542	0.014925	4.087	0.002
ln(estimated age):sex	0.00636	0.00636	0.012585	3.446	0.003
Residuals	0.36912	0.001846			
Total	0.50537				
C. Mandible					
ln(estimated age)	0.14751	0.147507	0.296	88.058	0.001
Sex	0.01135	0.011354	0.023	6.778	0.001
ln(estimated age):sex	0.00418	0.004178	0.008	2.494	0.018
Residuals	0.33502	0.001675			
Total	0.49806				

Bold P-values indicate significance ($\alpha = 0.05$). SS = sum of squares; MS = means squares.

ontogenetic change in lateral cranial shape and mandibular shape differed between the sexes. The ventral cranial view exhibited significant ontogenetic changes in skull shape with significant effects of sex but there was no significant interaction effect between sex and ln estimated age (Table 1).

For both sexes, the dominant ontogenetic shape changes in the ventral view of the cranium were the widening of the zygomatic arches and the mastoid processes (Fig. 2). In addition, the zygomatic arches lengthened along the anteroposterior axis, the rostrum narrowed and shortened, and the basicranium widened and lengthened relative to the anteroposterior axis of the cranium. In the lateral cranial view, posterodorsal expansion of the nuchal crest and occipital bone along with simultaneous ventral compression of the dorsal cranial profile contributed to the flattening of the skull through ontogeny (Fig. 3). Furthermore, the zygomatic arch exhibited anteroposterior and dorsal increases in size relative to the rest of the skull. The dominating ontogenetic changes in the mandible were the lengthening of the masseteric fossa and the anterodorsal expansion of the coronoid process, resulting in a more vertically oriented process through ontogeny (Figs 4). Additionally, the anterior portion of the mandibular body curved posterodorsally towards the tooth-row, whereas the posterior portion of the mandible expanded posteroventrally, both of which contribute to the relative shortening of the mandible along the anteroposterior axis.

Cranial shape changes within age classes

Separate Procrustes ANOVA and pairwise permutation analyses within each age class found that significant ontogenetic shape changes occurred during the pup and subadult stages in both cranial views (Fig. 5A–J ; Supporting Information, Tables S4 and S5). However, only the adult and aged adult stages exhibited significant effects of sex (Fig. 6A–D), and no age class exhibited a significant interaction between ln estimated age and sex (Supporting Information, Table S4).

During the pup stage, the dominant ontogenetic changes in the ventral cranium were the widening of the zygomatic arches and basicranium relative to the anteroposterior axis, the movement of the mastoid processes towards the anterior, and the lengthening of the palate (Fig. 5A). In the lateral cranial view, the braincase became much less bulbous due to posterodorsal expansion of the nuchal crest and occipital bones and simultaneous ventral compression of the dorsal cranial profile (Fig. 5F). In addition, the skull

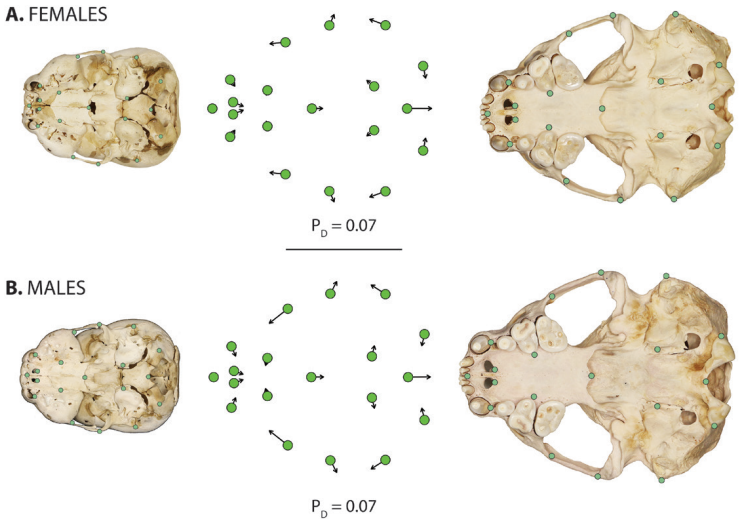

Figure 2. Ontogenetic changes of the ventral cranium. Vectors on landmarks and semilandmarks show the direction and magnitude of change from the mean pup shape to the mean aged adult shape of females (A) and males (B) after centroid size is scaled to the same size for each specimen. Vectors were magnified by a factor of 3 to display shape changes. P_D = Procrustes distance between youngest individual and oldest individual in each sex.

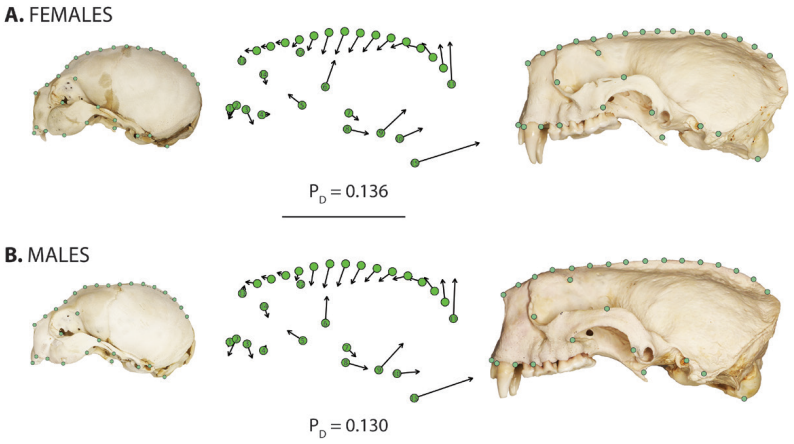

Figure 3. Ontogenetic changes of the lateral cranium. Vectors on landmarks and semilandmarks show the direction and magnitude of change from the mean pup shape to the mean aged adult shape of females (A) and males (B) after centroid size is scaled to the same size for each specimen. Vectors were magnified by a factor of 3 to display shape changes. P_D = Procrustes distance between youngest individual and oldest individual in each sex.

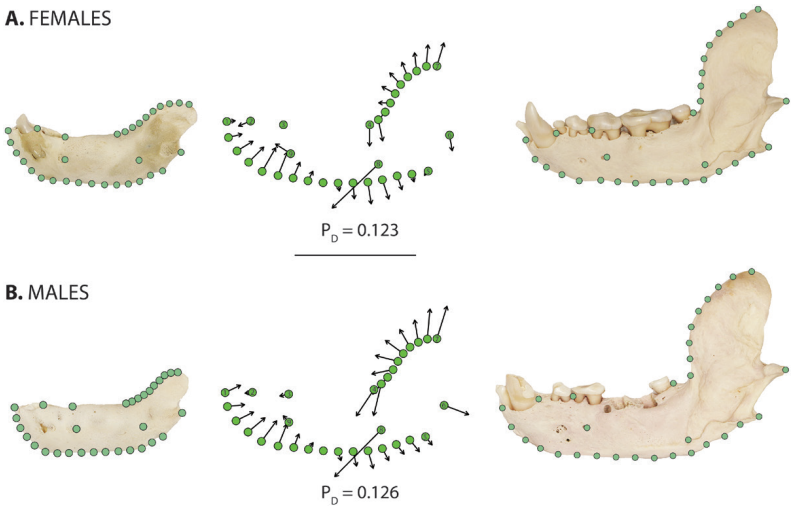

Figure 4. Ontogenetic changes of the mandible. Vectors on landmarks and semilandmarks show the direction and magnitude of change from the mean pup shape to the mean aged adult shape of females (A) and males (B) after centroid size is scaled to the same size for each specimen. Vectors were magnified by a factor of 3 to display shape changes. P_D = Procrustes distance between youngest individual and oldest individual in each sex.

began to lengthen relative to the anteroposterior axis as the temporal and occipital bones moved towards the posterior and the rostrum began to broaden on the dorsoventral axis (Fig. 5F).

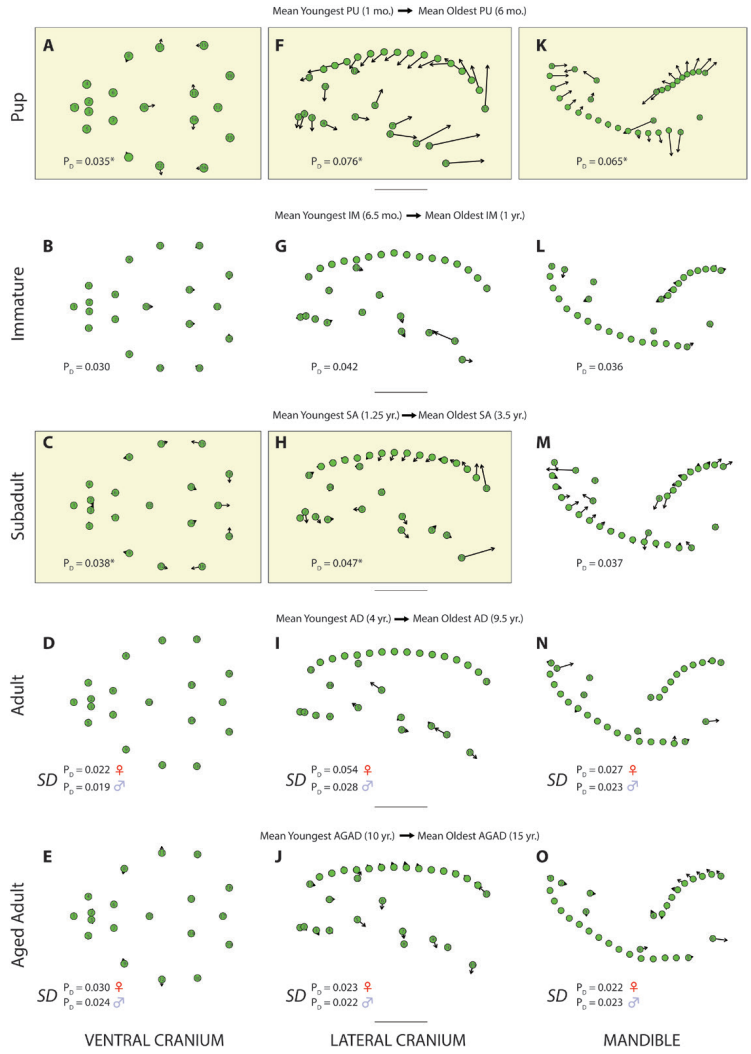

Figure 5. Ontogenetic shape changes of the ventral cranium (A–E), lateral cranium (F–J) and mandible (K–O) within each age class. Vectors on the landmarks and semilandmarks of each skull view show the direction and magnitude of change from the mean youngest shape to the mean oldest shape within each given age class. Skull views that exhibit significant shape changes through ontogeny are highlighted in yellow (see Supporting Information, Table S4 for full Procrustes ANOVA P-values). SD indicates significant effect of sex on shape changes. Vectors were magnified by a factor of 3 to display shape changes. P_D = Procrustes distance between youngest individual and oldest individual within each age class. Asterisks '*' indicate significant P_D based on permutation tests (see Supporting Information, Table S5 for full pairwise permutation P-values). AGAD, aged adult; AD, adult; SA, subadult; IM, immature; PU, pup.

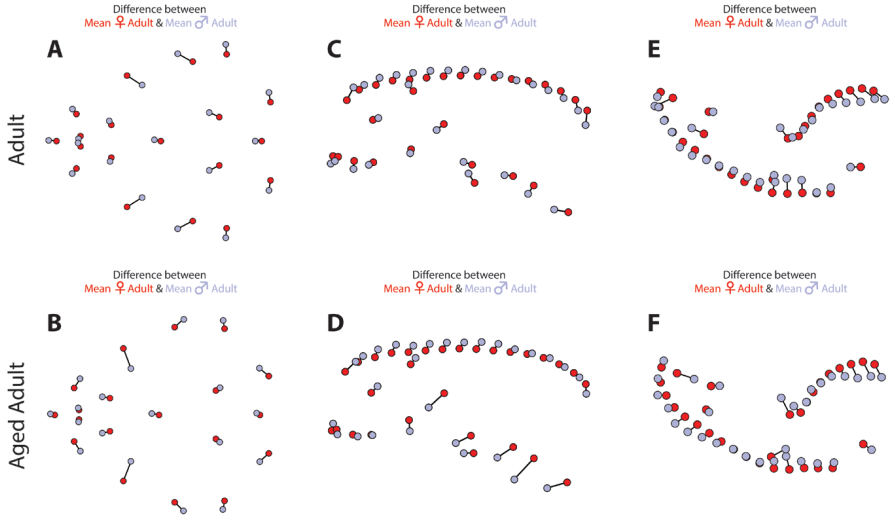

Figure 6. Ventral cranial (A and B), lateral cranial (C and D) and mandibular (E and F) shape differences between female and male southern sea otters in the adult and aged adult age classes. Red landmarks/semilandmarks indicate female shape and blue landmarks/semilandmarks indicate male shape. Lines linking female and male landmarks/semilandmarks indicate the relative direction and magnitude of change. Lines were magnified by a factor of 3 to display shape differences between the sexes.

Interestingly, no significant shape changes through ontogeny or effect of sex occurred during the immature stage (Fig. 5B, G). Ontogenetic shape changes resumed during the subadult stage when the mastoid processes widened anterolaterally, the basicranium and foramen magnum lengthened the skull along the anteroposterior axis, the braincase continued to flatten and the rostrum continued to broaden relative to the dorsoventral axis (Fig. 5C, H). The zygomatic arches also lengthened along the anteroposterior axis (Fig. 5C, H).

No significant ontogenetic changes in cranial shape occurred in both the adult and aged adult stages (Fig. 5D, E, I, J; Supporting Information, Tables S4 and S5). However, both of these age classes exhibited sexual dimorphism (Fig. 6A–D). Adult and aged adult males displayed relatively wider zygomatic arches and mastoid processes, shorter basicrania relative to the anteroposterior axis, slightly wider and longer rostrums and slightly more pronounced sagittal crests (Fig. 6A–D).

Mandibular shape changes within age classes

Significant ontogenetic changes in mandibular shape were found only in the pup stage (Fig. 5K; Supporting Information, Tables S4 and S5). The most dramatic mandibular shape change within this age class was the lengthening of the masseteric fossa (Fig. 5K). In addition, anterodorsal and ventral expansion of the coronoid process and posterior portion of the mandible, respectively, contributed to the lengthening and broadening of the ramus. Lastly, posterodorsal compression of the anterior portion of the mandibular body decreased the length of the mandible along the anteroposterior axis.

Significant effects of sex only occurred in the adult and aged adult stages. For both of these age classes, females exhibited larger mandibular rami relative to the dorsoventral and anteroposterior axes of the mandible (Fig. 6E, F). In addition, the anterior portion of the mandibular body was slightly broader in males compared to females.

The ventral and lateral cranial views exhibited significant interaction effects between sex and ln estimated age ($P < 0.001$; Table 2). Significant ontogenetic changes occurred in the mandible ($F_{1, 200} = 185.337$, $P < 0.001$) with no significant effect from sex ($F_{1, 200} = 1.477$, $P = 0.226$).

Within age classes, the pup, immature and subadult stages exhibited significant ontogenetic changes in ventral cranial size whereas only the pup stage exhibited significant ontogenetic changes in lateral cranial and mandibular size (Supporting Information, Table

Table 2. Results from ANCOVAs for ontogenetic changes and sex differences in cranial and mandibular centroid size across the entire lifespan

	$F_{1,200}$	P-value
A. Ventral cranium size		
ln(estimated age)	818.779	< 0.001
Sex	19.56	< 0.001
ln(estimated age):sex	13.095	< 0.001
B. Lateral cranium size		
ln(estimated age)	596.219	< 0.001
Sex	35.172	< 0.001
ln(estimated age):sex	12.063	< 0.001
C. Mandible size		
ln(estimated age)	185.337	< 0.001
Sex	1.477	0.226
ln(estimated age) × sex	2.826	0.094

Bold P-values indicate significance ($\alpha = 0.05$). ANCOVA, analysis of covariance.

S6). Furthermore, both views of the cranium displayed male-biased sexual size dimorphism in the subadult, adult and aged adult age classes. On average, the subadult ventral and lateral cranium is 4.5 and 5.0% larger in males, respectively; the adult ventral and lateral cranium is 4.8 and 5.8% larger in males, respectively and the aged adult ventral and lateral cranium is 6.7 and 8.2% larger in males, respectively. The mandible exhibited significant male-biased sexual size dimorphism in only the aged adult age class (Supporting Information, Table S6). SDI calculations indicate the male mandible is 6.9% larger than females on average.

Rates and age of cranial maturity

The model with the highest AICc weight was the Brody model:

$$x(t) = A\left(1 - Be^{-kt}\right)$$

where $x(t)$ is the measurement of interest at time t, A is the asymptotic maturity, k is the growth rate and B is the scaling constant (Supporting Information, Table S7). AICc weights for MA of the temporalis at the premolar for both males and females favoured the logistic model. However, we chose the Brody model rather than the logistic model for these two measurements to be able to compare model parameters with the other measurements.

With the exception of ventral cranial shape, asymptotic values of cranial shape and size significantly differed between male and female southern sea otters (Table 3; Fig. 7). Compared to females, males displayed faster growth rates in lateral cranial shape and ventral and lateral cranial size (Table 3). As a result, males exhibited earlier maturation (95% of the asymptotic values) in lateral cranial shape (1.1 years) than females (2.3 years) as well as earlier maturation in ventral cranial size (♂ 2.8 years; ♀ 3 years) and in lateral cranial size (♂ 3.3 years; ♀ 4.3 years; Table 3; Fig. 7). In contrast, growth rates between the sexes were not significantly different in ventral cranial shape (Table 3; Fig. 7).

While asymptotic values of mandibular shape and size were also significantly different between the sexes (Table 3; Fig. 7), mandibular developmental and growth rates were not. This indicates that the duration of development and growth of the mandible rather than rate were significantly different between males and females. Females reached mature mandibular shape earlier than males (♂ 2.8 years; ♀ 2.3 years) whereas, conversely, males reached mature mandibular size earlier than females (♂ 1.5 years; ♀ 1.9 years; Table 3; Fig. 7).

Asymptotic values and growth rates of all measured MAs did not significantly differ between male and female southern sea otters (Table 3; Fig. 8). Mature temporalis MAs at the canine (TMA_{can}) and at the premolar (TMA_{pre}) were reached at ages 1.6 and 1.9 years, respectively, and mature masseter MAs at the canine (MMA_{can}) and at the premolar (MMA_{pre}) were reached at ages 3.3 and 3.5 years, respectively (Table 3; Fig. 8). Complete eruption of adult dentition occurs a few months after weaning (around 1 year of age) for both sexes (Hatfield, 2006).

Body size maturation

Body size growth curves fit to data on mass-at age and length-at age from 386 female and 145 male sea otters show clear evidence of sexual dimorphism (Fig. 9). Males and females exhibited differences in the age of body size maturation: females reached maturity at 3.8 (based on length) or 4.1 (based on mass) years of age, while males did not reach maturity until 5.3 years of age (based on both length and mass). These differences were consistent with reported values for sexual maturity: females typically reach sexual maturity around 3–5 years (Jameson & Johnson, 1993), whereas males reach sexual maturity around 5–6 years (Green, 1978).

DISCUSSION

Asynchrony of skull development and growth

Southern sea otters of both sexes exhibit dramatic changes in cranial and mandibular shape and size

Table 3. Parameter estimates of growth curves generated with a Brody model

Skull view	Sex	A	K	B	Age of maturity
A. Skull shape					
Ventral cranium	♀	0.078 (0.076–0.080)	0.493 (0.33–0.656)	0.46 (0.406–0.513)	5.4
	♂	0.080 (0.0.77–0.083)	0.419 (0.238–0.600)	0.406 (0.345–0.466)	5.6
Lateral cranium	♀	0.140 (0.137–0.144)	1.465 (1.044–1.886)	0.711 (0.579–0.842)	2.3
	♂	0.123 (0.119–0.127)	3.090 (1.896–4.285)	0.911 (0.623–1.199)	1.1
Mandible	♀	0.129 (0.125–0.133)	1.361 (0.896–1.826)	0.719 (0.567–0.871)	2.3
	♂	0.124 (0.121–0.128)	1.125 (0.706–1.544)	0.647 (0.510–0.784)	2.8
B. Skull size					
Ventral cranium	♀	20.645 (20.361–20.929)	1.018 (0.684–1.352)	0.292 (0.242–0.0.342)	3
	♂	21.692 (21.462–21.922)	1.529 (1.271–1.788)	0.374 (0.321–0.428)	2.8
Lateral cranium	♀	24.068 (23.693–24.443)	0.588 (0.328–0.848)	0.192 (0.159–0.225)	4.3
	♂	25.452 (25.149–25.756)	0.988 (0.683–1.293)	0.309 (0.259–0.360)	3.3
Mandible	♀	15.0522 (14.787–15.317)	1.56 (0.895–2.255)	0.32 (0.229–0.41)	1.9
	♂	15.530 (15.139–15.921)	1.746 (0.684–2.807)	0.367 (0.211–0.524)	1.5
C. Mechanical advantage					
Temporalis canine	♀	0.40 (0.39–0.41)	1.620 (0.462–2.778)	0.201 (0.104–0.297)	1.5
	♂	0.39 (0.38–0.40)	1.472 (0.524–2.420)	0.168 (0.113–0.224)	1.6
Temporalis premolar	♀	0.49 (0.48–0.50)	1.405 (0.538–2.272)	0.215 (0.132–0.297)	1.8
	♂	0.48 (0.48–0.49)	1.097 (0.251–1.943)	0.142 (0.091–0.193)	2
Masseter canine	♀	0.46 (0.45–0.47)	0.619 (0.143–1.095)	0.191 (0.132–0.250)	3.2
	♂	0.45 (0.44–0.46)	0.701 (0.314–1.088)	0.274 (0.216–0.332)	3.4
Masseter premolar	♀	0.56 (0.55–0.57)	0.64 (0.250–1.020)	0.213 (0.161–0.265)	3.5
	♂	0.55 (0.54–0.57)	0.733 (0.392–1.073)	0.268 (0.219–0.317)	3.5

A is the asymptotic value, K is the growth rate constant and B is the scaling constant. 95% confidence intervals are given in parentheses. Bold values indicate significant differences between male and female parameters. Age of maturity indicates the ages (in years) at which skull shapes/sizes/mechanical advantage reach 95% of their respective asymptotic values.

over ontogeny. The flattening of the dorsal cranial profile, broadening of the zygomatic arches, lengthening of the cranium along the anteroposterior axis, development of a more pronounced sagittal crest, as well as overall increase in size follow the general developmental and growth patterns of the carnivoran cranium (Tanner et al., 2010; La Croix et al., 2011; Tarnawski et al., 2014; Segura, 2015). The majority of the shape and size changes occurred during the pup stage along with additional changes occurring during the subadult stage. However, neither cranial shape nor cranial size reached developmental maturity and full growth until after weaning and complete eruption of dentition. In fact, the crania of both sexes do not fully mature until the adult stage. Nonlinear modelling indicates that male and female otters exhibit differences in maturation ages (95% of the asymptotic values) of the cranium (see following section). Males reach adult cranial size maturity during the late-subadult stage (3.3 years), whereas females do not reach adult cranial size maturity until a year later during the early adult stage (4.3 years). Both sexes reach adult cranial shape maturity even later at ~5.5 years of age, after full body sizes have reached maturity (Fig. 10). Surprisingly, lateral cranial shape had reached adult maturity (95% of the asymptotic values) during the early subadult stage, much earlier than lateral cranial size and ventral cranial shape and size. Visual inspection of specimens, however, indicates discernible changes in lateral shape, specifically in the sagittal crest. As previously noted in spotted hyena (Crocuta crocuta) skulls (Tanner et al., 2010), this apparent inconsistency may be a result of distortion caused by projecting a 3D object onto a 2D photographic plane. We postulate that the development of the sagittal crest, particularly in males, portrays the braincase as deceptively round when projected onto a 2D plane. 2D geometric morphometric approaches may simply be unable to effectively characterize dorsal cranial shape changes between the bulbous braincase of the pup cranium to the artificially rounded, but in reality flatter, braincase of the adult cranium. Therefore, Procrustes distances of the lateral cranium may be an underestimation, resulting in earlier maturation times of shape.

The mandible reached adult maturity quicker than the cranium (Fig. 10). All significant changes in mandibular shape and size occurred only during the pup stage with no significant development and growth

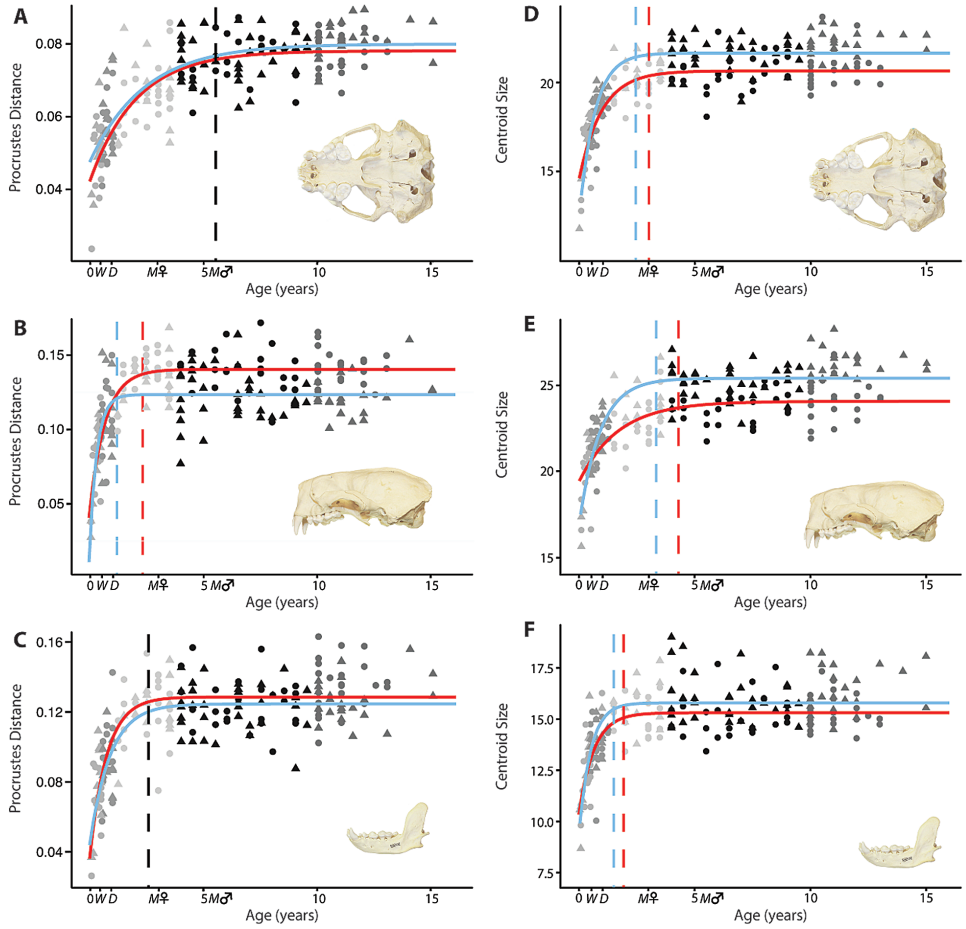

Figure 7. Growth curves for skull shape [ventral cranium (A), lateral cranium (B) and mandible (C)] and skull size [ventral cranium (D), lateral cranium (E) and mandible (F)]. Circles represent female skulls, triangles represent male skulls and colours represent the five age classes. The red (darker) curves are the female growth curves and the blue (lighter) curves are the male growth curves. Only the lateral cranium and mandible exhibited significantly intersexual differences in asymptotic values, and only the cranium exhibited significantly intersexual differences in growth rates (see Table 3). Red (darker) and blue (lighter) dashed lines indicate the times at which cranium shapes reach 95% of their asymptotic values for females and males, respectively, whereas the black dashed line indicate the ages at which mandibular shape reaches the minimum for the 95% confidence range for the asymptotic values for females and males combined. On the x-axis, W indicates age of weaning, D indicates age of complete gain of permanent dentition and SM ♀ and SM ♂ indicate earliest age of sexual maturity for female and male southern sea otters, respectively.

during subsequent stages. The relative lengthening and broadening of the coronoid process, ramus and masseteric fossa but relative shortening of the mandible along the anteroposterior axis all contribute to increasing MA. Higher MA is typically associated with increased force-modified jaws (Kardong, 2014) and thus serves as an adaptation in processing hard-shelled prey (Timm-Davis et al., 2015; Law et al.,

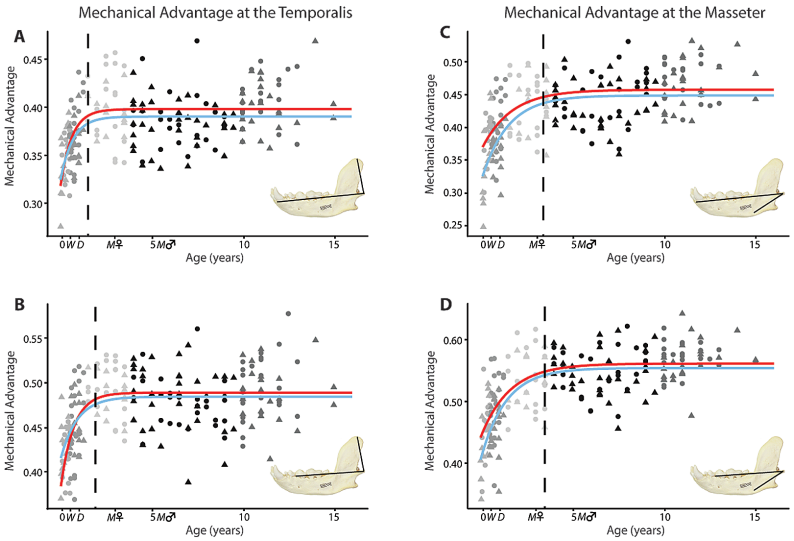

Figure 8. Growth curves for temporalis mechanical advantage to the canine (A) and premolar (B) and for masseter mechanical advantage to the canine (C) and the premolar (D). Circles represent female skulls, triangles represent male skulls and colours represent the five age classes. The red (darker) curves are the female growth curves and the blue (lighter) curves are the male growth curves. There was no significant difference in mechanical advantage between the sexes rates (see Table 3). Black dashed lines indicate the ages at which mechanical advantage reach 95% of their asymptotic values for both females and males combined. On the x-axis, W indicates age of weaning, D indicates age of complete gain of permanent dentition and SM ♀ and SM ♂ indicate earliest age of sexual maturity for female and male southern sea otters, respectively.

2016a, b). Mandibular size in both sexes reached adult maturity during the early subadult stage at age 1.5 years in males and 1.9 years in females, whereas females reached developmental maturity (2.3 years) slightly earlier than males (2.8 years) in mandibular shape.

That the cranium and mandible reached adult maturity at different life-history stages indicates cranial and mandibular development and growth are not in synchrony. A possible explanation for this asynchrony is that the mandible is a relatively simpler structure compared to the cranium. The mandible can reflect biting more easily due to its simple beam shaped structure, whereas the cranium is more complex and houses multiple structures that may pertain to other functions aside from processing food such as sensation and cognition (Wake & Roth, 1989 ; Hanken & Hall, 1993 ; Dumont et al., 2016). Therefore, selection on these other functions may result in slower cranial maturity. Although asynchrony between cranial and mandibular development has also been found in spotted hyenas (C. crocuta - Tanner et al., 2010) and coyotes (Canis latrans - La Croix et al., 2011), neither of these carnivorans exhibited asynchronous growth in the cranium and mandible. While asynchrony in cranial and mandibular development and growth can be one of the many diversifying patterns in the skulls, whether it is one of the more common mammalian patterns awaits further investigation with other taxa.

Despite exhibiting developmental and growth asynchrony, both patterns in cranium and mandible are congruent in that full developmental and growth maturity does not occur until several years after weaning. Newly weaned juveniles no longer have the benefit of obtaining food from their mothers and must compete with conspecific adults for the same food resources (Riedman & Estes, 1990) in already resource-poor environments (Tinker et al., 2008 ; Newsome et al., 2015 ; Tinker & Hatfield, 2015). Biting is an important mechanism used by sea otters to pry open some types of hard-shelled prey or crush other prey items prior to consumption (Riedman & Estes, 1990). Therefore, selective forces are expected to favour juveniles that exhibit fast maturation of the feeding apparatus so they may feed on preferable prey items sooner (Herrel & Gibb, 2006 ; Gignac & Santana, 2016). However, southern sea otters exhibit slow maturation of the skull, particularly in

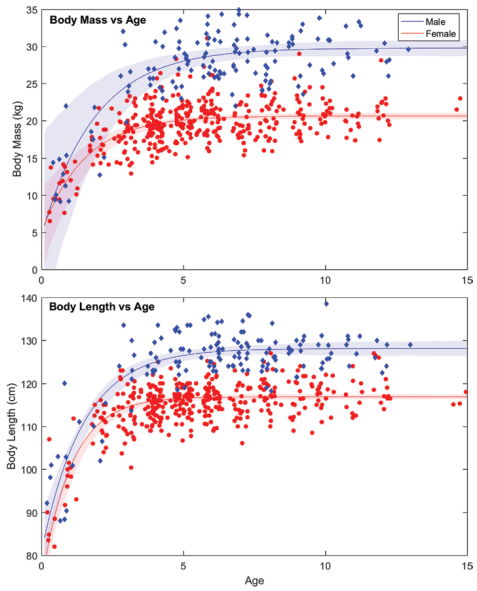

Figure 9. Growth curves for body mass (A) and body length (B). The red curves are the female growth curves and the blue curves are the male growth curves. Shaded red and blue represent 95% interval confidence range of the female and male growth curves, respectively.

the cranium, indicating that biting ability also exhibits slow maturation and is not yet achieved in newly weaned otters.

Over ontogeny, southern sea otters exhibit positive allometric increases in bite force generation relative to condylobasal length, and the temporalis muscle is the greatest contributor underlying these positive allometric increases (Law et al., 2016b). Changes in the cranial shape and size - broadening of the zygomatic arches, lengthening along the anteroposterior axis and development of a more pronounced sagittal crest - all provide additional attachment sites for the temporalis. The temporalis, however, inserts on the top of coronoid process of the mandible. During the mid-subadult stage, the mandible reaches full maturity much earlier than the cranium. The majority of mandibular shape changes are associated with increasing jaw adductor muscle in-levers, and unsurprisingly MA also reaches full maturation during the mid-subadult stage. The early maturation of MA in juvenile otters provides a potential boost in bite force during a period in which the rest of the skull remains smaller and less developed and prevents the jaw adductor muscles, particularly the temporalis, from reaching full development.

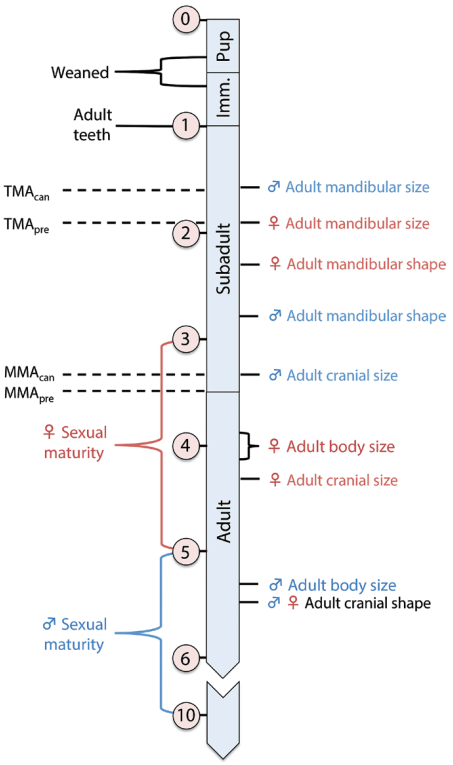

Figure 10. Timeline illustrating the maturation ages of southern sea otter skull morphology and mechanical advantage in relation to major life-history events. Maturation age was defined as the age at which skull shape/size/mechanical advantage and body size reached 95% of their asymptotic values. MMA = mechanical advantage of the masseter; TMA = mechanical advantage of the temporalis. Imm pup. = immature pup.

Therefore, our study suggests that although early maturation of the mandible and MA increase relative bite force with respect to juvenile sea otter body size, full maturation of bite force is not obtained until the temporalis muscles are fully developed, which in turn is constrained by the slow maturation of the cranium.

How immature biting ability affects the foraging ecologies (i.e. foraging success and dietary specialization) and survival of independent juveniles is unknown. Newly weaned juveniles already have the highest daily energy demands of all the immature age classes (Thometz et al., 2014), leading Thometz et al. (2014) to hypothesize that these high metabolic demands have the greatest impact on juvenile

survival during their first year post-weaning. Such a hypothesis is consistent with demographic analyses showing depressed juvenile survival in food-limited sea otter populations in both Alaska (Monson et al. , 2000) and California (Tinker et al. , 2006). Here, we build upon this hypothesis by suggesting that, along with high metabolic demands, immature shape and smaller size of the cranium also affects the survival of newly weaned juveniles by constraining biting abil - ity and thus potentially limiting foraging success on hard-shelled prey. These constraints and limitations suggest that juveniles may be unable to compete with mature sea otters.

Alternatively, novel feeding behaviours can poten - tially provide solutions to feeding with a less devel - oped feeding apparatus. One such feeding behaviour is tool use, an innovation that many animals use to gain otherwise inaccessible food sources (Bentley-Condit & Smith, 2010). Sea otters sometimes use rocks, shells or other hard objects as hammers or anvils to crack open heavily armoured invertebrate prey (Riedman & Estes, 1990). Therefore, tool use could potentially allow juveniles to gain access to hard-shelled prey items, despite having a relatively weak bite force. Indeed, sea otter pups begin playing with objects such as empty shells, often pounding them on their chests, and by 14 weeks of age, most pups are able to use a tool to open a prey item (Staedler, 2011). An important caveat, how - ever, is that individual southern sea otters along the central California coast exhibit pronounced specializa - tion in diet (Estes et al. , 2003 ; Tinker et al. , 2008) and this individual variation in diet is reflected by indi - vidual differences in tool use frequency (Fujii, Ralls & Tinker, 2015 ; Fuijii et al ., in press) . Diet specialists exhibit increased feeding efficiency on their preferred prey taxa (Tinker et al. , 2008 , 2012), apparently ben - efitting from learned handling skills that may include tool use. The frequency of tool use is highly correlated with specialization on prey species with thick, calcium carbonate shells, especially marine snails and larger bivalves (Fujii et al. , 2015). In contrast, individuals that specialize on prey types such as crustaceans and urchins are less likely to use tools with those prey or even when handling snails (Fuijii et al ., in press). Thus, whereas tool use may facilitate feeding on hard-shelled mollusks for some individual juveniles, biting appears to be the primary mechanism used to open other hard-shelled prey. Non-tool using juve - niles are likely susceptible to the presumed feeding disadvantages associated with a less developed feed - ing apparatus that we described above. Nevertheless, a comprehensive examination of the foraging ecology (i.e. dietary specialization, prey encounter rate and feeding efficiencies), feeding behaviour (i.e. tool use) and properties of consumed prey (i.e. prey material properties and prey size) across sea otter ontogeny are required to better understand how juvenile otters are able to compete against mature individuals and suc - cessfully forage for hard-shelled prey.

Pattern s of sexual dimorphi sm

The degree of sexual dimorphism in southern sea otter skulls varied across the five different age classes. We found no sexual dimorphism in skull size and shape of pup, immature and subadult sea otters, albeit we cannot discount the possibility that low and unbal - anced sample sizes between the sexes in these three age classes may have reduced the statistical power needed to distinguish intersexual differences. On the other hand, we found significant male-biased sexual size dimorphism in adult and aged adult cranioman - dibular morphology that are consistent with previous work (Scheffer, 1951 ; Roest, 1985 ; Wilson et al. , 1991 ; Law et al. , 2016a). These size differences translate to larger jaw adductor muscles and bite force in males (Law et al. , 2016b). Furthermore, we also found sig - nificant sexual shape dimorphism in adult and aged adult craniomandibular morphology. In the cranium, adult and aged adult males displayed relatively wider and larger morphological features including wider zygomatic arches and mastoid processes, slightly wider and longer rostrums and slightly more pro - nounced sagittal crests. In contrast, the female man - dible exhibits relatively larger and broader coronoid processes, masseteric fossas and mandibular rami compared to males. Although these craniomandibular shape differences suggest relatively greater tempo - ralis muscle attachment sites in males but relatively greater masseter attachment sites in females (Law et al. , 2016a), jaw adductor mass and bite forces do not significantly differ between the sexes when size cor - rected with either condylobasal length or body mass (Law et al. , 2016b).

Our nonlinear modelling indicated that sexual dimorphism in the skull arose through differences in developmental and growth rates and duration. Male crania, despite their larger sizes, displayed faster developmental and growth rates compared to female crania. Males that attain adult crania maturity ear - lier presumably reach adult biting ability faster and therefore may have a competitive advantage both in obtaining food and also in male–male agonistic inter - actions. As with many polygynous marine mammals, male sea otters compete with other males for access to reproductive females: successful males establish reproductive territories from which they exclude other mature males and maintain exclusive access to estrous females. Territorial defence can involve aggressive interactions with other males (Ames et al ., 1983; Pearson & Davis, 2005) and successful territorial holders are often larger, older males (Riedman & Estes

1990). Reproductive territories are established in kelp-dominated habitats where higher quality prey species occur, and females tend to congregate for all or most of the year (Jameson, 1989 ; Ralls, Eagle & Siniff, 1996).

It is important to note, however, that males rarely establish territories before reaching 6–7 years, just after the age of first reproduction. Nonterritorial males (including most juvenile and subadult males) instead congregate in 'bachelor areas' that are often located in suboptimal soft-sediment habitats or near the edges of the range (Jameson, 1989; Lafferty & Tinker, 2014).

Within bachelor groups, there are extensive male–male interactions ranging from playful to aggressive that may be important for the development of fighting skills and possibly even the establishment of social hierarchies. Play in many social species is hypothesized to be a way to increase the rate of physiological maturation (Burghardt, 2005) and to develop the skills necessary for reproductive success. That male otters reach cranial size maturity much earlier than sexual and body size maturity (Fig. 10) suggests selection for faster cranial growth would allow younger males to begin actively establishing hierarchical relationships much sooner than the onset of sexual and body size maturity. Because biting is the primary weapon used in territorial conflicts between males, we postulate that males that attain mature crania - and therefore bigger heads, greater jaw and possibly neck musculature and stronger biting ability - faster are able to rise through the hierarchical ranks and begin to venture out of bachelor groups to establish their own territories and mate with females. A recent analysis of male reproductive success found that the males that sired the most pups were those that could maintain a territory for the longest (Tarjan 2016): thus, early development of fighting skills could be critical for maximizing lifetime reproductive success.

CONCLUSION

The transition from depending on mother's milk to independently processing hard-shelled invertebrates represents a major ontogenetic dietary shift in southern sea otters. Here, we quantified the development and growth of the feeding apparatuses to elucidate when juveniles reach sufficient maturity required for durophagy. We found that southern sea otters of both sexes exhibit dramatic changes in cranial and mandibular shape and size over ontogeny. Although the majority of these changes occur in the pup stage, full development and growth of the skull does not occur until well after weaning. The mandible reaches adult maturity earlier during the subadult stage, whereas most aspects of cranial maturity do not occur until after mature body size is obtained. We hypothesize that the slower maturation of the crania of newly weaned juveniles serves as a handicap by constraining jaw adductor muscle size, and thus biting ability, and preventing feeding on hard-shelled prey. In addition, we found significant sexual shape and size dimorphism in adult and aged adult craniomandibular morphology that arose through differences in developmental and growth rates and duration. Male crania, despite their larger sizes, displayed faster developmental and growth rates compared to female crania. We postulate that males are selected to attain mature crania faster to presumably reach adult biting ability quicker and gain a competitive advantage in obtaining food and in male–male agonistic interactions.

Our study demonstrates how the analysis of morphological data can provide insight on the foraging ecologies of sea otters across ontogeny. Nevertheless, integrating our results with future investigations of sea otter foraging ecology, feeding behaviour and prey characteristics will elucidate how newly weaned pups are able to successfully forage as they grow as well as examine the mechanisms that contribute to the maintenance of sexual dimorphism.

ACKNOWLEDGEMENTS

We are grateful to Colleen Young (California Department of Fish and Wildlife) for obtaining sea otter specimens; Moe Flannery for access to the mammalian collection at the California Academy of Sciences; Sue Pemberton (California Academy of Sciences), Erin Dodd (California Department of Fish and Wildlife) and Francesca Batac (California Department of Fish and Wildlife) for helping clean the skulls; Vikram Venkatram for helping digitize landmarks; Pete Ramonidi (UCSC) and Carla Sette (UCSC) for helpful suggestions with the statistical analyses and Colleen Young and Brian Hatfield (U.S. Geological Survey) for obtaining the estimated ages of our specimens. Body size data from wild-caught sea otters were provided by U.S. Geological Survey in collaboration with California Department of Fish and Wildlife and the Monterey Bay Aquarium, and MTT is particularly grateful to Brian Hatfield, Mike Kenner, Joe Tomoleoni, Ben Witzman, Mike Harris, Jack Ames, Colleen Young, Michelle Staedler and Mike Murray for assistance with captures. CJL also thanks Mimi Zelditch and Don Swiderski for the training and advice in geometric morphometric methods during the 2016 UC Berkeley geometric morphometric workshop. Lastly, we thank Kristin Campbell and two anonymous reviewers for their helpful comments. Funding was provided partly by a Friends of Long Marine Lab Student Award, a Myers Trust Grant, a Rebecca and Steve Sooy Graduate Research Fellowship for

Marine Mammals and a National Science Foundation Graduate Research Fellowship (all to CJL). Any use of trade, product or firm names in this publication is for descriptive purposes only and does not imply endorsement by the US government.

REFERENCES

Adams DC, Otárola-Castillo E. 2013. geomorph: an r package for the collection and analysis of geometric morphometric shape data. Methods in Ecology and Evolution 4: 393–399.

Ames, J. A., Hardy, R. A., Wendell, F. E., & Geibel, J. J. 1983. Sea otter mortality in California . Sacramento, CA: Marine Resources Branch, California Department of Fish and Game.

Anderson MJ. 2001. A new method for non-parametric multivariate analysis of variance. Austral Ecology 26: 32–46.

Badyaev AV. 2002. Growing apart: an ontogenetic perspective on the evolution of sexual size dimorphism. Trends in Ecology & Evolution 17: 369–378.

Baliga VB, Mehta RS. 2014. Scaling patterns inform ontogenetic transitions away from cleaning in Thalassoma wrasses. The Journal of Experimental Biology 217: 3597–3606.

Bentley-Condit V, Smith EO. 2010. Animal tool use: current definitions and an updated comprehensive catalog. Behaviour 147: 185–221.

Bookstein FL. 1996. Combining the tools of geometric morphometrics. In: Marcus LF, Corti M, Loy A, Naylor GJP, Slice DE, eds. Advances in morphometrics . Boston: Springer US, 131–151.

Bookstein FL. 1997. Landmark methods for forms without landmarks: morphometrics of group differences in outline shape. Medical Image Analysis 1: 225–243.

Brunner S, Bryden MM, Shaughnessy PD. 2004. Cranial ontogeny of otariid seals. Systematics and Biodiversity 2: 83–110.

Burghardt GM. 2005. The genesis of animal play: testing the limits . Cambridge: MIT Press.

Christiansen P, Harris JM. 2012. Variation in cranioman - dibular morphology and sexual dimorphism in pantherines and the sabercat Smilodon fatalis . PLoS ONE 7: e48352.

Christiansen P, Wroe S. 2007. Bite forces and evolutionary adaptations to feeding ecology in carnivores. Ecology 88: 347–358.

Constantino PJ, Lee JJ, Morris D, Lucas PW, Hartstone-Rose A, Lee WK, Dominy NJ, Cunningham A, Wagner M, Lawn BR. 2011. Adaptation to hard-object feeding in sea otters and hominins. Journal of Human Evolution 61: 89–96.

Costa DP, Kooyman GL. 1982. Oxygen consumption, thermoregulation, and the effect of fur oiling and washing on the sea otter, Enhydra lutris . Canadian Journal of Zoology 60: 2761–2767.

Costa DP, Kooyman GL. 1984. Contribution of specific dynamic action to heat-balance and thermoregulation in the sea otter Enhydra lutris . Physiological Zoology 57: 199–203.

Dumont M, Wall CE, Botton-Divet L, Goswami A, Peigné S, Fabre A-C. 2016. Do functional demands associated with locomotor habitat, diet, and activity pattern drive skull shape evolution in musteloid carnivorans? Biological Journal of the Linnean Society 117: 858–878.

Estes JA, Riedman ML, Staedler MM, Tinker MT, Lyon BE. 2003. Individual variation in prey selection by sea otters: patterns, causes and implications. Journal of Animal Ecology 72: 144–155.

Estes JA, Underwood KE, Karmann MJ. 1986. Activity-time budgets of sea otters in California. The Journal of Wildlife Management 50: 626–636.

Fairbairn DJ. 2007. Introduction: the enigma of sexual size dimorphism. In: Fairbairn DJ, Blanckenhorn WU, Székely T, eds. Sex, size and gender roles evolutionary studies of sexual size dimorphism . Oxford: Oxford University Press, 1–10.

Fisher EM. 1941. Notes on the teeth of the sea otter. Journal of Mammalogy 22: 428.

Fujii JA, Ralls K, Tinker MT. 2015. Ecological drivers of variation in tool-use frequency across sea otter populations. Behavioral Ecology 26: 519–526.

Fujii, J.A., Ralls K, Tinker M.T. (In Press) Food abundance, prey morphology, and diet specialization influence individual sea otter tool-use. Behavioral Ecology

Gignac PM, Erickson GM. 2014. Ontogenetic changes in dental form and tooth pressures facilitate developmental niche shifts in American alligators. Journal of Zoology 295: 132–142.

Gignac PM, Santana SE. 2016. A bigger picture: organismal function at the nexus of development, ecology, and evolution: an introduction to the symposium. Integrative and Comparative Biology 56: 369–372.

Gittleman JL, Van Valkenburgh B. 1997. Sexual dimorphism in the canines and skulls of carnivores: effects of size, phylogency, and behavioural ecology. Journal of Zoology 242: 97–117.

Goodall C. 1991. Procrustes methods in the statistical analysis of shape. Journal of the Royal Statistical Society, Series B: Statistical Methodological 53: 285–339.

Gower JC. 1975. Generalized Procrustes analysis. Psychometrika 40: 33–51.

Green B. 1978. Sexual maturity and senescence of the male California sea otter (Enhydra lutris) . Unpublished Masters Thesis. San Jose State University.

Hanken J, Hall BK. 1993. The skull, volume 3: functional and evolutionary mechanisms . Chicago: University of Chicago Press, 1–168.

Hatfield B. 2006. Protocol for stranded and dead sea otters. California Department of Fish and Wildlife 1–15.

Hattori K, Burdin AM, Suzuki M, Ohtaishi N. 2003. Age-related change and allometry of skull and canine of sea otters, Enhydra lutris . The Journal of Veterinary Medical Science 65: 439–447.

Herrel A, Gibb AC. 2006. Ontogeny of performance in vertebrates. Physiological and Biochemical Zoology 79: 1–6.

Herrel A, O'reilly JC. 2006. Ontogenetic scaling of bite force in lizards and turtles. Physiological and Biochemical Zoology 79: 31–42.

Jameson RJ. 1989. Movements, home range and territories of male sea otters off central California. Marine Mammal Science 5: 159–172.

Jameson RJ, Johnson AM. 1993. Reproductive characteris - tics of female sea otters. Marine Mammal Science 9: 156–167.

Kardong KV. 2014. Vertebrates: comparative anatomy, func - tion, evolution . Boston: McGraw-Hill Education.

La Croix S, Holekamp KE, Shivik JA, Lundrigan BL, Zelditch ML. 2011. Ontogenetic relationships between cranium and mandible in coyotes and hyenas. Journal of Morphology 272: 662–674.

Lafferty KD, Tinker MT. 2014. Sea otters are recolonizing southern California in fits and starts. Ecosphere 5: 1–11.

Laidre KL, Estes JA, Tinker MT, Bodkin J, Monson D, Schneider K. 2006. Patterns of growth and body condition in sea otters from the Aleutian archipelago before and after the recent population decline. The Journal of Animal Ecology 75: 978–989.

Law CJ, Venkatram V, Mehta RS. 2016a. Sexual dimor - phismin craniomandibular morphology of southern seaot - ters (Enhydra lutris nereis). Journal of Mammalogy 97:1764–1773.

Law CJ, Young C, Mehta RS. 2016b. Ontogenetic scaling of theoretical bite force in southern sea otters (Enhydra lutris nereis). Physiological and Biochemical Zoology 89: 347–363.

Lindenfors P, Gittleman JL, Jones KE. 2007. Sexual size dimorphism in mammals. In: Fairbairn DJ, Blanckenhorn WU, Székely T, eds. Sex, size and gender roles evolutionary studies of sexual size dimorphism . Oxford: Oxford University Press, 16–26.

Lindenfors P, Tullberg B, Biuw M. 2002. Phylogenetic analyses of sexual selection and sexual size dimorphism in pinnipeds. Behavioral Ecology and Sociobiology 52: 188–193.

Lovich JE, Gibbons JW. 1992. A review of techniques for quantifying sexual size dimorphism. Growth, Development, Aging 56: 269–281.

Monson DH, Estes JA, Bodkin JL, Siniff DB. 2000. Life history plasticity and population regulation in sea otters. Oikos 90: 457–468.

Moors PJ. 1980. Sexual dimorphism in the body size of mus - telids (Carnivora): the roles of food habits and breeding sys - tems. Oikos 34: 147–158.

Morrison P, Rosenmann M, Estes JA. 1974. Metabolism and thermoregulation in the sea otter. Physiological Zoology 47: 218–229.

Newsome SD, Tinker MT, Gill VA, Hoyt ZN, Doroff A, Nichol L, Bodkin JL. 2015. The interaction of intraspecific competi - tion and habitat on individual diet specialization: a near range-wide examination of sea otters. Oecologia 178: 45–59.

Payne SF, Jameson RJ. 1984. Early behavioral development of the sea otter, Enhydra lutris . Journal of Mammalogy 65: 527–531.

Pearson, H. C., & Davis, R. W. 2005. Behavior of territorial male sea otters Enhydra lutris in Prince William Sound, Alaska. Aquatic Mammals , 31 (2): 226–233.

R Core Team. 2015. R: a language and environment for sta- tistical computing. R Foundation for Statistical Computing, Vienna. http://www.R-project.org/.

Radinsky LB. 1981a. Evolution of skull shape in carnivores. 1. Representative modern carnivores. Biological Journal of the Linnean Society 15: 369–388.

Radinsky LB. 1981b. Evolution of skull shape in carnivores. 2. Additional modern carnivores. Biological Journal of the Linnean Society 16: 337–355.

Ralls K, Harvey PH. 1985. Geographic variation in size and sexual dimorphism of North American weasels. Biological Journal of the Linnean Society 25: 119–167.

Ralls K, Siniff DB. 1990. Time budgets and activity patterns in California sea otters. The Journal of Wildlife Management 54: 251–259.

Ralls K, Eagle TC, Siniff DB. 1996. Movement and spatial use patterns of California sea otters. Canadian Journal of Zoology 74: 1841–1849.

Riedman M, Estes JA. 1990. The sea otter (Enhydra lutris): behavior, ecology, and natural history. Biological Report 90: 1–117.

Riley MA. 1985. An analysis of masticatory form and function in three mustelids (Martes americana , Lutra canadensis , Enhydra lutris). Journal of Mammalogy 66: 519–528.

Roest AI. 1985. Determining the sex of sea otters from skulls. California Fish Game 71: 179–183.

Rohlf FJ. 2010. tpsDig, 2.10. Ecology and Evolution, SUNY at Stony Brook Department of Ecology and Evolution, State University of New York, Stony Brook, NY 11794–524.

Rohlf FJ, Slice D. 1990. Extensions of the Procrustes method for the optimal superimposition of landmarks. Systematic Zoology 39: 40–21.

Sanfelice D, De Freitas TRO. 2008. A comparative descrip - tion of dimorphism in skull ontogeny of Arctocephalus aus - tralis , Callorhinus ursinus , and Otaria byronia (Carnivora: Otariidae). Journal of Mammalogy 89: 336–346.

Santana SE and Miller KE 2016. Extreme postnatal scaling in bat feeding performance: a view of ecomorphology from ontogenetic and macroevolutionary perspectives. Integrative and Comparative Biology 56:459-468.

Scheffer VB. 1951. Measurements of sea otters from western Alaska. Journal of Mammalogy 32: 10–14.

Schlager S. 2016. Morpho: calculations and visualisations related to geometric morphometrics. R-package version 2.4 .

Segura V. 2015. A three-dimensional skull ontogeny in the bobcat (Lynx rufus) (Carnivora: Felidae): a comparison with other carnivores. Canadian Journal of Zoology 93: 225–237.

Shea BT. 1986. Ontogenetic approaches to sexual dimorphism in anthropoids. Human Evolution 1: 97–110.

Smith RJ. 1999. Statistics of sexual size dimorphism. Journal of Human Evolution 36: 423–459.

Staedler MM. 2011. Maternal care and provisioning in the - southern sea otter (Enhydra lutris nereis): reproductive consequences of diet specialization in an apex predator. Unpublished D. Phil. Thesis. University of California, Santa Cruz.

Tanner JB, Zelditch ML, Lundrigan BL. 2010. Ontogenetic change in skull morphology and mechanical advantage in the spot - ted hyena (Crocuta crocuta). Journal of Morphology 271: 353–365.

Tarjan, L.M. 2016. Space Use and Reproductive Success of Male Sea Otters. Unpublished D. Phil. Thesis. University of California, Santa Cruz.

Tarjan LM, Tinker MT. 2016. Permissible home range estimation (PHRE) in restricted habitats: a new algorithm and an evaluation for sea otters. PLoS ONE 11: e0150547.
Tarnawski BA, Cassini GH, Flores DA. 2013. Allometry of the postnatal cranial ontogeny and sexual dimorphism in Otaria byronia (Otariidae). Acta Theriologica 59: 81–97.
Tarnawski BA, Cassini GH, Flores DA. 2014. Skull allometry and sexual dimorphism in the ontogeny of the southern elephant seal (Miroungaleonina leonina). Canadian Journal of Zoology 92: 19–31.
Thom MD, Harrington LA. 2004. Why are American mink sexually dimorphic? A role for niche separation. Oikos 105: 525–535.
Thometz NM, Tinker MT, Staedler MM, Mayer KA, Williams TM. 2014. Energetic demands of immature sea otters from birth to weaning: implications for maternal costs, reproductive behavior and population-level trends. The Journal of Experimental Biology 217: 2053–2061.
Thometz NM, Staedler MM, Tomoleoni JA, Bodkin JL,Bentall GB, Tinker MT. 2016. Trade-offs between energy maximization and parental care in a central place forager, the sea otter. Behavioral Ecology. doi: 10.1093/beheco/arw089
Timm-Davis LL, DeWitt TJ, Marshall CD. 2015. Divergent skull morphology supports two trophic specializations in otters (Lutrinae). PLoS ONE 10: e0143236.
Tinker MT, Hatfield BB. 2015. Southwest U.S. Southern sea otter annual range-wide census results. US Geological Surveydata release. http://dx.doi.org/10.5066/F7F47M5C.
Tinker MT, Doak DF, Estes JA, Hatfield BB, Staedler MM, Bodkin JL. 2006. Incorporating diverse data and realistic complexity into demographic estimation procedures for sea otters. Ecological Applications 16: 2293–2312.
Tinker MT, Staedler MM, Tarjan LM, Bentall G,Tomoleoni J, LaRoche NL. 2016. Geospatial data collected from tagged sea otters in central California, 1998–2012. US Geological Survey data release. http://www.dx.doi.org/10.5066/F76H4FH8.
Tinker MT, Bentall G, Estes JA. 2008. Food limitation leads to behavioral diversification and dietary specialization in sea otters. Proceedings of the National Academy of Sciences 105: 560–565.
Wake DB, Roth G. 1989. Complex organismal functions: integration and evolution in vertebrates . New York: John Wiley & Sons, 1–451.
Weckerly FW. 1998. Sexual-size dimorphism: influence of mass and mating systems in the most dimorphic mammals. Journal of Mammalogy 79: 33–52.
Wiley RH. 1974. Evolution of social organization and life-history patterns among grouse. The Quarterly Review of Biology 49: 201–227.
Wilson DE, Mittermeier RA. 2009. Handbook of the mammalsof the world. Vol. 1 Carnivora. Barcelona, Spain: Lynx Edicions.
Wilson DE, Bogan MA, Brownell RL, Burdin AM, Maminov MK. 1991. Geographic variation in sea otters, Enhydra lutris . Journal of Mammalogy 72: 22–36.
Yeates LC, Williams TM, Fink TL. 2007. Diving and foraging energetics of the smallest marine mammal, the sea otter (Enhydra lutris). The Journal of Experimental Biology 210: 1960–1970.
Zelditch ML, Lundrigan BL, David Sheets H, Garland T. 2003. Do precocial mammals develop at a faster rate? A comparison of rates of skull development in Sigmodon fulviventer and Mus musculus domesticus . Journal of Evolutionary Biology 16: 708–720.
Zelditch ML, Swiderski DL, Sheets HD. 2012. Geometric morphometrics for biologists: a primer. London: Academic Press.
Ziscovici C, Lucas PW, Constantino PJ, Bromage TG, van Casteren A. 2014. Sea otter dental enamel is highly resistant to chipping due to its microstructure. Biology Letters 10: 20140484.

SUPPORTING INFORMATION

Additional Supporting Information may be found in the online version of this article at the publisher's web-site:

Figure S1. Landmarks (black circles) and semilandmarks (white circles) digitized from the ventral cranium (A), lateral cranium (B) and mandible (C) used in the study. See Supporting Information, Table S3 for description of landmarks.
Table S1. Specimens used in this study.
Table S2. Age classes of the southern sea otter and the skull sample size per age class used in this study.
Table S3. Description of landmarks and semilandmarks used in this study.
Table S4. Results from Procrustes ANOVAs for intersexual cranial and mandibular shape differences within each age class. Bold P -values indicate significance ($\alpha = 0.05$).
Table S5. Results from pairwise permutation tests for intersexual cranial and mandibular shape differences in Procrustes distances (PD) within each age class. Bold P -values indicate significance ($\alpha = 0.05$).
Table S6. Results from analyses of covariance (ANCOVAs) for sex differences in cranial and mandibular centroid size within each age class. Bold P -values indicate significance ($\alpha = 0.05$).
Table S7. AICc and AICc weight scores of the seven growth models fitted to cranial shape, cranial centroid size and mechanical advantage. The AIC weight evaluates relative goodness-of-fit by balancing the distance between model and data by degrees of freedom.

Ontogenetic Scaling of Theoretical Bite Force in Southern Sea Otters (Enhydra lutris nereis)

Chris J. Law [1,*]
Colleen Young [2]
Rita S. Mehta [1]
[1]Department of Ecology and Evolutionary Biology, University of California, 100 Shaffer Road, Santa Cruz, California 95060; [2]California Department of Fish and Wildlife, Marine Wildlife Veterinary Care and Research Center, 1451 Shaffer Road, Santa Cruz, California 95060

Accepted 6/29/2016; Electronically Published 8/18/2016

ABSTRACT

Sexual dimorphism attributed to niche divergence is often linked to differentiation between the sexes in both dietary resources and characters related to feeding and resource procurement. Although recent studies have indicated that southern sea otters (Enhydra lutris nereis) exhibit differences in dietary preferences as well as sexual dimorphism in skull size and shape, whether these intersexual differences translate to differentiation in feeding performances between the sexes remains to be investigated. To test the hypothesis that scaling patterns of bite force, a metric of feeding performance, differ between the sexes, we calculated theoretical bite forces for 55 naturally deceased male and female southern sea otters spanning the size ranges encountered over ontogeny. We then used standardized major axis regressions to simultaneously determine the scaling patterns of theoretical bite forces and skull components across ontogeny and assess whether these scaling patterns differed between the sexes. We found that positive allometric increases in theoretical bite force resulted from positive allometric increases in physiological cross-sectional area for the major jaw adductor muscle and mechanical advantage. Closer examination revealed that allometric increases in temporalis muscle mass and relative allometric decreases in out-lever lengths are driving these patterns. In our analysis of sexual dimorphism, we found that scaling patterns of theoretical bite force and morphological traits do not differ between the sexes. However, adult sea otters differed in their absolute bite forces, revealing that adult males exhibited greater bite forces as a result of their larger sizes. We found intersexual differences in biting ability that provide some support for the niche divergence hypothesis. Continued work in this field may link intersexual differences in feeding functional morphology with foraging ecology to show how niche divergence has the potential to reinforce sexual dimorphism in southern sea otters.

Keywords: biomechanics, cranial musculature, durophagy, feeding performance, Mustelidae, niche divergence, sexual dimorphism.

Introduction

Dietary specialization by some individuals within the same population is a prevalent phenomenon that is not well understood (Bolnick et al. 2011). The sex structure of populations introduces natural variability in morphology and behavior that may contribute to feeding differences between individuals. While sexual selection may drive morphological disparity between the sexes (Darwin 1871; Clutton-Brock 2007), natural selection may also select for traits that reduce competition for food resources (Darwin 1871; Hedrick and Temeles 1989; Shine 1989). The latter hypothesis is known as niche divergence and suggests that sexual dimorphism is linked to dietary partitioning (Darwin 1871). Sexual dimorphism attributed to niche divergence is often expressed as differences in cranial size and shape (Darwin 1871; Camilleri and Shine 1990; Radford and Plessis 2003; Thom and Harrington 2004), which further translates to differences in feeding performances between the sexes (Herrel et al. 1999, 2007; Bulté et al. 2008; McGee and Wainwright 2013; Thomas et al. 2015).

In many vertebrates, biting is the primary mechanism to capture, kill, and consume prey (Kardong 2014). Bite force, a widely used measure of feeding performance, has been shown to be a strong link between cranial morphology and dietary ecology (Herrel et al. 2007; Anderson et al. 2008; Bulté et al. 2008; Santana et al. 2010). Greater bite forces also strongly correlate with reduced handling times for both prey capture and consumption (Herrel et al. 2001; Verwaijen et al. 2002; van der Meij and Bout 2006; Anderson et al. 2008). In most cases, individuals with larger heads exert greater forces and can therefore expand their dietary breadth by consuming larger or more robust food items (Verwaijen et al. 2002; Herrel et al. 2006; Bulté et al. 2008). Therefore, by growth alone, both males and females exhibit increases in bite force that can lead to increased foraging efficiency and net energy intake (Binder and Valkenburgh 2000; Huber et al. 2006; Pfaller et al. 2011; Marshall et al. 2014).

The ability to generate large forces during feeding is particularly important for durophagous vertebrates, those that specialize on hard items such as bones, seeds, or shelled organisms

*Corresponding author; e-mail: cjlaw@ucsc.edu.

Physiological and Biochemical Zoology 89(5):347–363. 2016. 1522-2152/2016/8905-6037$15.00. DOI: 10.1086/688313

(Van Valkenburgh 2007; Collar et al. 2014). Unsurprisingly, a plethora of studies have revealed that bite force in durophagous species scales with positive allometry relative to body size through ontogeny (Erickson et al. 2003; Pfaller et al. 2011; Marshall et al. 2012; Kolmann et al. 2015). Ontogenetic increases in bite force can occur from a disproportionate increase in (1) head size (Anderson et al. 2008); (2) physiological cross-sectional area (PCSA) of the jaw adductor muscles, which can be altered by changing various components of muscle architecture including mass, pennation angle, and muscle fiber lengths (Pfaller et al. 2011; Kolmann et al. 2015); (3) mechanical advantage, which can be enhanced by shifting muscle insertion points or the bite point (Grubich 2005; Huber et al. 2008); or (4) any combination of the aforementioned changes (Hernandez and Motta 1997; Huber et al. 2006; Kolmann and Huber 2009). Although an increasing number of studies have examined the differential scaling of head size, jaw muscle force, mechanical advantage, and their contributions to bite force, few studies have examined these parameters in mammals (Santana and Miller 2016). Furthermore, even fewer studies have investigated whether scaling patterns of bite force and its underlying components differ between the sexes, particularly within mammals.

Southern sea otters (Enhydra lutris nereis) are an excellent mammalian system with which to examine scaling patterns of bite force and dimorphism in biting ability. These durophagous marine mustelids feed on a variety of hard-shelled invertebrates such as chitinous crabs and calcifying bivalves and gastropods (Riedman and Estes 1990). Like many durophagous mammals, sea otters exhibit several cranial adaptations that facilitate durophagy including short, blunt skulls (Riley 1985); taller and wider mandibular rami (Timm-Davis et al. 2015; bunodont dentition (Fisher 1941; Constantino et al. 2011); and fracture-resistant dental enamel (Ziscovici et al. 2014). Recent work on adult southern sea otters indicated that although size is the primary axis of craniomandibular variation, a handful of craniomandibular traits demonstrated significant shape differences between the sexes (Law et al., forthcoming). These size-corrected differences in jaw adductor muscle in-levers, cranial height, and postorbital constriction breadth suggest differences in biting ability between the sexes for a given body size.

In this study, we tested the hypothesis that the scaling patterns of muscle dissection–based estimations of bite force and the underlying anatomical components differ between the sexes. To test our hypothesis, we first investigated the anatomical traits that contribute to bite force generation in southern sea otters. We then simultaneously determined the scaling patterns of theoretical bite forces and skull components across ontogeny and assessed whether these scaling patterns differed between the sexes. Last, we elucidated which of these factors are responsible for the strong allometric patterns of bite force production.

Methods and Material

Specimens and Gross Dissections

We obtained 55 naturally deceased southern sea otters (24 females and 31 males; table A1) from the California Department of Fish and Wildlife (CDFW) Marine Wildlife Veterinary Care and Research Center from October 2013 to February 2016. The age class of each specimen was determined using a suite of morphological characteristics including total body length, tooth wear, and closure of cranial sutures (table A2; Hat field 2006). Body mass was also measured for each specimen. All specimens stranded along the central California coast, within and throughout the current southern sea otter range (Pigeon Point in the north to Gaviota in the south).

We dissected the major jaw adductor muscles (superficial temporalis, deep temporalis, superficial masseter, deep masseter, and zygomaticomandibularis) following Scapino 's (1968) cranial musculature description of various mustelids including the northern sea otter (Enhydra lutris kenyoni). While there was distinct separation between the superficial and deep temporalis, there was inadequate separation between the superficial masseter, deep masseter, and zygomaticomandibularis muscles (Scapino 1968). Therefore, we treated the three subdivisions as one muscle, the masseter (fig. 1A). Furthermore, because the medial pterygoid is positioned deep along the medial side of the mandible and cannot be excised intact, we did not include this muscle in our analyses. Muscles were removed from the left side of the skull, blotted dry, and weighed to the nearest 0.1 g using a digital scale.

We then measured the length and pennation angle of muscle fibers by digesting and separating the muscles in a solution of 15% aqueous nitric acid for 3–7 d depending on muscle size (Biewener and Full 1992). Muscle fiber lengths were measured to the nearest 0.01 mm using a digital caliper. Skulls were subsequently cleaned by a dermestid beetle colony at the California Academy of Sciences or with a maceration tank at CDFW. We then photographed and digitally measured the condylobasal length (distance from the anteriormost point on the premaxillae to the plane of the posterior surface of the occipital condyles), zygomatic breadth (greatest distance across the zygomatic arches), and cranial height (distance perpendicular to the palate plane from the lateralmost point of the mastoid process to the point of the sagittal crest directly superior to the mastoid process) of each cranium using ImageJ (Schneider et al. 2012; fig. 1C, 1D).

Bite Force Model

Because of its craniostylic characteristics, the mammalian jaw can be modeled as a static third-class lever where an axis passing through the temporomandibular joints (TMJs) serves as the fulcrum and muscle forces generated by jaw adductor muscle contractions create rotation of the lower jaw about this fulcrum (Davis et al. 2010). Under static lever equilibrium, the force of biting balances the rotation of the lower jaw created by these muscle forces (fig. 1A, 1B).

We first calculated PCSA for each muscle based on muscle mass (m), mean fiber length (f), muscle density (r), and fiber pennation angle (v; Sacks and Roy 1982):

$$\text{PCSA} = \frac{m \cos[\theta]}{r \quad f}.$$

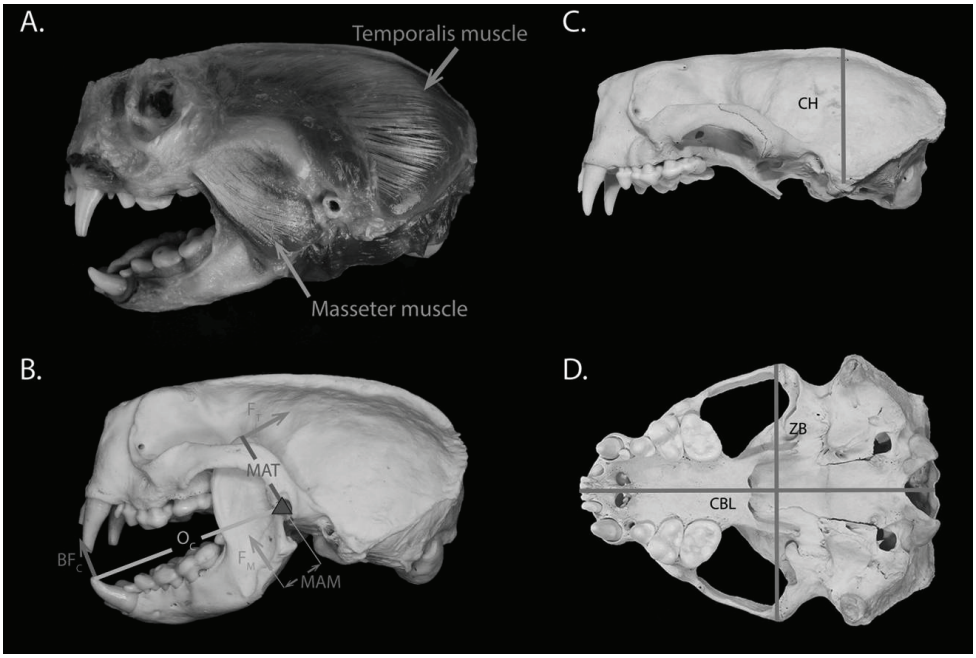

Figure 1. A, Photograph of the two major jaw adductor muscles of an adult male sea otter. B, Force of the temporalis and masseter muscles (F_T and F_M) are applied at given distances (MAT and MAM) from the fulcrum (triangle), creating rotation of the lower jaw. Bite forces, at given distances (O_C and O_M), balance these muscle forces. Using the model $BF_X = 2[(F_T \times MAT + F_M \times MAM)/O_X]$, theoretical bite forces are calculated at the canine (BF_C) and the molar (BF_M). C, D, Cranial dimensions used in this study. CBL = condylobasal length; CH = cranial height; ZB = zygomatic breadth. A color version of this figure is available online.

We used a mammalian muscle density of 1.06 g/cm^3 (Mendez and Keys 1960). Jaw muscle fibers were parallel; thus, we used a fiber pennation angle of 0°. PCSA of the temporalis muscle was totaled as a sum of the PCSA calculated for the superficial and deep temporalis subdivisions and modeled as a single muscle. To estimate muscle forces of the temporalis and masseter, we multiplied PCSA by a muscle stress value of 25 N/cm^2 (Herzog 1994), a value that is commonly used in other dissection-based estimations of bite force (Herrel et al. 2008; Davis et al. 2010; Santana et al. 2010; Pfaller et al. 2011). We then modeled each muscle force as a single force vector (F_T and F_M) and applied them to the insertion points of the temporalis, the top of the coronoid process of the mandible, and the masseter, the midpoint between the anteriormost edge of the masseteric fossa and the angular process of the mandible. Our estimation of muscle forces assumed that all of the jaw muscles were maximally activated.

We calculated maximum theoretical bite forces (BF_X) by adding the moment (product of the force vector and in-lever length) of each jaw adductor muscle, dividing by the out-lever, and multiplying by 2 to account for bilateral biting:

$$BF_X = 2\left(\frac{F_T \times MAT + F_M \times MAM}{O_X}\right),$$

where F_T and F_M are the force vectors of the temporalis and masseter, respectively; MAT is the perpendicular in-lever length of the temporalis, measured as the perpendicular distance from the temporalis muscle force vector to the TMJ; MAM is the perpendicular in-lever length of the masseter, measured as the perpendicular distance from the masseter muscle force vector to the TMJ; and O_X is the out-lever length, measured as the distance between the bite point and the TMJ (Davis et al. 2010). Muscle force vectors were estimated based on gape angle measured from the maxillary tip to the condyle to the mandibular tip. Because data for gape angles were unavailable for all age classes, we estimated maximum gape angle based on measurements from osteological specimens. We used constant gape angles of 45°, 55°, 60°, and 62° for pups, immatures, subadults, and adults, respectively. Our estimation of adult gape angles is similar to the mean gape angle range (66.5°) obtained from observational studies of adult sea otter feeding (Timm 2013). We calculated theoretical bite forces at two locations, the lower canine (BF_C) and in be-

Table 1: Scaling of cranial dimensions against body mass and body length

	Sex effects		Scaling relationships				
	Intercept	P	R^2	Slope (95% CI)	P	Isometric prediction	Scaling patterns
A. Cranial dimensions against BM:							
CBL	F 4.35, M 4.35	.679	.89	.17 (.15–.19)	! .001	.33	NA
ZB	F 4.02, M 4.05	.959	.9	.18 (.17–.20)	! .001	.33	NA
CH	F 3.81, M 3.74	.929	.65	.12 (.09–.13)	! .001	.33	NA
B. Cranial dimensions against BL:							
CBL	F 2.48, M 2.57	.051	.91	.53 (.49–.58)	! .001	1	NA
ZB	F 1.86, M 2.11	.195	.91	.57 (.52–.63)	! .001	1	NA
CH	F 2.72, M 2.43	.621	.57	.36 (.30–.42)	! .001	1	NA

Note. Cranial dimensions served as dependent variables, while body mass (BM; pt. A) and body length (BL; pt. B) served as independent variables. P values from tests of sex effects reflect differences in elevation between the sexes, and P values from tests of isometry reflect differences from isometric predictions. All P values are reported as Benjamini-Hochberg-corrected values. Bold P values indicate significance ($\alpha = 0.05$). See table A3 for tests in difference of slopes. CI = confidence interval. For scaling patterns, NA = negative allometry. CBL = condylobasal length; CH = cranial height; F = female; M = male; ZB = zygomatic breadth.

tween the first and second molars of the lower jaw (BF/M). These two bite points represent important bite positions in prey processing for sea otters; biting at the canine is used to pry open hard-shelled invertebrates such as bivalves, whereas the molars are used to crush items before consumption (Riedman and Estes 1990). All in-lever and out-lever measurements were taken from photographs of the lateral view of the mandible in ImageJ v. 1.48 (Schneider et al. 2012).

Statistical Analyses

We performed all statistical analyses in R 3.2.3 (R Core Team 2015). We natural log transformed (ln) all variables to reduce skewness and heteroscedasticity across values of all variables and ensure that traits exhibited linear relationships with each other. To determine which cranial dimension (condylobasal length, zygomatic breadth, cranial height) and body size metric (body mass, body length) were the best predictors of bite force, we performed separate sex-specific multiple regression analyses. In each analysis, we used theoretical bite force as the dependent variable and cranial dimensions and body size as the independent variables. Following Baliga and Mehta (2014), we estimated the R^2 decomposition of each model (Zuber and Strimmer 2011) by computing correlations between the response and the Mahalanobis-decorrelated predictors (CAR scores) using the R package relaimpo (Grömping 2006). Comparing these scores allowed us to assess the relative importance of each predictor, enabling us to identify which measurement most strongly predicted each sex's ontogenetic bite force trajectory.

We used the R package smatr (Warton et al. 2011) to simultaneously (1) examine scaling patterns between/within the body size, cranial dimensions, theoretical bite forces, and components of our bite force model and (2) assess whether these scaling patterns differed between the sexes. To examine scaling among body size and cranial dimensions, we performed standardized major axis (SMA) regressions with cranial dimensions as dependent variables, body mass and body length as independent variables, and sex as the main factor. Similarly, to examine scaling of bite force generation, we performed SMA regressions with theoretical bite forces, model components (in-levers, out-levers, jaw muscle masses, and muscle fiber lengths), mechanical advantage, and muscle PCSAs as dependent variables, body size and cranial dimensions as the independent variables, and sex as the main factor. In each independent analysis, we first tested the null hypothesis that the mean SMA regression slopes and elevation did not significantly differ between the sexes. Because we found nonsignificant differences between slopes in all of our analyses (see "Results"), we pooled the male and female data sets for subsequent scaling analyses. Scaling relationships between all SMA regression slopes were compared with null predictions of isometry (linear measurements = 1.0; areas and forces = 2.0; masses = 3.0), based on Euclidean geometry (Hill 1950; Schmidt-Nielsen 1984; Emerson and Bramble 1993). Using modified t-tests, we tested whether each slope significantly deviated from isometry (i.e., allometry). Predicted slopes significantly greater or less than the 95% confidence intervals of the observed SMA regression slopes were interpreted as positive or negative allometry, respectively. We adjusted all P values using a Benjamini-Hochberg correction to reduce the type I error probability across multiple comparisons (Benjamini and Hochberg 1995). We then ran a second set of sex-specific multiple regression analyses and calculated CAR scores to assess which component of the bite force model contributed the most to theoretical bite forces in each sex. In these analyses, we used theoretical bite force as the dependent variable and model components (out-levers, in-levers, jaw muscle masses, and jaw fiber length) as the independent variables.

Last, we used ANOVAs to test for sexual size differences of each trait and theoretical bite force in the adult specimens. We used only adults because differential dietary specialization between the sexes has been examined only in adult southern sea otters. We did not use natural log–transformed values for these ANOVA tests.

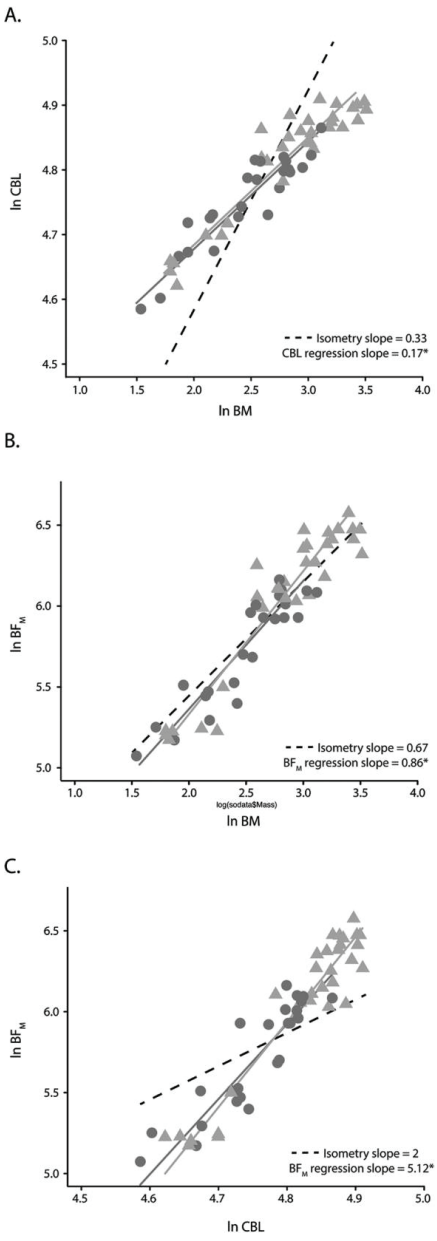

Figure 2. Scaling of condylobasal length (CBL) on body mass (BM) for female and male southern sea otters (A), bite force at the molar (BF_M) on condylobasal length (B), and bite force at the molar on body mass (C). Circles indicate female otters, and triangles indicate male otters. Dark gray and light gray solid lines represent standardized major axis regressions for females and males, respectively. Dotted lines indicate line of isometry. An asterisk indicates that the slope is significantly different from isometry. See tables 1, 2, and A3 for more details. A color version of this figure is available online.

Results

Mean slopes between the sexes were not significantly different in all SMA analyses (table A3), indicating that scaling patterns of cranial morphology and biting ability do not differ between females and males.

Scaling of Cranial Morphometrics

Condylobasal length, zygomatic breadth, and cranial height all scaled with negative allometry relative to body mass and body length (table 1; fig. 2A). Among cranial traits, zygomatic breadth scaled isometrically to condylobasal length ($b = 1$, $P = 0.153$), whereas cranial height scaled with negative allometry ($b < 1$, $P < 0.001$). These trends were observed in both males and females.

Scaling of Biting Biomechanics

Theoretical bite force at the canine and molar showed positive allometric relationships with body and cranial dimensions (table 2; fig. 2B, 2C). CAR scores indicated that ln condylobasal length and ln body mass were the greatest head and body predictors of theoretical bite force in both sexes (table 3).

All bite force model components, mechanical advantage at the canine, and muscle PCSA displayed positive allometry relative to ln condylobasal length (all $P \leq 0.001$–0.012; table 4; figs. 3, 4). However, we found no relationship between ln condylobasal length and mechanical advantage at the molar for both jaw muscles (table 4).

Conversely, disparate scaling patterns emerged when we examined the ontogeny of the bite force model components against ln body mass (table A4, pt. A). Ln lengths of the out-levers and temporalis in-lever scaled with negative allometry relative to ln body mass ($b < 0.33$, $P \leq 0.001$–0.041), whereas ln masseter in-lever length scaled isometrically ($b = 0.33$, $P = 0.408$). Masses of the jaw adductor muscles also differed in allometric scaling: ln temporalis mass scaled with positive allometry relative to ln body mass ($b > 1$, $P = 0.041$), and ln masseter mass scaled with negative allometry relative to ln body mass ($b < 1$, $P = 0.047$). Last, ln fiber lengths for both jaw adductor muscles scaled isometrically relative to ln body mass ($b = 0.33$, $P = 0.183$–0.578). Examination of mechanical advantage and PCSA against ln body mass also revealed disparate scaling patterns (table A4, pt. B, C). Ln temporalis and masseter mechanical advantage at the canine scaled with positive allometry ($b > 0$, both $P < 0.001$; table A4, pt. B). In contrast, there was no significant relationship between ln body mass and ln mechanical advantage at the molar for both jaw muscles ($R^2 = 0.00$–0.10, $P = 0.067$–0.561). Overall ln PCSA of the temporalis and of the masseter scaled with positive allometry ($b > 0.67$, $P < 0.001$) and isometry ($b = 0.67$, $P = 0.198$), respectively (table A4, pt. C).

Table 2: Scaling of estimated bite forces against body and cranial dimensions

	Sex effects		Scaling relationships				
	Intercept	P	R^2	Slope (95% CI)	P	Isometric prediction	Scaling pattern
A. BF_C against body and cranial dimensions:							
BM	F 3.03, M 2.71	.996	.88	.92 (.84–1.01)	! .001	.67	PA
BL	F 2 6.40, M 2 7.62	.297	.88	2.89 (2.63–3.18)	! .001	2	PA
CBL	F 2 18.90, M 2 22.49	.621	.9	5.47 (5.02–5.96)	! .001	2	PA
ZB	F 2 14.54, M 2 18.87	.959	.9	4.98 (4.56–5.44)	! .001	2	PA
CH	F 2 29.85, M 2 26.69	.929	.61	8.06 (6.79–9.57)	! .001	2	PA
B. BF_M against body and cranial dimensions:							
BM	F 3.77, M 3.55	.831	.89	.86 (.78–.95)	! .001	.67	PA
BL	F 2 5.15, M 2 5.94	.130	.87	2.61 (2.33–2.91)	! .001	2	PA
CBL	F 2 16.97, M 2 19.61	.929	.89	5.12 (4.36–5.59)	! .001	2	PA
ZB	F 2 12.85, M 2 16.29	.929	.89	4.66 (4.25–5.11)	! .001	2	PA
CH	F 2 27.33, M 2 23.48	.996	.62	7.46 (6.30–8.84)	! .001	2	PA

Note. Bite force at the canine (BF_C; pt. A) and molar (BF_M; pt. B) served as dependent variables, while body and cranial dimensions served as independent variables. P values from tests of sex effect reflect differences in elevation between the sexes, and P values from tests of isometry reflect differences from isometric predictions. All P values are reported as Benjamini-Hochberg-corrected values. Bold P values indicate significance ($\alpha = 0.05$). See table A3 for tests in difference of slopes. For scaling patterns, PA = positive allometry. BM = body mass; BL = body length; CBL = condylobasal length; CH = cranial height; F = female; M = male; ZB = zygomatic breadth.

CAR scores revealed that out of the seven components in our bite force model, the temporalis muscle mass was the greatest contributor to theoretical bite force in both sexes (table 5). A second CAR score analysis also found that temporalis muscle mass contributed to the bite force model more than mechanical advantage (table A5).

Effects of Sexual Dimorphism on the Ontogeny of Biting Biomechanics

Mean slopes between the sexes were not significantly different in all SMA analyses (table A3). In addition, we did not find significant elevation effects between the sexes in our SMA regressions of cranial dimensions against body size metrics (table 1; fig. 2A) or theoretical bite forces against body size and cranial dimensions (table 2; fig. 2B, 2C). However, SMA regressions of the bite force model components against body mass and condylobasal length revealed significant elevation effects in some model components (tables 4, A4; fig. 4). These analyses suggested that for a given condylobasal length or body mass, female sea otters exhibit relatively longer temporalis and masseter in-levers but shorter molar out-levers (tables 4A, A4, pt. A; fig. 4). In addition, overall temporalis and masseter mechanical advantage to the canine was relatively higher in females than in males (tables 4, pt. B; A3).

Adult Characteristics

Males were significantly larger than females for absolute values of body size and cranial dimensions ($P = 0.001$–0.013; table 6).

Table 3: Multiple regression analyses of morphological predictors of estimated bite force

	CAR scores for BF_C								
	BM	BL	CBL	ZB	CH	Adjusted R^2	F ratio	df	P
Female	.301	.260	.217	.143	.026	.93	54.32	5, 25	! .001
Male	.283	.147	.296	.119	.097	.93	55.75	5, 18	! .001
	CAR scores for BF_M								
	BM	BL	CBL	ZB	CH				
Female	.299	.273	.212	.132	.021	.92	44.5	5, 25	! .001
Male	.281	.160	.276	.108	.110	.92	48.41	5, 18	! .001

Note. Bold correlation-adjusted correlation (CAR) scores represent the best body and cranial predictors of estimated bite force at the canine (BF_C) and at the molar (BF_M). Bold P values indicate significance ($\alpha = 0.05$). BM = body mass; BL = body length; CBL = condylobasal length; CH = cranial height; ZB = zygomatic breadth.

Table 4: Scaling of bite force model components (pt. A), mechanical advantage (pt. B), and physiological cross-sectional area against condylobasal length (CBL; pt. C)

	Sex effects		Scaling relationships				
	Intercept	P	R^2	Slope (95% CI)	P	Isometric prediction	Scaling patterns
A. BF components against CBL:							
O_C	F 2 3.75, M 2 3.21	.057	.94	1.09 (1.02–1.16)	.012	1	PA
O_M	F 2 6.37, M 2 6.47	.000	.93	1.58 (1.45–1.72)	! .001	1	PA
MAT	F 2 8.14, M 2 7.59	.000	.89	1.74 (1.59–1.91)	! .001	1	PA
MAM	F 2 8.09, M 2 9.39	.000	.67	1.87 (1.59–2.18)	! .001	1	PA
m_{TEM}	F 2 25.89, M 2 30.85	.959	.92	6.81 (6.31–7.36)	! .001	3	PA
m_{MAS}	F 2 22.18, M 2 25.36	.228	.88	5.33 (4.83–5.86)	! .001	3	PA
f_{TEM}	F 2 10.10, M 2 8.85	.610	.64	2.15 (1.83–2.54)	! .001	1	PA
f_{MAS}	F 2 8.65, M 2 8.15	.056	.4	1.83 (1.48–2.26)	! .001	1	PA
B. MA against CBL:							
$temMA_C$	F 2 4.93, M 2 4.98	.002	.56	.77 (.64–.92)	! .001	0	PA
$temMA_M$			NS				
$masMA_C$	F 2 6.40, M 2 7.33	.000	.17	1.05 (.79–1.39)	! .001	0	PA
$masMA_M$			NS				
C. PCSA against CBL:							
$PCSA_{TEM}$	F 2 20.13, M 2 23.58	.996	.89	5.11 (4.66–5.60)	! .001	2	PA
$PCSA_{MAS}$	F 2 22.18, M 2 25.36	.228	.88	5.35 (4.84–5.86)	.001	2	PA

Note. Bite force (BF) components, mechanical advantage, and physiological cross-sectional area (PCSA) served as dependent variables, while body mass served as the independent variable. *P* values from tests of sex effect reflect differences in elevation between the sexes, and *P* values from tests of isometry reflect differences from isometric predictions. All *P* values are reported as Benjamini-Hochberg-corrected values. Bold *P* values indicate significance (α p 0.05). NS p nonsignificant relationship (R^2 p 0.00–0.08, P p 0.067–0.680). See table A3 for tests in difference of slopes. For scaling patterns, I p isometry, PA p positive allometry, and NA p negative allometry. f_{MAS} p masseter fiber length; f_{TEM} p temporalis fiber length; M p male; m_{MAS} p masseter mass; m_{TEM} p temporalis mass; MAM p masseter in-lever; MAT p temporalis in-lever; $masMA_C$ p masseter mechanical advantage to the canine; $masMA_M$ p masseter mechanical advantage to the molar; O_C p out-lever to canine; O_M p out-lever to molar; $PCSA_{MAS}$ p physiological cross-sectional area of masseter; $PCSA_{TEM}$ p physiological cross-sectional area of temporalis; $temMA_C$ p temporalis mechanical advantage to the canine; $temMA_M$ p temporalis mechanical advantage to the molar.

Males also exhibited significantly greater theoretical bite forces ($P < 0.001$) and larger jaw adductor muscle masses ($P < 0.001$). Despite differences in bite force, we found no significant size differences in out-lever lengths, in-lever lengths, mechanical advantage, and muscle fiber lengths (P p 0.053–0.766; table 6).

Discussion

Scaling of Craniomuscular Traits and Bite Force

Our study focused on measurements of body size (body mass and length), cranial measurements, and muscular traits (temporalis and master mass, fiber lengths, pennation angle, and insertion points) to understand scaling patterns in male and female southern sea otters. Our bite force model relied on the derivations of these measurements and other variables such as muscle tissue density, peak muscle stress, and gape angle for which values were taken from the literature and not directly measured.

The negative allometric relationship between body mass and condylobasal length suggests that sea otters have shorter heads relation to their body. While this pattern is intuitive, closer examination of the scaling patterns of out-lever lengths indicates that shorter jaws may also contribute to allometric increases in theoretical bite force. The out-levers exhibit less of a positive allometric relationship compared to all the components of the bite force model. Furthermore, this allometric pattern reverses when examining the scaling relationship between out-levers and body mass; out-lever lengths are highly negatively allometric compared to all other bite force model components. Thus, these patterns strongly suggest that bite force may be partly driven by the disproportionate decreases in out-lever lengths. Theoretical bite force in southern sea otters scaled with positive allometry relative to cranial dimensions and body size through ontogeny. Studies across a broad range of taxa demonstrate that allometric increases in bite force can be attributed to allometric increase in PCSA of the jaw muscles (Pfaller et al. 2011; Kolmann et al. 2015), mechanical advantage (Grubich 2005; Huber et al. 2008), or a combination of both (Hernandez and Motta 1997; Huber et al. 2006; Kolmann and Huber 2009). In turn, allometric increases in PCSA and mechanical advantage can be achieved by changes in the underlying components:

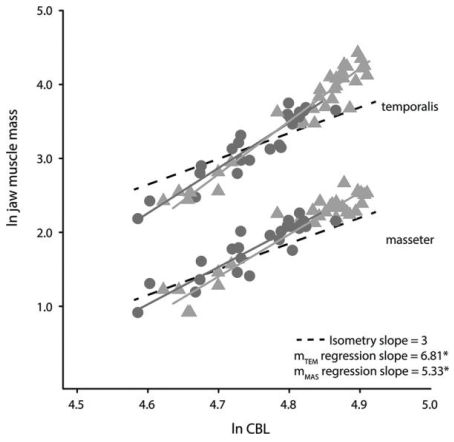

Figure 3. Scaling of temporalis (m_{TEM}) and masseter (m_{MAS}) muscle masses on condylobasal length (CBL). Circles indicate female otters, and triangles indicate male otters. Dark gray and light gray solid lines represent standardized major axis regressions for females and males, respectively. Dotted lines indicate the line of isometry. An asterisk indicates that the slope is significantly different from isometry. See table 4 for more details. A color version of this figure is available online.

scaling patterns in muscle PCSA can be altered by changes in jaw muscle mass, muscle fiber lengths, and/or pennation angle (Pfaller et al. 2011; Kolmann et al. 2015), and scaling patterns of mechanical advantage can be altered by changes in in-lever and out-lever lengths (Grubich 2005; Huber et al. 2008). In sea otters, we found that positive allometry of theoretical bite force is the product of allometric increases in both muscle PCSA and mechanical advantage relative to condylobasal length. Examination of the bite force model components revealed that out-lever lengths, in-lever lengths, jaw muscle masses, and jaw muscle fiber lengths all scaled with positive allometry with respect to condylobasal length, suggesting that all these components contribute to the allometric increase in bite force. Nevertheless, CAR scores show that temporalis mass is the most important contributor to bite force estimation, indicating that ontogenetic changes in temporalis mass contributed more strongly to the ontogenetic patterns in bite force than did lever lengths or muscle fiber lengths. This is corroborated by the fact that temporalis mass was the only model component to exhibit strong positive allometry relative to body mass, suggesting that the disproportionate increase in theoretical bite force with respect to body mass is driven by the disproportionate increase in temporalis mass.

Our finding that the temporalis mass is the most important contributor to theoretical bite force is not surprising. It is well documented that the temporalis is the dominant jaw adductor muscle in carnivores (Scapino 1968; Turnbull 1970). In mustelids, the temporalis (deep and superficial) can comprise up to 80% of the jaw adductor mass (Turnbull 1970; Riley 1985; Timm 2013; Davis 2014). Large temporalis muscles are used to generate the high bite forces at large gape angles necessary to capture and kill prey (Turnbull 1970). In addition, the temporalis helps to resist dislocation of the condyle during forceful posterior biting (Maynard Smith and Savage 1959). In the durophagous southern sea otter, hard-shelled prey are often crushed with molars (carnassial position) where bite forces are greatest. Therefore, large temporalis muscles are essential in generating the high bite forces at large gape angles that are necessary to break open these heavily armored invertebrate prey (Timm 2013).

Patterns of Sexual Dimorphism

Our data indicated that adult males exhibited significantly larger cranial dimensions, bigger jaw musculature, and greater theoretical bite forces than adult females. Our finding of larger cranial traits is consistent with previous findings (Scheffer 1951; Roest 1985; Wilson et al. 1991; Law et al., forthcoming). Sexual selection may drive male sea otters to have greater biting ability than females, as they use that ability to fight with other males to defend territories (Garshelis et al. 1984) and for copulating with females, during which they grasp a female's nose with their teeth (Fisher 1939). However, a difference in absolute theoretical bite force between the sexes also is consistent with the niche divergence hypothesis, which suggests that intersexual differences in traits related to feeding are linked to dietary partitioning between the sexes (Darwin 1871; Hedrick and Temeles 1989; Shine 1989). Law et al. (forthcoming) attributed the morphological differences in the sea otter feeding apparatus as an indication of niche divergence, which also aids in the maintenance of sexual dimorphism. Southern sea otter foraging and habitat use patterns may corroborate the niche divergence hypothesis. Male sea otters utilize larger home ranges than females (Smith et al. 2015) and often are the first to explore and occupy new areas (Garshelis et al. 1984), facilitating range expansion. In addition, sea otter foraging studies in California have indicated a strong pattern of dietary specialization (Estes et al. 2003; Tinker et al. 2007), particularly in food-limited areas (Tinker et al. 2008), with females showing a greater degree of specialization (Smith et al. 2015). Generalists are typically better equipped to use a broader array of habitats and prey types (Bolnick et al. 2007; Darimont et al. 2009). Therefore, in southern sea otters, greater biting ability may benefit males as they move through and establish new territories, which may host larger or novel prey items that require greater bite force to obtain, whereas female sea otter prey diversity is constrained by their relatively small home ranges and their tendency to specialize on a few prey items. This difference may allow male sea otters to take advantage of different foraging opportunities than females and may be explained by the niche divergence hypothesis.

In contrast, when the morphological and functional traits are size corrected with either condylobasal length or body mass, we found that ontogenetic scaling patterns of cranial dimensions and theoretical bite forces do not significantly differ between the sexes, suggesting that for a given condylobasal length or body

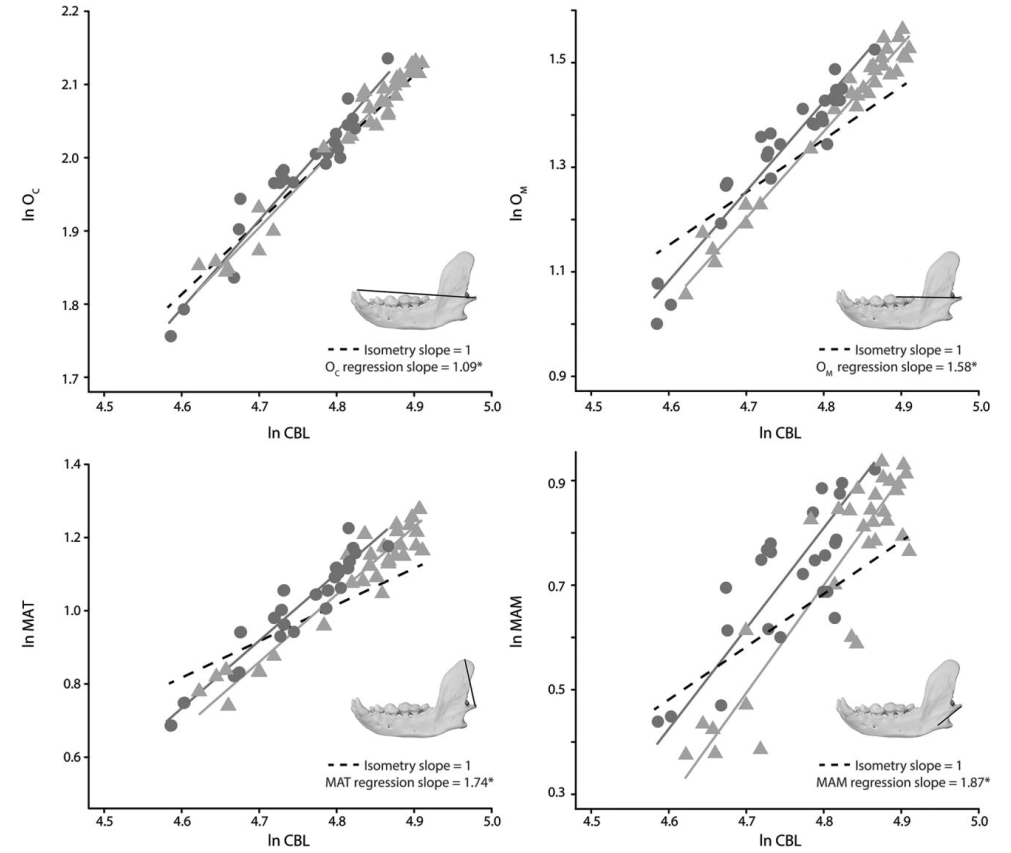

Figure 4. Scaling of out-levers and in-levers on condylobasal length. Circles indicate female otters, and triangles indicate male otters. Dark gray and light gray solid lines represent standardized major axis regression for females and males, respectively. Dotted lines indicate line of isometry. An asterisk indicates that the slope is significantly different from isometry. See table 4 for more details. A color version of this figure is available online.

mass, males and females do not differ in cranial features related to biting or theoretical bite force. Similarly, the majority of the muscular components of our model exhibited no significant differences between the sexes when corrected for size. These results indicate that male southern sea otters exhibit greater theoretical bite forces because of their larger crania and greater jaw muscle sizes rather than differences in scaling patterns.

Despite not finding size-corrected differences in theoretical bite force between the sexes, we observed size-corrected differences in the mechanical advantage at the canine, with females exhibiting relatively higher mechanical advantage compared to males. These differences in jaw mechanics can be traced back to relative differences in lever lengths between the sexes; females exhibited relatively longer in-levers for both the temporalis and masseter muscles, whereas females and males did not exhibit relatively different canine out-lever lengths. Intersexual differences in size-corrected in-lever lengths but not size-corrected out-lever lengths are consistent with recent work based on linear measurements of 112 adult southern sea otter skulls (Law et al., forthcoming). Because higher mechanical advantage is typically associated with increased force-modified jaws (Kardong 2014), it is surprising that females exhibited relatively higher mechanical advantage than males yet did not exhibit relatively higher theoretical bite forces. A possible explanation for this observed pattern is the role of temporalis muscle mass—a trait that did not exhibit size-controlled intersexual differences—in biting performance. As the greatest contributor to bite force, temporalis muscle mass may have simply masked the signal of intersexual

Table 5: Multiple regression analyses of model components that contribute to estimated bite force

	CAR scores for BF_C components										
	O_C	MAT	MAM	m_{TEM}	m_{MAS}	f_{TEM}	f_{MAS}	Adjusted R^2	F ratio	df	P
Female	.084	.209	.073	.392	.210	.000	.032	1	79,730	7, 16	! .001
Male	.117	.168	.109	.349	.179	.035	.042	.99	50,240	7, 23	! .001
	CAR scores for BF_M components										
	O_M	MAT	MAM	m_{TEM}	m_{MAS}	f_{TEM}	f_{MAS}				
Female	.095	.210	.090	.359	.205	.000	.040	1	47,000	7, 13	! .001
Male	.111	.184	.103	.351	.193	.027	.032	.99	36,140	7, 15	! .001

Note. Correlation-adjusted correlation (CAR) scores representing relative contribution of model components to estimated bite force at the canine (BF_C) and at the molar (BF_M). Bold CAR scores represent the best model component predictor. Bold P values indicate significance ($\alpha = 0.05$). f_{MAS} = masseter fiber length; f_{TEM} = temporalis fiber length; m_{TEM} = temporalis mass; m_{MAS} = masseter mass; MAM = masseter in-lever; MAT = temporalis in-lever; O_C = out-lever to canine; O_M = out-lever to molar.

differences from mechanical advantage in our overall estimation of bite force.

Modeling Biting Ability

Our study is one of the few ontogenetic scaling studies examining the underlying muscular and skeletal components that contribute to biting ability in a single mammalian species. While the focus of our article is on the ontogenetic pattern of bite force development, our model came with two caveats. First, we were unable to empirically test our bite force model with measured bite forces from live sea otters. Southern sea otters are protected under the US Marine Mammal Protection Act as well as the US Endangered Species Act, making in vivo

Table 6: Summary statistics for raw morphological and estimated bite-force data and results of ANOVAs to assess sexual differences in each craniodental trait

Traits	Adult females (n = 7; mean ± SE)	Adult males (n = 12; mean ± SE)	$F_{1, 17}$	P
BM (kg)	17.09 ± 1.07	24.75 ± 1.31	15.0901	.002
BL (cm)	89.17 ± .99	97.27 ± .96	28.9562	! .001
CBL (cm)	123.70 ± .83	130.97 ± .97	24.3057	! .001
ZB (cm)	96.75 ± .63	101.79 ± 1.00	11.9562	.004
CH (cm)	59.30 ± .63	62.60 ± .63	11.2042	.005
BF_C (N)	227.73 ± 6.40	318.53 ± 12.04	27.465	! .001
BF_M (N)	420.48 ± 11.70	582.16 ± 19.12	33.7689	! .001
O_C (cm)	7.77 ± .11	8.11 ± .07	8.2809	.013
O_M (cm)	4.21 ± .07	4.43 ± .06	4.9634	.053
MAT (cm)	3.13 ± .05	3.21 ± .06	.848	.452
MAM (cm)	2.19 ± .07	2.33 ± .05	2.7134	.158
$temMA_C$	.40 ± .00	.40 ± .01	.7653	.455
$temMA_M$	.74 ± .01	.73 ± .01	1.9873	.225
$masMA_C$	.28 ± .01	.29 ± .01	.2967	.653
$masMA_M$	.52 ± .01	.53 ± .01	.1195	.766
m_{TEM} (g)	37.32 ± 1.03	60.64 ± 3.05	29.4098	! .001
m_{MAS} (g)	8.15 ± .34	10.93 ± .37	23.3904	! .001
f_{TEM} (cm)	4.18 ± .05	4.75 ± .13	9.295	.010
f_{MAS} (cm)	3.34 ± .10	3.40 ± .12	.0909	.766
$PCSA_{TEM}$ (cm^2)	8.42 ± .21	12.00 ± .45	31.5618	! .001
$PCSA_{MAS}$ (cm^2)	2.31 ± .10	3.07 ± .11	21.4458	! .001

Note. All P values are reported as Benjamini-Hochberg-corrected values. Bold P values indicate significance ($\alpha = 0.05$). BF_C = bite force at canine; BF_M = bite force at molar; BL = body length; BM = body mass; CBL = condylobasal length; CH = cranial height; f_{MAS} = masseter fiber length; f_{TEM} = temporalis fiber length; m_{MAS} = masseter mass; m_{TEM} = temporalis mass; MAM = masseter in-lever; MAT = temporalis in-lever; O_C = out-lever to canine; O_M = out-lever to molar; $PCSA_{MAS}$ = physiological cross-sectional area of masseter; $PCSA_{TEM}$ = physiological cross-sectional area of temporalis; $temMA_C$ = temporalis mechanical advantage to the canine; $temMA_M$ = temporalis mechanical advantage to the masseter; ZB = zygomatic breadth.

studies challenging. Regardless, in vivo studies would be invaluable in providing cranial and bite force measurements needed to validate our model. However, we found that our theoretical bite forces ofjust the adult specimens (mean adult BF Cp 270.4 N; mean adult BF Mp 482.2 N) are comparable to theoretical bite forces using the dry skull method (mean BF Cp 281.0 N; mean BF Mp 394.2 N), which uses photographs of dorsoposterior and ventral views of the cranium to estimate muscle cross-sectional area (Christiansen and Wroe 2007). In addition, our estimations of adult temporalis muscle force (310.7 N) and mass (52.6 g) and adult masseter muscle force (84.3 N) and mass (10.0 g) were similar to muscle force estimations in Alaskan sea otters (temporalis force, 313.0 N; temporalis mass, 53.6 g; and masseter force, 59.4 N; masseter mass, 7.9 g; Timm 2013). Despite our lack ofin vivo bite forces, our study primarily focuses on the ontogenetic scaling of bite force generation rather than absolute values.

Second, our model does not account the force generated by the medial pterygoid, which can contribute to biting ability. However, the medial pterygoid is greatly reduced in mustelids, making up approximately 3.3% of the jaw adductor muscle volume in Alaskan sea otters (Enhydra lutris kenyoni ; Timm 2013), 4% in ferrets (Mustela putorius furo; Davis 2014), and 4.2% in Eurasian otters (Lutra lutra ; Turnbull 1970). Because ofits relatively small size, the medial pterygoid is a weak adductor and more likely serves in stabilizing the jaws during biting in mustelids (Davis 2014). Estimation of medial pterygoid force generation (19.5 N) accounted for just 4.9% of total jaw muscle force generation in Alaskan sea otters (Timm 2013). Therefore, the medial pterygoid is unlikely to signi ficantly contribute to biting ability.

Conclusion

We found that in southern sea otters, allometric increases of PCSA for the major jaw adductor muscle and mechanical advantage underlie the pattern of positive allometry for theoretical bite force. Although all the components of our model scaled with positive allometry relative to condylobasal length, CAR scores indicated that temporalis muscle mass was the greatest contributor to theoretical bite force. This is corroborated by the fact that temporalis mass was the only model component out of eight variables to exhibit positive allometry relative to body mass. Alternatively, allometric decreases in out-lever lengths also contribute to allometric increases in theoretical bite force. In our analysis of sexual dimorphism, we found no differences in scaling patterns of bite force and morphological traits between the sexes through ontogeny. Although we did not find size-corrected differences in theoretical bite forces, muscle PCSA, and the majority of cranial traits between the sexes, we found that for a given condylobasal length or body mass, female sea otters exhibit relatively longer temporalis and masseter in-levers but shorter molar out-levers. We postulate that as the greatest contributor to theoretical bite force, temporalis muscle mass may have masked the signal of sex effects from lever lengths in our overall estimation of bite force. In adults, we found that adult male sea otters can generate greater bite forces than adult female sea otters, and these intersexual differences are a result of differences in overall size (in which males are larger) rather than differences in scaling patterns. Our results demonstrating a difference in absolute theoretical bite force between the sexes are consistent with the niche divergence hypothesis. Nevertheless, additional field studies in sea otter foraging ecology will further validate the role of the niche divergence hypothesis in the maintenance of sexual dimorphism in sea otters.

Acknowledgments

We are grateful to Erin Dodd (California Department of Fish and Wildlife [CDFW]), Francesca Batac (CDFW), and Sue Pemberton (California Academy of Sciences) for helping clean out the skulls; Lilian Carswell (US Fish and Wildlife Service) for permitting logistics; Tim Tinker (US Geological Survey) for helpful discussions on sea otter life history; Sharlene Santana (University of Washington) for providing PDFs of rare references; and Vikram Baliga (University of California –Santa Cruz) for guidance with the statistical analyses. We also thank Vikram Baliga, Ben Higgins, Jacob Harrison, and two anonymous reviewers for helpful comments and discussions on various versions of this manuscript. Funding was provided partly by a Grant-in-Aid of Research from the American Society of Mammalogists, a Lerner-Gray Fund through the American Museum of Natural History, a Rebecca and Steve Sooy Graduate Research Fellowship for Marine Mammals, and a National Science Foundation Graduate Research Fellowship (all awarded to C.J.L.).

Literature Cited

Anderson R.A., L.D. McBrayer, and A. Herrel. 2008. Bite force in vertebrates: opportunities and caveats for use of a nonpareil whole-animal performance measure. Biol J Linn Soc 93:709–720.

Baliga V.B. and R.S. Mehta. 2014. Scaling patterns inform ontogenetic transitions away from cleaning in Thalassoma wrasses. J Exp Biol 217:3597–3606.

Benjamini Y. and Y. Hochberg. 1995. Controlling the false discovery rate: a practical and powerful approach to multiple testing. J R Stat Soc B 57:289–300.

Biewener A.A. and R.J. Full. 1992. Force platform and kinematic analysis. Pp. 45–73 in A.A. Biewener, ed. Biomechanics structures and systems: a practical approach. Oxford University Press, New York.

Binder W.J. and B. Valkenburgh. 2000. Development of bite strength and feeding behaviour in juvenile spotted hyenas (Crocuta crocuta). J Zool 252:273–283.

Bolnick D.I., P. Amarasekare, M.S. Araújo, R. Bürger, J.M. Levine, M. Novak, V.H.W. Rudolf, et al. 2011. Why intraspecific trait variation matters in community ecology. Trends Ecol Evol 26:183–192.

Bolnick D.I., R. Svanbäck, M.S. Araújo, and L. Persson. 2007. Comparative support for the niche variation hypothesis that more generalized populations also are more heterogeneous. Proc Natl Acad Sci USA 104:10075–10079.

Bulté G., D.J. Irschick, and G. Blouin-Demers. 2008. The reproductive role hypothesis explains trophic morphology dimorphism in the northern map turtle. Funct Ecol 22:824–830.

Camilleri C. and R. Shine. 1990. Sexual dimorphism and dietary divergence: differences in trophic morphology between male and female snakes. Copeia 1990:649–658.

Christiansen P. and S. Wroe. 2007. Bite forces and evolutionary adaptations to feeding ecology in carnivores. Ecology 88: 347–358.

Clutton-Brock T. 2007. Sexual selection in males and females. Science 318:1882–1885.

Collar D.C., J.S. Reece, M.E. Alfaro, and P.C. Wainwright. 2014. Imperfect morphological convergence: variable changes in cranial structure underlie transitions to durophagy in moray eels. Am Nat 183:E168–E184. doi:10.1086/675810.

Constantino P.J., J.J.W. Lee, D. Morris, P.W. Lucas, A. Hartstone-Rose, W.-K. Lee, N.J. Dominy, et al. 2011. Adaptation to hard-object feeding in sea otters and hominins. J Hum Evol 61:89–96.

Darimont C.T., P.C. Paquet, and T.E. Reimchen. 2009. Landscape heterogeneity and marine subsidy generate extensive intrapopulation niche diversity in a large terrestrial vertebrate. J Anim Ecol 78:126–133.

Darwin C. 1871. The descent of man and selection in relation to sex. J. Murray, London.

Davis J.L., S.E. Santana, E.R. Dumont, and I.R. Grosse. 2010. Predicting bite force in mammals: two-dimensional versus three-dimensional lever models. J Exp Biol 213:1844–1851.

Davis J.S. 2014. Functional morphology of mastication in musteloid carnivorans. PhD diss. Ohio State University, Columbus.

Emerson S.B. and D.M. Bramble. 1993. Scaling, allometry, and skull design. Pp. 384–421 in J. Hanken and B.K. Hall, eds. The skull. Vol. 3. Functional and evolutionary mechanisms. University of Chicago Press, Chicago.

Erickson G.M., A.K. Lappin, and K.A. Vliet. 2003. The ontogeny of bite-force performance in American alligator (Alligator mississippiensis). J Zool 260:317–327.

Estes J.A., M.L. Riedman, M.M. Staedler, M.T. Tinker, and B.E. Lyon. 2003. Individual variation in prey selection by sea otters: patterns, causes and implications. J Anim Ecol 72:144–155.

Fisher E.M. 1939. Habits of the southern sea otter. J Mammal 20:21.

———. 1941. Notes on the teeth of the sea otter. J Mammal 22:428.

Garshelis D.L. and A.M. Johnson. 1984. Social organization of sea otters in Prince William Sound, Alaska. Can J Zool 62: 2648–2658.

Grömping U. 2006. Relative importance for linear regression in R: the package relaimpo. J Stat Softw 17:1–27.

Grubich J.R. 2005. Disparity between feeding performance and predicted muscle strength in the pharyngeal musculature of black drum, Pogonias cromis (Sciaenidae). Environ Biol Fish 74:261–272.

Hatfield B. 2006. Protocol for stranded and dead sea otters. California Department of Fish and Wildlife, Sacramento.

Hedrick A.V. and E.J. Temeles. 1989. The evolution of sexual dimorphism in animals: hypotheses and tests. Trends Ecol Evol 4:136–138.

Hernandez L.P. and P.J. Motta. 1997. Trophic consequences of differential performance: ontogeny of oral jaw-crushing performance in the sheepshead, Archosargus probatocephalus (Teleostei, Sparidae). J Zool 243:737–756.

Herrel A., R.V. Damme, B. Vanhooydonck, and F.D. Vree. 2001. The implications of bite performance for diet in two species of lacertid lizards. Can J Zool 79:662–670.

Herrel A., A. De Smet, L.F. Aguirre, and P. Aerts. 2008. Morphological and mechanical determinants of bite force in bats: do muscles matter? J Exp Biol 211:86–91.

Herrel A., R. Joachim, B. Vanhooydonck, and D.J. Irschick. 2006. Ecological consequences of ontogenetic changes in head shape and bite performance in the Jamaican lizard Anolis lineatopus. Biol J Linn Soc 89:443–454.

Herrel A., L.D. McBrayer, and P.M. Larson. 2007. Functional basis for sexual differences in bite force in the lizard Anolis carolinensis. Biol J Linn Soc 91:111–119.

Herrel A., L. Spithoven, R. Van Damme, and F. De Vree. 1999. Sexual dimorphism of head size in Gallotia galloti: testing the niche divergence hypothesis by functional analyses. Funct Ecol 13:289–297.

Herzog W. 1994. Muscle. Pp. 154–187 in B.M. Nigg and W. Herzog, eds. Biomechanics of the musculoskeletal system. Wiley, Chichester.

Hill A.V. 1950. The dimensions of animals and their muscular dynamics. Sci Prog 38:209 –230.
Huber D.R., M.N. Dean, and A.P. Summers. 2008. Hard prey, soft jaws and the ontogeny offeeding mechanics in the spotted ratfish Hydrolagus colliei. J R Soc Interface 5:941 – 952.
Huber D.R., C.L. Weggelaar, and P.J. Motta. 2006. Scaling of bite force in the blacktip shark Carcharhinus limbatus . Zoology 109:109–119.
Kardong K.V. 2014. Vertebrates: comparative anatomy, function, evolution. McGraw-Hill, Boston.
Kolmann M.A. and D.R. Huber. 2009. Scaling offeeding biomechanics in the horn shark Heterodontus francisci: ontogenetic constraints on durophagy. Zoology 112:351–361.
Kolmann M.A., D.R. Huber, P.J. Motta, and R.D. Grubbs. 2015. Feeding biomechanics of the cownose ray,Rhinoptera bonasus, over ontogeny. J Anat 227:341 –351.
Law C.J., V. Venkatram, and R.S . Mehta. Forthcoming. Sexual dimorphism in the craniomandibular morphology of southern sea otters (Enhydra lutris nereis). J Mammal.
Marshall C.D., A. Guzman, T. Narazaki, K. Sato, E.A. Kane, and B.D. Sterba-Boatwright. 2012. The ontogenetic scaling of bite force and head size in loggerhead sea turtles (Caretta caretta): implications for durophagy in neritic, benthic habitats. J Exp Biol 215:4166 –4174.
Marshall C.D., J. Wang, A. Rocha-Olivares, C. Godinez-Reyes, S. Fisler, T. Narazaki, K. Sato, et al. 2014. Scaling of bite performance with head and carapace morphometrics in green turtles (Chelonia mydas). J Exp Mar Biol 451:91 –97.
Maynard Smith J. and R. Savage. 1959. The mechanics of mammalian jaws. Sch Sci Rev 141:289 –301.
McGee M.D. and P.C. Wainwright. 2013. Sexual dimorphism in the feeding mechanism of threespine stickleback. J Exp Biol 216:835 –840.
Mendez J. and A. Keys. 1960. Density and composition of mammalian muscle. Metab Clin Exp 9:184 –188.
Pfaller J.B., P.M. Gignac, and G.M. Erickson. 2011. Ontogenetic changes in jaw-muscle architecture facilitate durophagy in the turtle Sternotherus minor. J Exp Biol 214:1655 –1667.
R Core Team. 2015. R: a language and environment for statistical computing. R Foundation for Statistical Computing, Vienna. http://www.R-project.org/.
Radford A.N. and M.A. Du Plessis. 2003. Bill dimorphism and foraging niche partitioning in the green woodhoopoe. J Anim Ecol 72:258 –269.
Riedman M. and J.A. Estes. 1990. The sea otter (Enhydra lutris): behavior, ecology, and natural history. Biol Rep 90:1 –117.
Riley M.A. 1985. An analysis of masticatory form and function in three mustelids (Martes americana, Lutra canadensis, Enhydra lutris). J Mammal 66:519 –528.
Roest A.I. 1985. Determining the sex of sea otters from skulls. Calif Fish Game 71:179 –183.
Sacks R.D. and R.R. Roy. 1982. Architecture of the hind limb muscles of cats: functional significance. J Morphol 173:185 – 195.
Santana S.E., E. Dumont, and J.L. Davis. 2010. Mechanics of bite force production and its relationship to diet in bats. Funct Ecol 24:776 –784.
Santana S.E. and K.E. Miller. 2016. Extreme postnatal scaling in bat feeding performance: a view of ecomorphology from ontogenetic and macroevolutionary perspectives. Integr Comp Biol. doi:10.1093/icb/icw075.
Scapino R.P. 1968. Biomechani cs offeeding in Carnivora. PhD diss. University of Illinois, Chicago.
Scheffer V.B. 1951. Measurements of sea otters from western Alaska. J Mammal 32:10 –14.
Schmidt-Nielsen K. 1984. Scaling. Cambridge University Press, Cambridge.
Schneider C.A., W.S. Rasband, and K.W. Eliceiri. 2012. NIH Image to ImageJ: 25 years ofimage analysis. Nat Methods 9: 671–675.
Shine R. 1989. Ecological causes for the evolution of sexual dimorphism: a review of the evidence. Q Rev Biol 64:419 –461.
Smith E.A., S.D. Newsome, J.A. Estes, and M.T. Tinker. 2015. The cost of reproduction: differential resource specialization in female and male California sea otters. Oecologia 178: 17–29.
Thom M.D. and L.A. Harrington. 2004. Why are American mink sexually dimorphic? a role for niche separation. Oikos 105:525–535.
Thomas P., E. Pouydebat, I. Hardy, F. Aujard, C.F. Ross, and A. Herrel. 2015. Sexual dimorphism in bite force in the grey mouse lemur. J Zool 296:133 –138.
Timm L.L. 2013. Feeding biomechanics and craniodental morphology in otters (Lutrinae). PhD diss. Texas A&M University, College Station.
Timm-Davis L.L., T.J. DeWitt, and C.D. Marshall. 2015. Divergent skull morphology supports two trophic specializations in otters (Lutrinae). PLoS ONE 10:e0143236.
Tinker M.T., G. Bentall, and J.A . Estes. 2008. Food limitation leads to behavioral diversification and dietary specialization in sea otters. Proc Natl Acad Sci USA 105:560 –565.
Tinker M.T., D.P. Costa, J.A. Estes, and N. Wieringa. 2007. Individual dietary specialization and dive behaviour in the California sea otter: using archival time-depth data to detect alternative foraging strategies. Deep Sea Res II 54: 330–342.
Turnbull W.D. 1970. Mammalian masticatory apparatus. Field Museum of Natural History, Chicago.
van der Meij M.A.A. and R.G. Bout. 2006. Seed husking time and maximal bite force in finches. J Exp Biol 209:3329 –3335.
Van Valkenburgh B. 2007. Deja vu: the evolution offeeding morphologies in the Carnivora. Am Zool 47:147 –163.
Verwaijen D., R. Van Damme, and A. Herrel. 2002. Relationships between head size, bite force, prey handling efficiency and diet in two sympatric lacertid lizards. Funct Ecol 16: 842–850.
Warton D.I., R.A. Duursma, D.S. Falster, and S. Taskinen. 2011. smatr 3: an R package for estimation and inference about allometric lines. Methods Ecol Evol 3:257 –259.

Wilson D.E., M.A. Bogan, R.L. Brownell, A.M. Burdin, and M.K. Maminov. 1991. Geographic variation in sea otters, Enhydra lutris . J Mammal 72:22 –36.

Ziscovici C., P.W. Lucas, P.J. Constantino, T.G. Bromage, and A. van Casteren. 2014. Sea otter dental enamel is highly resistant to chipping due to its microstructure. Biol Lett 10: 20140484.

Zuber V. and K. Strimmer. 2011. High-dimensional regression and variable selection using CAR scores. Stat Appl Genet Mol Biol 10:1 –34.

Conclusion

As a comparative biologist, my research investigates how morphological variation affects the performance, behavior, and ecology of different species across evolutionary time as well as between individuals within single populations. In my first three dissertation chapters, I examined how size, shape, and performance of the cranial and post-cranial systems affect species diversity and phenotypic disparity. In Chapters 1 and 2, I examined the role of morphological innovations in the diversification of species. I first used novel molecular- and fossil-based methods to uncover if musteloids exhibited rapid rates of lineage diversification and phenotypic variation as predicted under adaptive radiation theory. Surprisingly, I found no evidence for rapid bursts of lineage diversification across the entire clade as previously hypothesized. Instead, I found an increase in a species carrying capacity within a subclade of Mustelidae (weasels, otters, martens) that is nearly twice as high as the remaining musteloid clade. Supporting decoupled diversification dynamics between the subclade of elongate mustelids and the ancestral musteloid regime is our finding of increased rates of body length evolution, but not body mass evolution, within the decoupled mustelid subclade. Coincidently, mustelids within this subclade have been consistently described as small and "elongate," which suggest body elongation may have served as a morphological innovation leading to increased species richness. I further tested this hypothesis in Chapter 2 by quantifying musteloid body shapes with 401 osteological specimens. I found that a derived clade consisting of weasels, otters, and martens exhibited evolutionary shifts towards more

elongate body plans and reduced limb lengths compared to the rest of Musteloidea. This supports the hypothesis that body elongation served as an innovation that may have enabled the exploitation of new open habitats and their associated rodent and lagomorph faunas during the continual cooling and drying of the Late Miocene to Pliocene, which resulted in their relatively higher species richness.

Chapters 1 and 2 produced two major accomplishments. First, I revealed that body shape can serve as an innovation leading to increased species richness within a clade and that phenotypic evolutionary rates under a single morphological metric, even one as influential as mass, may not capture the evolution of diversity in clades that exhibit elongate body shapes. Second, my study was the first to compile a quantitative database of mammalian body shapes for comparative analyses and document the underlying components of the axial skeleton that contribute to the diversity of body shapes. Furthermore, I found that more elongate bodies correlate negatively with forelimb length but not hindlimb length, a relationship that has not previously been described in mammals but follows the major trend exhibited by other ectothermic vertebrate clades. Because osteological specimens are used, my body shape metric can be extended for more thorough examination of the underlying morphological traits that drive the evolution towards more extreme body shape patterns across the mammalian tree of life.

In Chapter 3, I examined the interface between interspecific and intraspecific variation; specifically, I examined how sexual dimorphism evolved across an entire clade. The evolution and maintenance of sexual dimorphism has long been attributed to sexual selection. Alternatively, niche divergence, a non-mutually exclusive

mechanism for the evolution of sexual dimorphism is rarely tested. My examination of sexual dimorphism revealed that selection via dietary divergence rather than sexual selection is a greater factor in maintaining cranial sexual dimorphism. I found that the greatest degree of cranial size and bite force dimorphism occurred in terrestrial carnivores, which reduces dietary competition between the sexes because competition for terrestrial vertebrate prey is greater than other dietary groups. Therefore, Chapter 3 highlights niche divergence as an important mechanism that maintains the evolution of sexual dimorphism. Furthermore, I found a much stronger relationship between the degree of cranial size dimorphism and bite force dimorphism compared to relationships between the degree of cranial shape dimorphism and the degree of cranial size dimorphism as well as the degree of bite force dimorphism. These results support a hypothesis that cranial size plays a larger role in facilitating bite force generation over cranial shape. I further tested this hypothesis by examining the relationships between cranial size and shape and bite force. I found a strong relationship between cranial size and estimated bite force but not between cranial shape and relative bite force (Law et al. in revision). Many-to-one mapping of form to function may explain this pattern because a variety of evolutionary shape changes rather than a single shape change may have contributed to an increase in relative biting ability. I also found that while musteloids with different diets exhibit different cranial shapes, they have similar estimated bite forces. This suggests that other feeding performance metrics and potentially non-feeding traits are also important contributors to cranial evolution. Overall, Chapter 3 revealed that morphological

diversity does not always lead to the same functional diversity, and that these relationships can differ between the sexes.

In my last two chapters (Chapters 4 and 5), I examined how growth, development, and sexual dimorphism affects the form and function of the southern sea otter feeding apparatus. The development and growth of the feeding apparatus are among the most salient changes across an organism's ontogeny as they are directly related to ontogenetic shifts in diets and resource use. A complete understanding of the development and growth of the feeding apparatus, however, is not possible without knowledge of the effects of sex. Selective pressures underlying sexual dimorphism act not only on adult morphology but also on the development and growth of traits throughout ontogeny. Therefore, understanding how ontogeny and sexual dimorphism affect the morphology and performance of individuals is essential for a complete understanding of the fitness and survival of an entire population. Overall, I found significant sexual dimorphism in adult sea otter skulls and bite force that arose through differences in developmental and growth rates and duration of the craniomandibular morphology. I postulate that males are selected to attain mature crania faster to presumably reach adult biting ability sooner, gaining a competitive advantage in obtaining food and in male–male agonistic interactions. The next steps in this research project are to quantify dietary differences between the sexes and across ontogeny. Together with my previous work, these data will further elucidate how newly weaned pups are able to successfully forage as they grow as well as examine the mechanisms that contribute to the maintenance of sexual dimorphism.

Although my dissertation attempts to examine the mechanisms that generate phenotypic variation both between and within species, I acknowledge that much work is still needed to bridge these macroevolutionary and microevolutionary processes. New phylogenetic comparative methods are always in development; however, the field as a whole still struggles to incorporate intraspecific variation into these large macroevolutionary analyses and most researchers use mean trait values for species in broad interspecific comparisons, leaving the role of intraspecific variation on phenotypic disparity poorly studied. Only with the development of new methods will researchers be able to examine how intraspecific variation produced by sexual dimorphism or growth and development contributes to macroevolutionary patterns of phenotypic disparity. I am just beginning to examine how sexual dimorphism affects cranial morphospace in musteloids, specifically if males and females in each species will occupy mostly non-overlapping parts of cranial morphospace. Therefore, I predict that the inclusion of both sexes will fill morphospace that was previously unoccupied when the analysis focused on a single sex. This pattern would indicate significant increases in cranial disparity and niche packing, which would allow species to increase their overall niche space by reducing dietary competition between the sexes. These results would demonstrate that ignoring sexual variation would lead to underestimations of cranial disparity.

My research with the southern sea otter population also led to additional questions left to be answered. Although I have found significant differences in skull morphology and bite force between the sexes across ontogeny, additional work is needed to determine if there is a corresponding difference in diet. Together with

Chapters 4 and 5, these data will further elucidate how newly weaned pups are able to successfully forage as they grow and develop as well as examine the mechanisms that contribute to the maintenance of sexual dimorphism in this population of southern sea otters. Furthermore, some individual sea otters use tools feed; therefore, this innovative behavior may influence the growth and development of the skull and therefore biting ability. Overall, additional research is needed to simultaneously examine how tool use behavior and biting performance affects foraging success (biomechanically and energetically) and fitness (profitability and injury prevention) in individual sea otters. This research project will help provide us with an understanding of the energetic mechanisms underlying variation in tool use and show us whether tool-using otters enjoy greater energetic profitability using tools.

Examining the link between morphology, performance, behavior, and ecology and its contribution to biological diversity between and within species has been the central motivation for my life's work and I look forward to investigating how these processes led to the great diversity we find across the Tree of Life.